

ISSN 1407-5806

**COMPUTER
MODELLING**
AND
NEW TECHNOLOGIES

Volume 17
No 2

2013

Transporta un sakaru institūts
(Transport and Telecommunication Institute)

Computer Modelling and New Technologies

Volume 17, No. 2 – 2013

ISSN 1407-5806
ISSN 1407-5814
(On-line: www.tsi.lv)

Riga – 2013

EDITORIAL BOARD:

Prof. Igor Kabashkin (Chairman of the Board), *Transport & Telecommunication Institute, Latvia*;
Prof. Yuri Shunin (Editor-in-Chief), *Information Systems Management Institute, Latvia*;
Prof. Adolfas Baublys, *Vilnius Gediminas Technical University, Lithuania*;
Dr. Brent D. Bowen, *Purdue University, USA*;
Prof. Olgierd Dumbrajs, *University of Latvia, Solid State Physics Institute, Latvia*;
Prof. Sergey Maksimenko, *Institute for Nuclear Problem, Belarus State University, Belarus*;
Prof. Vladimir Litovchenko, *V. Lashkaryov Institute of Semiconductor Physics of National Academy of Science of Ukraine*;
Prof. Pavel D'yachkov, *Kurnakov Institute for General and Inorganic Chemistry, Russian Academy of Sciences, Russia*;
Prof. Stefano Bellucci, *Frascati National Laboratories – National Institute of Nuclear Physics, Italy*;
Prof. Eugene Kopytov, *Transport & Telecommunication Institute, Latvia*;
Prof. Arnold Kiv, *Ben-Gurion University of the Negev, Israel*;
Prof. Juris Zakis, *Higher School of Social Technologies, Latvia*;
Prof. Edmundas Zavadskas, *Vilnius Gediminas Technical University, Lithuania*;
Prof. Michael Schenk, *Fraunhofer Institute for Factory Operation and Automation IFF, Germany*.

Host Organization:

Transport and Telecommunication Institute

Supporting Organizations:

Latvian Transport Development and Education Association
Latvian Academy of Sciences
Latvian Operations Research Society

THE JOURNAL IS DESIGNED FOR PUBLISHING PAPERS CONCERNING THE FOLLOWING FIELDS OF RESEARCH:

- mathematical and computer modelling
- mathematical methods in natural and engineering sciences
- physical and technical sciences
- computer sciences and technologies
- material science, solid state physics and chemistry
- nanomaterials, nanodevices and nanotechnologies
- aviation and aerospace technologies
- electronics and telecommunication
- transport and logistics
- economics and management
- innovative education
- social sciences

In journal articles can be presented in English. All articles are reviewed.

EDITORIAL CORRESPONDENCE

Transporta un sakaru institūts (Transport and Telecommunication Institute)
Lomonosova iela 1, LV-1019, Riga, Latvia. Phone: (+371) 67100593. Fax: (+371) 67100535
E-mail: journal@tsi.lv, www.tsi.lv

COMPUTER MODELLING AND NEW TECHNOLOGIES, 2013, vol. 17, no. 2

ISSN 1407-5806, ISSN 1407-5814 (on-line: www.tsi.lv)

Scientific and research journal of Transport and Telecommunication Institute (Riga, Latvia)

The journal is being published since 1996.

The papers published in Journal “Computer Modelling and New Technologies” are included in

INSPEC (since 2010), **VINITI** (since 2011), **CAS Database**

www.theiet.org/resources/inspec/

<http://www2.viniti.ru/>

<http://www.cas.org/>

Copyright © Transport and Telecommunication Institute, 2013

CONTENTS

Editors' remarks	5
Operation Research	
Repayment Problem at a Settlement of Debts M. Rebezova	7
A Research on Transport Planning Strategic Environmental Assessment (Sea): Incorporating System Dynamics into the Environmental Carrying Capacity Methods for Adaptation of Markov Models to Requested Maintenance Policies Y. Chai, X. Meng, Sh. Ma, L. Xu, Ya. Li, Lu Shen, Ch. Jiang	15
Computer Simulation	
A Novel Online Assessment Scheme for Power System Security Level of Transient Stability Based on Relationships Exploration in a Large Data Set F. Qian, S. Liu, W. Yang, H. Wei, Yo. Fan	24
Numerical Simulation of Air Leakage in Goaf of Fully Mechanized Face with High Dip and Hard Roof Zh. Xie, T. Luan, Na He	36
Simulation of Systems Information Security S. Amanzholova, N. Zhakayev	44
Real-Time Facial Feature Point Detection and Tracking in a Video Sequence B. B. Abisheva, B. M. Baisakov, M. M. Maratov	48
Design And Analysis of Negative Value Circuit Components in PSpice Simulation Software A. Ferikoğlu, Ya. Sari, R. Köker	53
Computer Technologies	
Is there Any Truth in „Projectlibre the Open Source Replacement of Microsoft Project“? K. S. Tsvetkov, M. M. Petrova	60
Mathematical Modelling	
Study on Model of Component Reliability Based on Dynamic Strength Interference Theory X. Ma, Cu. Jiang	65
Authors' Index	73
Personalia	74
Cumulative index	78
Preparation of publications	84



Editors' Remarks

Closed Path

by Rabindranath Tagore

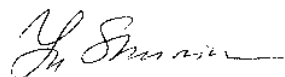
I thought that my voyage had come to its end
at the last limit of my power, that the path before me was closed,
that provisions were exhausted
and the time come to take shelter in a silent obscurity.

But I find that thy will knows no end in me.
And when old words die out on the tongue,
new melodies break forth from the heart;
and where the old tracks are lost,
new country is revealed with its wonders.

Rabindranath Tagore (1861–1941) *

This 17th volume no. 2 presents actual papers on main topics of Journal specialization, namely, Operation Research, Computer Simulation, Computer Technologies and Mathematical Modelling. Contributors of this issue represent scientific institutions of Russia, China, Bulgaria, Turkey and Kazakhstan. Our journal policy is directed on the fundamental and applied sciences researches, which are the basement of a full-scale modelling in practice. This edition is the continuation of our publishing activities. We hope our journal will be interesting for research community, and we are open for collaboration both in research and publishing. We hope that Journal's contributors will consider the collaboration with the Editorial Board as useful and constructive.

EDITORS



Yu.N. Shunin



I.V. Kabashkin

* **Rabindranath Tagore** (1861–1941) – Greatest writer in modern Indian literature, Bengali poet, novelist, educator, who won the Nobel Prize for Literature in 1913. Tagore was awarded the knighthood in 1915, but he surrendered it in 1919 as a protest against the Massacre of Amritsar, where British troops killed some 400 Indian demonstrators protesting colonial laws. Tagore's reputation in the West as a mystic has perhaps misled his Western readers to ignore his role as a reformer and critic of colonialism.



REPAYMENT PROBLEM AT A SETTLEMENT OF DEBTS

M. Rebezova

*Transport Clearing House
 Bolshaja Gruzinskaja 59, Moscow 123056, Russia
 E-mail: rebezova@tch.ru*

In different areas of practical activity the mutual payment liabilities occur between the subjects. Mutual repayment can be done to reduce the real money transfers between subjects. The problem consists in finding the corresponding chain of subjects. The problem is formulated in language of the graph theory and on the one hand it is the classical linear programming problem, on the other hand it is the classical problem of the graph theory. The algorithm and software have been developed for the solution of the problem.

Keywords: graph theory, tree, contour, linear programming, settlement of debts

1. Introduction. Problem Statement

Mathematically, the problem can be formulated in language of graph theory in the following way [1–3]. We consider directed finite graph $G = (V, E)$ whose vertex set V corresponds to subjects of settlement and arc set E corresponds to payment liabilities. An arc from vertex $v_i \in V$ to vertex $v_j \in V$ is denoted as $e_{i,j} \in E$. Its length $d(e_{i,j}) > 0$ equals to an amount of money from subject i to subject j . Mutual repayment can be done to reduce the real money transfers. It is possible if such a closed chain c between subjects (vertices) there exists that if one and the same amount of money is passed along the chain then initial subject receives amount of money, which he sent. The maximal possible passed amount of money equals to minimal payment (arc length) in this chain: $\min\{d(e) : e \in c\}$. It corresponds to a simple contour (without repeating vertices) on graph and indicated passed amount must not exceed the minimal length of the arcs included in the contour. We call this amount as *the weight* $x(c)$ of the contour c or *the transaction*.

The problem consists in finding the set of such contours that: 1. For any graph arc $e \in E$ the sum of weights of contours, in which arc included, must not exceed weight of the arc $d(e)$. 2. The sum of all contours weights (transactions) is maximal.

We formalize the problem more exactly. Let C is some set of simple contours; $k = |C|$ is the number of contours. We introduce the indicator function $\delta_e(c)$, which equals 1 if the arc e is included in the contour c , and $\delta_e(c)$ equals 0 – otherwise. Weights $\{x(c)\}$ of contours $\{c\}$, included in the set C , must satisfy the condition:

$$\sum_{c \in C} x(c) \delta_e(c) \leq d(e), \quad (1)$$

where $x(c) \geq 0, \forall c \in C, \forall e \in E$

and maximize the objective function

$$f(C) = \sum_{c \in C} x(c) v(c), \quad (2)$$

where $v(c)$ is number of arcs included in the contour c .

Solution of formulated problem involves two components. Firstly, we must determine the set of simple contours C . Secondly we must assign weights for contours satisfying condition (1).

2. The Linear Programming Problem

We begin from second component when the set of simple contours C has been specified. We want to assign weights $x(c)$ of contours (transactions) in the formula (2).

Let n denote the number of graph arcs, k denote the number of contours in C . We number all arcs and contours of the graph and introduce into consideration $n \times k$ - matrix A , where the element $A_{i,j} = 1$,

if the i -th arc is included in the j -th contour, and $A_{i,j} = 0$ - otherwise. So i -th row contains the list of contours that include the arc i , and j -th column contains the list of arcs included in the j -th contour c . Next, we consider n -dimensional vector of lengths of arcs: $d = (d_1, \dots, d_n)$.

Weights $\{x(c)\}$ of contours are unknown variables of linear programming problem. In accordance with the standard designations of this theory we shall designate weights x_j of contours for j -th contour, so $x = (x_1, \dots, x_k)$ is nonnegative k -vector.

Then in matrix form the condition (1) is the following:

$$Ax \leq d. \quad (3)$$

The objective function (2) is as follows:

$$f(x) = v^T x, \quad (4)$$

where v is k -dimension vector whose j -th component is equal to the number of arcs included 0 into the j -th contour.

So we have a classical problem of linear programming. Solution methods of this problem are well known [4, 5]. On the other hand, enumeration of all simple contours is the classical problem of the graphs theory [2, 3]. However, solution of this problem is very laborious. So we will use heuristic approximate method and further we proceed to its description.

3. The Proposed Method of Simple Contour Enumeration

The stated method is an approximate since it does not work with the whole set of simple contours, but only with a subset thereof. Thereby computational laboriousness of the method decreases. We construct the contours taking into account their possible maximal weight. It is done to reduce the loss of method efficiency caused by the latter circumstance. The formal description of the procedure of forming of simple contours is as follows.

3.1. Maxi-min contours

The method is based on the conception of the theory of directed graphs analogous to the conception "the shortest path tree". This tree contains the shortest paths from origin to the all other vertices of graph to which path from origin exists. The shortest path is defined as the path having minimal length, i.e. minimal sum of arcs lengths included in the path. *In our case we sense under length of path minimal length among all lengths of arcs included in the path.* We select the maximal length path among all paths between two vertices. We will call such path *maxi-min path*. Algorithms of construction of the shortest paths tree are well known [2, 3]. We will call tree, constructed by that method (in our treatment of the path length), *tree of maxi-min paths*. Applied algorithm is presented in Section 3.3.

The vertices, that do not have arcs outgoing of them, are called *end vertices* in the constructed tree. We find among all end vertices such vertices from which there are arcs, directed to the origin, in the graph. These vertices are called *terminal vertices*. If a is a terminal vertex and e is an arc corresponding to this vertex, then attachment of this arc to the path from origin to vertex a produces the contour. We will call it *maxi-min contour*. Length of this contour is equal to the minimal length of arc e and the considered path. We designate by $C(a)$ the set of all *maxi-min contours* for initial vertex a . Union of all such contours for all vertices $a \in V$ give the whole set of vectors under consideration $C = \bigcup_{a \in V} C(a)$.

3.2. Replenishment of the contour set

We consider the path α included vertices $(\alpha_1 \dots \alpha_{k-1} \alpha_k \alpha_{k+1} \dots \alpha_m)$ and its non-end vertex α_k . We call α_k by *the head* of path $(\alpha_1 \dots \alpha_{k-1} \alpha_k)$ and by *the tail* of path $(\alpha_k \alpha_{k+1} \dots \alpha_m)$ respectively. We will designate these paths $T_k(\alpha)$ and $H_n(\beta)$. Let for two paths α and β α_k -tail of $T_k(\alpha)$ and β_n -head of $H_n(\beta)$ do not have common vertices and there is arc $e = (\alpha_k, \beta_n)$ in graph. Then adding $e = (\alpha_k, \beta_n)$ to α_k -tail and β_n -head gives a new path $T_k(\alpha)eH_n(\beta)$.

If the first vertex α_1 of path α coincides with the last vertex β_n of path β , then we obtain the new contour $\alpha\beta$. For example it happens, when considered paths α and β have one and the same vertex as the end vertices ($\alpha_1 = \alpha_k = \beta_1 = \beta_n$), namely the paths α and β are contours. Therefore we can apply given procedure to the *maxi-min contours*. We will call this procedure **replenishment of contours**.

As a result the set of contours C will be formed for which the indicated above linear programming problem is applied.

3.3. D-algorithm of formation the maxi-min paths tree

The stated algorithm is a certain modification of Dijkstra's algorithm [2, 3], so it is named *D-algorithm*.

Input: M and $i0$. 1. $M = (M_{i,j}) = (d(e_{i,j}))$ is an adjacency matrix whose rows and columns correspond to vertices of graph; $M_{i,j}$ is the length of the arc between corresponding vertices. Therein 0 means that arc absents itself. 2. $i0$ is the number of some vertex of the graph.

Output. The maxi-min paths tree T with origin $i0$.

Method. We use two s -dimensional vectors T and L , where s is number of graph vertices (rows or columns of matrix M). The value of L_i equals to maximal length of path from origin $i0$ to i -th vertex, which is known at the given moment of the algorithm work. The value T_i contains the number of vertex. This vertex is preceded by the vertex i on the current path from $i0$ to i . The algorithm consists in the gradual increase of the vector L values. It finishes its work when such increase becomes impossible.

The algorithm.

Step 0. Let $T_i = i0$, $L_i = 0$, $i = 1, \dots, s$; $n = 1$.

Step n. All pair of vertices with numbers i and j are examined. If a strict inequality

$$L_j < \min\{L_i, M_{i,j}\},$$

occurs then vectors T and L are corrected:

$$L_j = \min\{L_i, M_{i,j}\}, \quad T_j = i.$$

If change of vectors T and L has been occurred when step n was executed, then we set $n = n + 1$ and go to step n . Otherwise – end. T is the required tree.

The described algorithm is implemented in the procedure $Tree(M, i0)$, that is considered below.

4. The Software

The software has been developed in the language Mahcad. It is intended for the representation input data for the linear programming problem (3), (4): restrictions matrix A , free coefficients vector b and vector v of coefficients of the objective function. Adjacency matrix M of the graph describes payments between subjects. Above we designated the set of subjects (graph vertices) by V . Now we designate its dimension (the number of subjects) by s . As earlier, $d(e_{i,j})$ is an amount of money (value of transaction) from subject i to subject j . Corresponding matrix is the adjacency matrix of the graph $M = (M_{i,j}) = (d(e_{i,j}))$. It is a square matrix of order s .

We give a short description of the software. The text below can be explained by illustrations contained in the example of Section 5. Listings of all programs can be got at author.

4.1. The main procedures

Procedure $Tree(M, i0)$ issues mini-max tree with origin $i0$ in the graph given by adjacency matrix M . Wherein Dijkstra's algorithm described in Section 3.1 is implemented.

Procedure $Path(Tr, i, i0)$ issues mini-max path in the tree Tr from vertex $i0$ to vertex i . The last element of issued vector is a weight of path.

Procedure $MMCon(M, i0)$ issues all mini-max contours for vertex $i0$ in the graph given by adjacency matrix M . These contours are calculated on the basis of closure of paths issued by the procedure $Path(Tr, i, i0)$.

Procedure $ContF(LLoki, c)$ forms the column of the matrix A corresponding to the contour c . List of graph arcs $LLoki$ is input to the procedure. This list forms by the auxiliary procedure $Edges(M)$ – see below. Separate rows in the list correspond to certain arc. A row has three elements containing information about initial and final vertices of arc and about a length of arc. The row number equals the number of the corresponding arc. Contour c is described by a column vector containing numbers of its vertices. The first and last elements of vector must coincide.

Procedure $MatrixForm(M)$ forms whole matrix A . It is the main procedure.

4.2. The auxiliary procedures

Procedure $Edges(M)$ issues the list of arcs (edges) for the adjacency matrix M of the graph. It contains three columns. The first two columns contain initial and final vertices of arcs; the third column contains the lengths of the arcs. Issued list fixes numbering of graph arcs.

Procedure $Who(Edg, i, j)$ issues the number of the arc from vertex i to vertex j with respect to list $Edgr$.

Procedure $Cont(v, M)$ determines whether there is a vector v among columns of matrix M : 1, if there is.

Procedure $WithoutZ(v)$ copies elements of vector v starting from the first element and finishing copying when the first element will be copied repeatedly. The procedure is applied to rejection unnecessary elements when the matrix A is formed.

5. The Numerical Example

In our numerical example number of subject's s is equal to 8. Adjacency matrix M contains mutual payments: $M_{i,j}$ means a value of payment from i -th subject to j -th subject. In our case the numerical values are presented in Table 1 (see Figure 1, too).

The table shows that the total number of payments (transactions) equals to 26. Therefore the corresponding graph contains 26 arcs and 8 vertices. The list of arcs and arc characteristics (numbers of initial and final vertices and arc lengths) are presented in Table 2.

Table 1. Values of payments

	$i=1$	$i=2$	$i=3$	$i=4$	$i=5$	$i=6$	$i=7$	$i=8$
$j=1$	0	1	0	3	0	4	5	0
$j=2$	0	0	7	1	0	0	3	0
$j=3$	4	0	0	4	4	1	0	10
$j=4$	0	0	0	0	4	0	0	2
$j=5$	3	2	0	0	0	8	0	0
$j=6$	0	4	0	1	0	0	2	2
$j=7$	0	0	4	2	4	0	0	7
$j=8$	7	0	0	0	0	0	0	0

Table 2. Arcs of the graph, and theirs lengths

N	1	2	3	4	5	6	7	8	9	10	11	12	13
i	1	1	1	1	2	2	2	3	3	3	3	3	4
j	2	4	6	7	3	4	7	1	4	5	6	8	5
d	1	3	4	5	7	1	3	4	4	4	1	10	4

N	14	15	16	17	18	19	20	21	22	23	24	25	26
i	4	5	5	5	6	6	6	6	7	7	7	7	8
j	8	1	2	6	2	4	7	8	3	4	5	8	1
d	2	3	2	8	4	1	2	2	4	2	4	7	7

The first our task is the formation of simple contours that allow madding mutual payments. The maxi-min paths trees for some vertices are presented in Table 3 and Figure 2 (see Section 3.1).

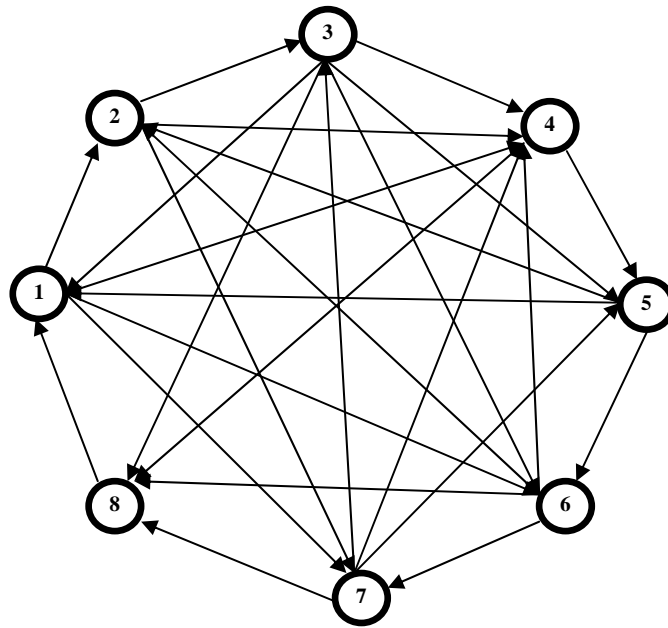


Figure 1. The graph corresponding to Table 1

Table 3. The maxi-min paths trees

$$\begin{aligned}
 Tree(1) &= \begin{pmatrix} 1 & \times \\ 6 & 4 \\ 2 & 4 \\ 3 & 4 \\ 3 & 4 \\ 1 & 4 \\ 1 & 5 \\ 7 & 5 \end{pmatrix}, &
 Tree(2) &= \begin{pmatrix} 8 & 7 \\ 2 & \times \\ 2 & 7 \\ 3 & 4 \\ 3 & 4 \\ 1 & 4 \\ 1 & 5 \\ 3 & 7 \end{pmatrix}, &
 Tree(4) &= \begin{pmatrix} 3 & 4 \\ 6 & 4 \\ 2 & 4 \\ 4 & \times \\ 4 & 4 \\ 5 & 4 \\ 1 & 4 \\ 3 & 4 \end{pmatrix}, &
 Tree(6) &= \begin{pmatrix} 3 & 4 \\ 6 & 4 \\ 2 & 4 \\ 3 & 4 \\ 3 & 4 \\ 6 & \times \\ 1 & 4 \\ 3 & 4 \end{pmatrix}.
 \end{aligned}$$

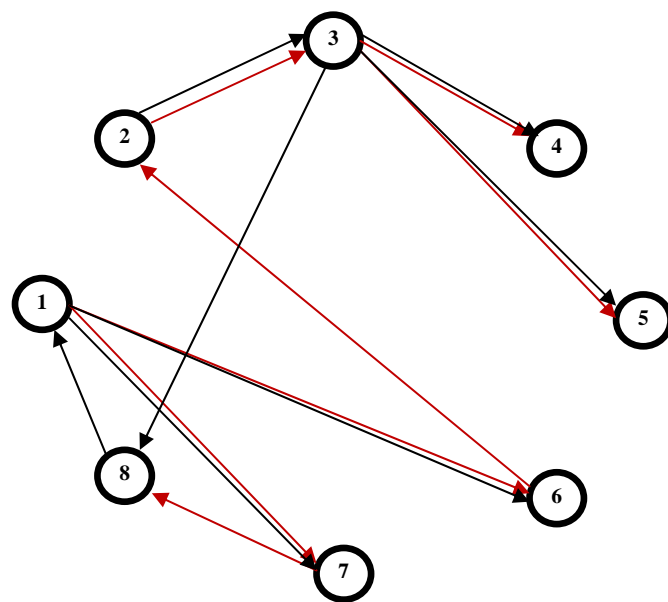


Figure 2. The maxi-min paths trees corresponding to vertex 1 and vertex 2

The maxi-min contours are constructed on the basis of maxi-min paths trees. The list of contours is presented in Table 4 (see Figure 3, too). Each represented matrix corresponds to certain initial vertex specified in the name of the matrix. Each column corresponds to certain contour in which specified vertex is repeated twice. Weight (length) of contour is specified after the second indication of the initial vertex. The zeros should be ignored.

Table 4. The maxi-min contours

$$\begin{aligned}
 MMC(1) &= \begin{pmatrix} 1 & 1 & 1 \\ 6 & 6 & 7 \\ 2 & 2 & 8 \\ 3 & 3 & 1 \\ 1 & 5 & 5 \\ 4 & 1 & 0 \\ 0 & 3 & 0 \end{pmatrix}, &
 MMC(2) &= \begin{pmatrix} 2 & 2 & 2 \\ 3 & 3 & 3 \\ 8 & 5 & 8 \\ 1 & 2 & 1 \\ 2 & 2 & 6 \\ 1 & 0 & 2 \\ 0 & 0 & 4 \end{pmatrix}, &
 MMC(3) &= \begin{pmatrix} 3 & 3 \\ 8 & 8 \\ 1 & 1 \\ 6 & 7 \\ 2 & 3 \\ 3 & 4 \\ 4 & 0 \end{pmatrix}, \\
 \\
 MMC(4) &= \begin{pmatrix} 4 & 4 & 4 & 4 & 4 \\ 5 & 5 & 5 & 5 & 5 \\ 6 & 6 & 6 & 6 & 6 \\ 2 & 2 & 2 & 4 & 2 \\ 3 & 4 & 3 & 1 & 3 \\ 1 & 1 & 4 & 0 & 1 \\ 4 & 0 & 4 & 0 & 7 \\ 3 & 0 & 0 & 0 & 4 \\ 0 & 0 & 0 & 0 & 2 \end{pmatrix}, &
 MMC(5) &= \begin{pmatrix} 5 & 5 & 5 \\ 6 & 6 & 6 \\ 2 & 2 & 2 \\ 3 & 3 & 3 \\ 5 & 4 & 1 \\ 4 & 5 & 7 \\ 0 & 4 & 5 \\ 0 & 0 & 4 \end{pmatrix}, &
 MMC(6) &= \begin{pmatrix} 6 & 6 & 6 \\ 2 & 2 & 2 \\ 3 & 3 & 3 \\ 1 & 6 & 5 \\ 6 & 1 & 6 \\ 4 & 0 & 4 \end{pmatrix}, \\
 \\
 MMC(7) &= \begin{pmatrix} 7 & 7 & 7 \\ 8 & 8 & 8 \\ 1 & 1 & 1 \\ 7 & 6 & 6 \\ 5 & 2 & 7 \\ 0 & 7 & 2 \\ 0 & 3 & 0 \end{pmatrix}, &
 MMC(8) &= \begin{pmatrix} 8 & 8 & 8 & 8 \\ 1 & 1 & 1 & 1 \\ 6 & 6 & 6 & 7 \\ 2 & 2 & 8 & 8 \\ 3 & 3 & 2 & 5 \\ 8 & 4 & 0 & 0 \\ 4 & 8 & 0 & 0 \\ 0 & 2 & 0 & 0 \end{pmatrix}.
 \end{aligned}$$

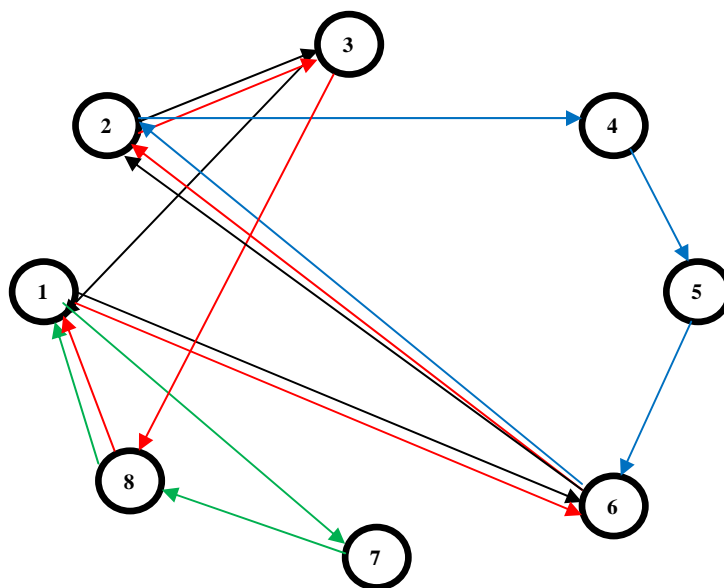


Figure 3. Examples of the maxi-min contours

The set of all represented contours is replenished according to the algorithm of Section 3.2. As a result the set of contours is formed from which the optimal contours are selected. In our case the number of such contours equals 19.

Further we need to construct the incidence matrix A from formula (3). This matrix has $n = 26$ rows (it is equal to number of arcs) and $k = 19$ columns (it is equal to number of considered different contours). The matrix is presented in Table 5. Value 1 means that a considered arc (the number of which corresponds to Table 2) is included in the contour indicated in column. Value 0 means the contrary case.

Table 5. The incidence matrix “arcs-contours” A

	1	2	3	4	5	6	7	8	9	10	11	12	13	14	15	16	17	18	19
1	0	0	0	1	0	0	0	0	0	0	0	0	0	0	0	0	0	0	0
2	0	0	0	0	0	0	0	1	0	0	0	0	0	0	0	0	0	0	0
3	1	1	0	0	0	1	0	0	0	0	0	0	0	0	0	1	1	1	1
4	0	0	1	0	0	0	1	0	0	0	0	1	0	1	0	0	0	0	0
5	1	1	0	1	1	1	0	1	0	1	0	1	1	1	1	0	0	1	0
6	0	0	0	0	0	0	0	0	1	0	0	0	0	0	0	0	0	0	0
7	0	0	0	0	0	0	0	0	0	0	0	0	0	0	0	1	0	0	0
8	1	0	0	0	0	0	0	1	0	0	0	1	0	1	0	0	0	0	0
9	0	0	0	0	0	0	0	0	0	1	0	0	0	0	0	0	0	1	0
10	0	1	0	0	1	0	0	0	0	0	0	0	1	0	0	0	0	0	0
11	0	0	0	0	0	0	0	0	0	0	0	0	0	0	1	0	0	0	0
12	0	0	0	1	0	1	1	0	0	0	0	0	0	0	0	0	0	0	0
13	0	0	0	0	0	0	0	1	1	1	1	1	0	0	0	0	0	0	0
14	0	0	0	1	0	0	0	0	0	0	0	0	0	0	0	0	0	1	0
15	0	1	0	0	0	0	0	0	0	0	0	0	0	0	0	0	0	0	0
16	0	0	0	0	1	0	0	0	0	0	0	0	0	0	0	0	0	0	0
17	0	0	0	0	0	0	0	1	1	1	1	1	1	1	0	0	0	0	0
18	1	1	0	0	0	1	0	1	1	1	0	1	1	1	1	1	0	1	0
19	0	0	0	0	0	0	0	0	0	0	1	0	0	0	0	0	0	0	0
20	0	0	0	0	0	0	0	0	0	0	0	0	0	0	0	0	1	0	0
21	0	0	0	0	0	0	0	0	0	0	0	0	0	0	0	0	0	0	1
22	0	0	0	0	0	0	1	0	0	0	0	0	0	0	0	0	0	0	0
23	0	0	0	0	0	0	0	0	0	0	0	1	0	0	0	0	0	0	0
24	0	0	0	0	0	0	0	0	0	0	0	0	0	1	0	0	0	0	0
25	0	0	1	0	0	0	0	0	0	0	0	0	0	0	0	1	1	0	0
26	0	0	1	1	0	1	1	0	0	0	0	0	0	0	0	1	1	1	1

Let us consider other components of linear programming problem (3). 26-dimensional vector of free coefficients consists of the lengths of the arcs. These lengths are presented in the last line of the Table 2. 19-dimensional vector of objective function coefficients v equal to the sum of all rows of matrix M , namely, $v = (4 \ 5 \ 3 \ 4 \ 3 \ 5 \ 4 \ 6 \ 4 \ 5 \ 3 \ 6 \ 6 \ 5 \ 3 \ 5 \ 4 \ 6 \ 3)^T$.

So, all the input data of linear programming problem have been defined. A solution can be found by using any linear programming package. The corresponding solution is presented in Table 6. Used (basic) column (contour) numbers, numbers of the arcs and corresponding amounts of settlements (transactions) are shown in Table 6. The maximal amount of all transactions turned out to be 64.

Table 6. The optimal solution

Contour j	3	4	5	7	8	11	13	14	17	19
Number of arcs	3	4	3	4	6	3	6	5	4	2
Transaction, x_j	0	1	2	4	3	1	0	1	2	2

References

1. Christofides, N. (1975). *Graph Theory. An Algorithmic Approach*. New York-London-San-Francisco: Academic Press. 432 p.
2. Ore, O. (1962). *Theory of Graphs*. Providence: American Mathematical Society. 352 p.
3. Swamy, M. N. S., Thulasiraman, K. (1981). *Graphs, Networks, and Algorithms*. New York: John Wiley & Sons.
4. Andronovs, A. *Transporta sistēmu optimizācijas metodes. 1. daļa. Lineārā programmēšana*. Rīga: Rīgas Tehniskā Universitāte. 72 p.
5. Murtagh, B. P. (1981). *Advanced Linear Programming: Computation and Practice*. New York: McGraw-Hill. 224 p.

Received on the 1st of April 2013

A RESEARCH ON TRANSPORT PLANNING STRATEGIC ENVIRONMENTAL ASSESSMENT (SEA): INCORPORATING SYSTEM DYNAMICS INTO THE ENVIRONMENTAL CARRYING CAPACITY

Y. Chai^a, X. Meng^{a}, Sh. Ma^b, L. Xu^{b*}, Ya. Li^a, Lu Shen^a, Ch. Jiang^a*

^a*Chinese Research Academy of Environmental Science, Beijing 100012, P. R. China*

^b*Key Laboratory of Industrial Ecology and Environmental Engineering (MOE), School of Environmental Science and Technology, Dalian University of Technology, Dalian, Liaoning 116024, P. R. China*

** Corresponding authors: Xiaojie Meng*

E-mail: mengxj@craes.org.cn; Ling Xu. E-mail: xuling@dlut.edu.cn

Transport construction plays an important role in promoting prosperity in the development process of a city. However, the environmental impacts it bring shouldn't be ignored. It is necessary to adopt strategic environmental assessment (SEA) before the transport planning is carried out. Environmental carrying capacity (ECC) is often used as a measuring tool in SEA to see whether a region is suitable to exploit. However, this static snapshot of ECC accounting fails to present the dynamic, multi-levelled relationship among the driving forces. In order to refine the SEA theory and conduct the transport planning in Dalian, China, this paper attempts to incorporate system dynamic (SD) into ECC to develop a SD-ECC forecasting framework, and provide a platform to support policy making for urban transport planning.

Keywords: transport planning, strategic environmental assessment, system dynamic, environmental carrying capacity, scenario analysis

1. Introduction

As an important driving force of regional economic growth, Transport construction has always been government's priority. However, transport industry is a high energy-consumption industry. In 2004, transport energy-consumption accounted for 26% of world's energy use. In Canada, energy-consumption of transport system accounts for 66% of total social energy consumption, and most consumed by automobiles. While the energy-consumption of transport system accounts for 60% in the United States, 73% consumed by automobile [1]. In developing countries, energy use is increasing faster than that in the developed nations, and is projected to grow from 31% in 2002 to 43% of global transport energy use by 2025 [2].

Contaminations emitted by traffic system are the main source of atmospheric pollution. The atmospheric pollutants include carbon monoxide (CO), nitrogen oxides (NO_x), hydrocarbons (C_xH_y), sulfur dioxide(SO₂) and other harmful substances (such as lead, volatile organic compounds (VOC), fluorine chlorinated hydrocarbons, etc.). CO and NO_x from vehicle emission account for 80% and 60% of total atmospheric pollutant emission respectively in Europe [1]. Besides, so many cases of photochemical smoke and acid rain are also relevant to the traffic pollution.

In addition, land occupation due to transport construction is supposed to have a bad effect on ecological environment, not only on environmental factors, such as soil, water, gas, heat, but also on the survival rate of vegetation, animal deaths, distribution pattern and migration of wild animals [3].

Based on problems above, it is imperative to implement transport planning strategic environmental assessment (SEA) before the transport construction. It was not until the 90s in last century when SEA was introduced to transport planning in European countries. In May 2001, a synthesis of the cases and an analysis of the data proceeded in a workshop held in Finland. The aim of the workshop was to gain an overview of environmental assessments in the transport sector of the UN/ECE as well as to identify the factors influencing the effectiveness of SEA [4]. Viewing from SEA practice of transport planning in Europe and USA, SEA techniques mostly focus on scenario analysis, GIS analysis and model simulation. The United States also put emphasis on benefits-cost analysis. Currently, model simulation technology has become the research focus all around the world. The main purpose is to develop the traffic prediction models, atmospheric pollutants and noise prediction models [5].

European research and practice had great inspiration on Chinese SEA study in urban transport planning with technical route, intervention time, evaluation content and methods. In 2002, Yang Jin [6] first introduced SEA into urban transport planning and had a research on working procedures, element and indicator selection. In the following years, Meng Qingtang et al. [7] evaluated four alternatives in urban transport planning based on status of urban development. Song Guohua and Yu Lei [8] put forward integrated urban transport planning environmental impact assessment method based on the analysis of traffic exhaust emissions, theoretical model of traffic noise. These studies provide insights for SEA. However, most of them rely on theoretical abstraction and qualitative analysis without paying more attention on the complex quantitative relationship among the impact factors.

Environmental impact of transportation has close relationship with social economy, population resource and policy. It is an unbreakable organic unity with elements, which has complex causal relationship and hard to analysis quantitatively. SD model was designed to simulate complex system with an interactive web of feedback loops and nonlinear relationships. Thus, it has an incomparable advantage in this field. ECC analysis is used to evaluate the carrying capacity of basic element, such as resource and environment, for development activities. There are researches using these two methods separately in transport planning SEA. Such as Chen Chong et al.'s [9] "Application research on transport planning impact prediction", Ji Han and Yoshitsugu Hayashi's [10] "A system dynamics model of CO₂ mitigation in China's inter-city passenger transport", Upham Paul et al.'s [11] "Environmental capacity and European air transport: stakeholder opinion and implications for modeling", Yang Rihui's [12] "Transport strategic environmental assessment for urban sustainable development".

However, it can't describe regional carrying capacity by using SD method merely. Meanwhile, the complex relationship can't be regarded if SD is not adopted. Based on the above problems, this work attempts to generate a methodological synthesis of SD and ECC (Namely, SD-ECC), and provides an integrated framework of sustainability policy-making. Then, scenario analysis is adopted to formulate the best policy portfolio for transport planning.

2. System Dynamics Model

2.1. Modelling

The SD model in this work takes Dalian's transport planning as a case. Dalian transport planning regulation system is a complex integrated organic system whose elements involve all aspects of economic life. These elements are close with each other, interact each other, restrain each other. This traffic planning SD model takes the environmental impacts as a key point, and mainly considers about the following four aspects: people's demand for traffic facilities and their impetus for economic growth; the economic and environmental impacts by land use; the transportation development demand for energy. Based on the above considerations, overall research framework is design (Fig. 1).

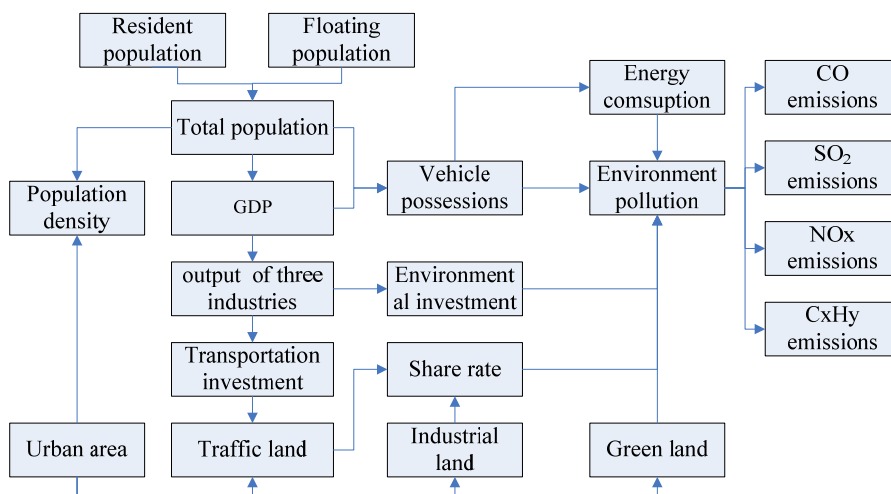


Figure 1. Overall research framework of transport planning SEA

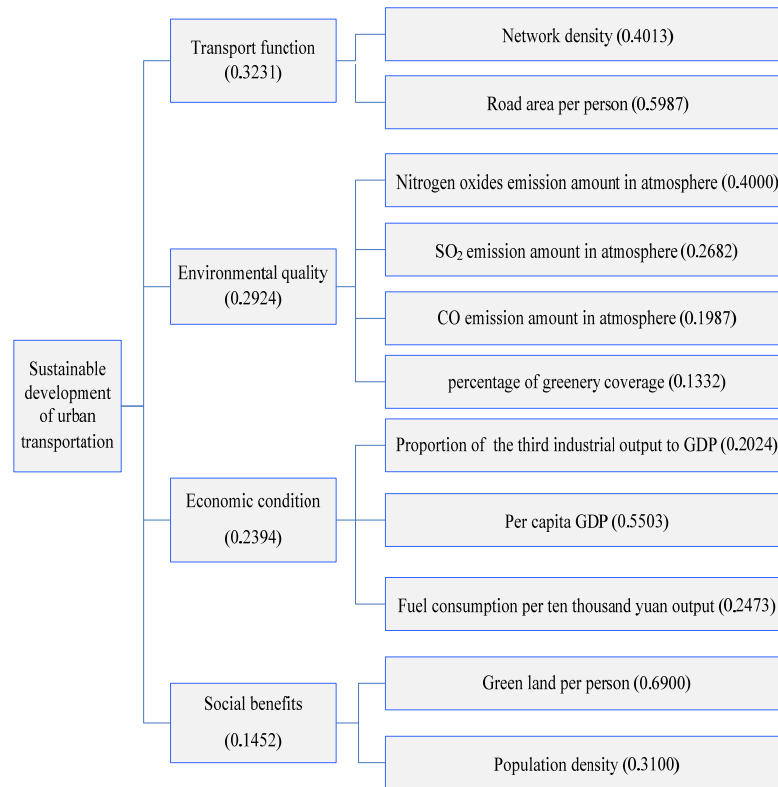
2.2. Scenario design

This model mainly analyses the impacts on traffic system, social economy and environmental quality under different policies. The related parameters change in view of different policy orientations. The scenarios are shown in Table 1.

Table 1. Details on scenarios design

Scenarios	Description
Scenario 0	No action plan. Namely, plan isn't carried out. The aim of this scenario is to illustrate possible tendency if no further road construction is implemented
Scenario 1	High traffic network growth plan. This scenario puts high emphasis on network construction in order to avoid road jam while the environment refinement is neglected
Scenario 2	Planning scenario. This scenario is designed according to Dalian development planning. It expects refinement of traffic jam as well as environment protection, but less emphasis is put on environment
Scenario 3	High population growth scenario. This scenario maintains high population growth rate through mechanical growth rate regulation. The aim is to predict the tendency under population boom and to show how important it is to control population growth in China
Scenario 4	High economy growth scenario. This scenario maintains high GDP growth by setting high growth rate of each industry, especially the second industry. Economy growth mainly depends on high consumption heavy industry
Scenario 5	Environment protection scenario. This scenario expects maximum realization of environmental targets by increasing investment on environment, setting stricter laws and regulations on environment and energy conservation
Scenario 6	Integrated scenario. The target of this scenario is to realize fine transport function and high-quality environment, that is, to achieve a win-win situation. Besides, the scenario tries best to achieve coordinate development among social economy, transportation and environment

According to analysis of designed scenarios, indicator values setting are as Figure 2.



GRR: Growth rate of railway; GIF: Growth rate of the first industry;
 GRE: Growth rate of express road; GIS: Growth rate of the second industry;
 GRA: Growth rate of arterial road; GIT: Growth rate of the third industry;
 GRS: Growth rate of subsidiary road; EIC: Environmental investment coefficient;
 GRB: Growth rate of branch road; MGRP: Mechanical growth rate of population.

Figure 2. Parameter setting of each scenario

2.3. Data

Annual data on transport and model parameters are taken from the following items: 1) Dalian Statistical Yearbook [13]. 2) Dalian Development Planning (2003–2020) [14]. 3) Dalian Overall Planning [15]. 4) Dalian Statistical information web. The time frame spans from 2003 to 2020 with 2003 to 2008 used as validation year, and with time step of one year in simulation.

2.4. Model verification

Before running the simulation, historical behaviour-matching test are conducted to ensure the model validity. It compares the simulated values with the historic ones after the model is established. This work chooses population, GDP per people and vehicle possessions capacity as validating values. It turns out these three variables have errors under 5%, which indicates that the model established in this paper is reasonable.

2.5. Simulation

The purpose of this model is to investigate the impact on society, economy and environment with different policy orientations. Based on this target, seven designed scenarios are simulated. The simulated results of main driving forces are used in ECC calculation in Section 3.

3. Environmental Carrying Capacity (ECC)

3.1. Indicator system

Evaluation indicator system of SEA for urban transport planning should be established before ECC is calculated [17–19]. The hierarchy consists of goal level, criteria level and alternatives level with 11 indicators. Analysis Hierarchy Process (AHP) is used for weight determination [20]. The overall inconsistency ratio (RI) for the entire analysis (0.0132) is well within the acceptable rang (< 0.1), indicating consistent judgments by the participants. Indicators and their weights are shown on Figure 3.

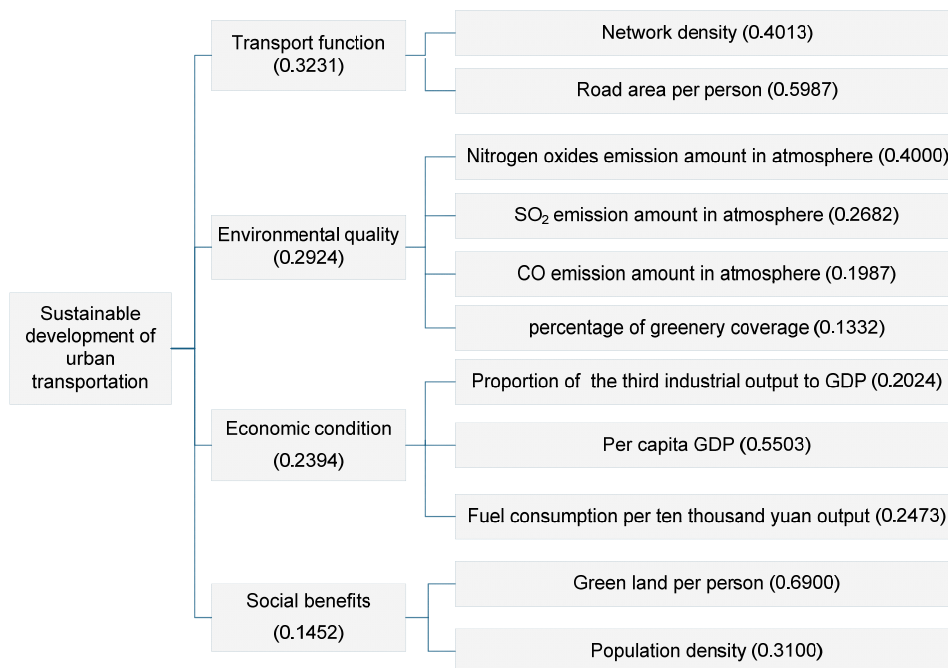


Figure 3. Evaluation indicator system and weights in urban transport planning

3.2. Calculation

Then, ECC is calculated using fuzzy evaluation method referring to ECC quantitative research literature [21]. Simulated values in Section 2 are adopted in the following equations to compute Environmental Carrying Capacity Indicators (ECCI).

1) “Benefit” or “Cost” indicator

“Benefit” Indicators refer to those are the bigger the better indicators, such as network density, area of total road per capita, percentage of greenery coverage, proportion of the third industrial output to GDP, GDP per capita and green land per capita. “Cost” indicators refer to those are the smaller the better indicators, such as population density, fuel consumption per ten thousand yuan output. These two kinds of indicators are suitable for different equations, which are shown below.

Equation for “Benefit” indicators

$$C_i = \begin{cases} 1 & (P_i \geq P_{i\max}) \\ \frac{P_i - P_{i\min}}{P_{i\max} - P_{i\min}} & (P_{i\min} < P_i < P_{i\max}) \\ 0 & (P_i \leq P_{i\min}) \end{cases} \quad (1)$$

Where subscript i denotes a certain indicator; C_i is ECCI of i ; P_i is simulated value of i from SD model; $P_{i\max}$ is maximum standard value of i ; $P_{i\min}$ is minimum standard value of i .

Equation for “Cost” indicators:

$$C_i = \begin{cases} 1 & (P_i \leq P_{i\min}) \\ \frac{P_{i\max} - P_i}{P_{i\max} - P_{i\min}} & (P_{i\min} < P_i < P_{i\max}) \\ 0 & (P_i \geq P_{i\max}) \end{cases} \quad (2)$$

The letters in Eq. (2) mean the same as in Eq. (1).

2) Indicators using “surplus carrying rate”

NO_x emission amount in atmosphere, SO_2 emission amount in atmosphere, CO emission amount in atmosphere are such kind of indicators. When pollutants emission exceeds environmental capacity, the ECCI is 0; the ECCI is 1 when no pollutant emits into the atmosphere.

$$C_i = \begin{cases} 0, (R_i \geq S_i) \\ 1 - \frac{R_i}{S_i}, (0 < R_i < S_i) \\ 1, (R_i = 0) \end{cases} \quad (3)$$

Where subscript i denotes a certain indicator; C_i is ECCI of i ; R_i is simulated value of i in SD model; S_i is standard value of i .

Table 2. List of ECCI for each alternative scenario

Scenarios	Years	ECCI of transport function	ECCI of environment quality	ECCI of economic condition	ECCI of social benefits	Regional integrated ECCI
Scenario 0	2010	0.313778	0.700068	0.323555	0.243896	0.418954
	2015	0.295439	0.743644	0.467973	0.261288	0.46287
	2020	0.277909	0.819366	0.638906	0.301919	0.526168
Scenario 1	2010	0.408282	0.680751	0.345809	0.218094	0.445421
	2015	0.45161	0.717983	0.498904	0.209649	0.505732
	2020	0.487342	0.781894	0.684872	0.204155	0.579688
Scenario 2	2010	0.395837	0.707756	0.414198	0.23726	0.468452
	2015	0.431907	0.739217	0.673502	0.248365	0.552995
	2020	0.465547	0.801346	0.848649	0.281132	0.628719
Scenario 3	2010	0.377014	0.662091	0.370581	0.192857	0.432129
	2015	0.398899	0.696036	0.523402	0.523402	0.505529
	2020	0.41806	0.779818	0.657711	0.152086	0.542633
Scenario 4	2010	0.395837	0.681505	0.410021	0.228589	0.458517
	2015	0.431907	0.705487	0.608812	0.231764	0.525235
	2020	0.465547	0.767637	0.742517	0.254874	0.589641
Scenario 5	2010	0.359127	0.757672	0.387106	0.247113	0.466131
	2015	0.371117	0.813269	0.563612	0.274669	0.532518
	2020	0.3823	0.870272	0.753746	0.320011	0.604901
Scenario 6	2010	0.397582	0.741285	0.454102	0.243808	0.489323
	2015	0.430993	0.779406	0.733835	0.261379	0.580785
	2020	0.462207	0.844106	0.973431	0.301172	0.672925

Eq. (4) is used to calculate ECCI of each level and integrate ECCI. Results are listed in Table 2.

$$ECCI = \sum_{i=1}^n \sum_{j=1}^m C_{i,j} \cdot W_{i,j} \cdot W_i \quad (4)$$

where subscripts i and j denote an indicator level and a certain indicator of i level; n and m denote a number of indicator levels and a number of indicators; $C_{i,j}$ is ECCI of j ; $W_{i,j}$ is the weight of j ; W_i is the weight of i .

4. Results

ECCI, whose numerical interval is [0, 1], is divided into four ranks to indicate the degree of environmental carrying saturation, as is shown in Table 3.

Table 3. ECCI classify standard [21]

Level	I	II	III	IV
Range	(0.8,1]	(0.6,0.8]	(0.2,0.6]	[0,0.2]
Condition	unsaturated	sub-saturated	saturated	over-saturated

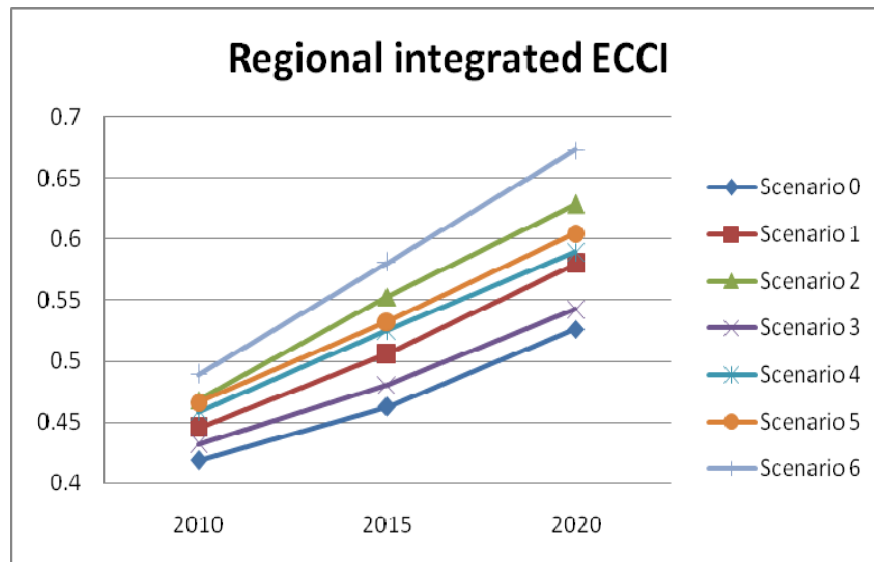


Figure 4. ECCI tendency of each scenario

Figure 4 presents the projected trends of ECCI of each scenario. It shows that most ECCI of all scenarios are between 0.4 to 0.6. According to classify standard in Table 3, ECC is saturated with balanceable development intensity. The whole system is in the weak carrying state. However, ECCI of each scenario are rising gradually in 2010, 2015, 2020. According to Figure 4, quality order of alternative scenario is as follows:

Scenario 6 > Scenario 2 > Scenario 5 > Scenario 4 > Scenario 1 > Scenario 3 > Scenario 0 subsequently.

This paper compares different scenarios in the same criteria level to see the different results under various policies.

Scenario 0 has the worst ECC. Smaller network density and road area per capita lead to worse transport function (Fig. 5 (a)). Low traffic capacity slows down the growth of economy, which directly affects on GDP per capita (Fig. 5 (c)). Then, vehicle possessions will lessen due to smaller purchasing power. In this point of view, pollutants from traffic will reduce. On the other hand, if transport land shrinks, land for industry is likely to expand. Then, the contaminants from industry increase. It turns out that the quality of environment can't improve that much (Fig. 5 (b)).

Scenario 1 has the best traffic function due to road development policy (Fig. 5 (a)). Elegant transport system makes freightage and passenger transport more convenient, which contributes to GDP growth. On the other hand, increasing the investment to road construction slows down the pace of GDP growth (see Fig. 5 (c)). In environmental aspect, transportation development can lead to air pollution

as well as land occupancy, which has a bad impact on ecological system (Fig. 5 (b)). Besides, Social benefits may be affected for the decline of green land (Fig. 5 (d)).

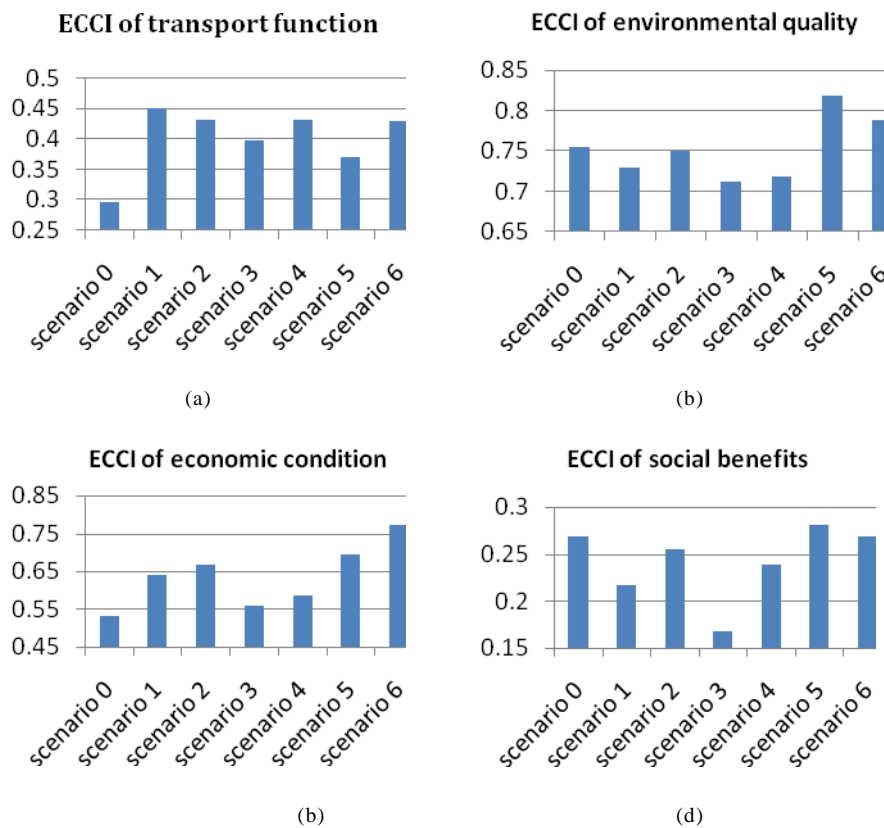


Figure 5. ECCI of criteria levels of each scenario in 2015

Scenario 2 is the planning scenario. It takes both the traffic function and the environmental quality into consideration, but more emphasis on traffic function while less on environment (Fig. 5 (a), (b)). Environmental quality is improving yet not so fast.

Scenario 3 has the largest population due to loose population control policy. As GDP creators, population can stimulate economic growth. However, driving factors concerning per capita is getting worse (Fig. 5 (a), (c), (d)). Larger population tends to let out more pollutants, making the environment even worse (Fig. 5 (b)). Thus, it can be seen that population control policy, as a basic national policy in China, is a necessity considering the current situation in China.

Scenario 4 is seeking high economic growth through promoting the second industry. GDP grows fastest of all seven scenarios. However, relying on exaggerate the proportion of the second industrial output to GDP to accelerate economic growth is unsustainable. So the ECCI of economy presents a low value (Fig. 5 (c)). The second industry boom is bound to bring environmental deterioration. In additional, growing number of vehicles possessing capacity due to increased purchasing power makes the pollution even worse (Fig. 5 (b)), at the same time, contributes to traffic jam (Fig. 5 (a)).

Scenario 5 tends to protect the environment at full stretch. It promotes the environmental improvement by exaggerating environmental investment, exploiting renewable and clean energy and making regulations to encourage green trip mode. Scenario 5 has the best environmental quality (Fig.5 (d)). However, exaggerating environmental investment hinders the rapid growth of economy (Fig. 5 (c)).

Scenario 6 integrates planning scenario. Proper road construction leads to fine transportation (Fig. 5 (a)), while reasonable population control policy achieves high living standard (Fig. 5 (d)). Economic growth is conducted by enlarging the proportion of the third industry to avoid environmental problem brought by high-speed growth of the second industry. As a result, economy grows fast while resource consumption declines. In additional, this scenario increases investment in environment protection to develop energy conservation and emission reduction technology for vehicle.

Due to the measures above, ECC of environmental quality improves a lot. Regional ECCI is becoming bigger and bigger and will soar to 0.63758 by the year 2020 (Fig. 5 and Table 2). ECCI will reach to sub-saturated state in terms of Table 3. The system is bearable with proper develop intensity. Accordingly, scenario 6 is the best scenario.

5. Conclusions

Transport planning SEA, which has inevitable impact on environment and human beings should be conducted based on the comprehensive understanding of the concept and methodology of SEA. In this study, a SD-ECC model is developed to provide a platform to support policy-making towards Dalian city's transport planning after comprehending these terms deeply. Through a series of simulations and calculations, ECCI for all the scenarios are presented in the chart, implying that integrate scenario can provide guidance for reasonable policy-making in Dalian city's transport planning.

Acknowledgement

Financial supports from the National Natural Science Foundation of China (NSFC) (Grant No. 40801228) are highly appreciated.

References

1. Wang, W., Xiang, Q.J., Chang, Y.L., Li, T.Z., Li, X.G. (2010). *Energy Consumption and Environmental Impact Analysis Method of Urban Transportation System*. Beijing: Science Publisher. (In Chinese).
2. Jin, W., Xu, L., & Yang, Z. (2008). Modeling a policy making framework for urban sustainability: Incorporating system dynamics into the Ecological Footprint. *Ecological Economics*, 68(12), 2938–2949.
3. Yin, Z., Li, Y., Gu, Z., Zhao, F., Zhao, T. & Zhou, X. (2006). Ecological environmental impact of road construction and ecological road constructon. *Reserch on Water and soil conservation*, 4, 161–164.
4. Hilden, M., Eeva, F., Minna, K. (2004). Views on planning and expectations of SEA: the case of transport planning. *Environmental Impact Assessment Review*, 24, 519–536.
5. Li, Q. R., Qian, X. & Lu, Y. (2009). Review on strategic enironment assessment researches of transport planning. *Transport science in Hunan*, 1, 145–148.
6. Yang, J. (2002). Transport strategic environment assessment for urban sustainable development. *Environmental protection in transportation*, 5, 40–42.
7. Meng, Q. T., Ju, M. T., Li, H. Y. (2004). Alternatives analysis in urban transport planning environmental impact assessment. *Transport environmental protection*, 3, 21–23. (In Chinese).
8. Song, G., & Yu, L. (2007). Methodology and application of strategic environmental assessment for urban transport planning. *Safety and environment engineering*, 3, 6–10.
9. Chen, C., Shao, L. G., Xu, L., Ji, S. C. (2006). Application research on transport planning impact prediction. In *National intercommunication on methodology and management of planning environmental impact assessment*. Suzhou. (In Chinese).
10. Ji, H., Yoshitsugu, H. (2008). A system dynamics model of CO2 mitigation in China's inter-city passenger transport. *Transportation Research Part D*, 13, 298–305.
11. Upham, P., Raper, D., Thomas, C., McLellan, M., Lever, M. & Lieuwen, A. (2004). Environmental capacity and European air transport: stakeholder opinion and implications for modelling. *Journal of Air Transport Management*, 10(3), 199–205.
12. Yang, R. (2006). Environment impact assessment of road construction based on Environmental carrying capacity. Changsha University of Science and Technology.
13. Dalian Bureau of Statistics. (2003). *Dalian Statistical Yearbook*. Dalian: National Statistical Publisher. (In Chinese)
14. Dalian City Planning and Design Institute, Dalian City Planning Bureau of Land and Resources. (2004). *City development planning of Dalian (2003–2020)*. Dalian. (In Chinese)
15. Dalian City Planning Bureau. (2000). *Dalian Overall Planning*. Dalian. (In Chinese)
16. Donnelly, A., et al. (2007). Selecting environmental indicator for use in strategic environmental assessment. *Environmental Impact Assessment Review*, 27(2), 161–175.

17. Zhao, W. (2007). *Research on atmosphere carrying capacity of urban transport*. Southwest Communication University.
18. Jiang, H. (2008). Research on strategic environment assessment and application based on environmental carrying capacity. Hunan University. (In Chinese).
19. Alison, D., Mike, J., Tadhg, O., Gerry, B. (2007). Selecting environmental indicator for use in strategic environmental assessment. *Environmental Impact Assessment Review*, 27(2), 161–175.
20. Leung, P., Muraoka, J., Nakamoto, S.T. & Pooley, S. (1998). Evaluating fisheries management options in Hawaii using analytic hierarchy process (AHP). *Fisheries Research*, 36(2–3), 171–183.
21. Xu, Q.B. (2009). *Application research on Environment carrying capacity in strategic environment assessment*. Huazhong Agriculture University. (In Chinese)

Received on 20th of May 2013

A NOVEL ONLINE ASSESSMENT SCHEME FOR POWER SYSTEM SECURITY LEVEL OF TRANSIENT STABILITY BASED ON RELATIONSHIPS EXPLORATION IN A LARGE DATA SET

F. Qian², S. Liu¹, W. Yang², H. Wei², Yo. Fan¹

¹ *School of Electrical Engineering, Wuhan University, Wuhan 430072, China*

² *Electric power dispatching control center, Guangdong Power Grid, China Southern Power Grid, Guangzhou 510000, China*

E-mail: 2011202070013@whu.edu.cn. E-mail: 1612234945@qq.com

In this paper, a scheme based on data mining and relationships exploration is presented for security level assessment of transient stability. The proposed scheme can select the optimal variables as input features by detecting the relationship between critical clearing time (CCT) and each variable in a large power flow data set. The data set is created based on a series of power flow simulation and fault simulation in the software PSS/E. The relationships exploration statistical tool used is based on the maximal information coefficient (MIC) and the Pearson product-moment correlation coefficient (PPMCC). The variables selected are corresponding to the relationships highly ranked by MIC and PPMCC, including linear relationships and especially nonlinear ones. These relationships are also shown in the paper and some of them are explained from the perspective of power system operation. If the measured values of these variables are obtained in real-time from wide area measurement system (WAMS), the CCT can be estimated in real time since its relationships with these variables are explored. Then the security level of transient stability can be assessed for a new operation state. The scheme is tested on a 21-bus system provided by PSS/E and various test results indicate the scheme is accurate and effective, as well as the way to select input features is more intelligent than the current techniques.

Keywords: Maximal information coefficient (MIC), Pearson product-moment correlation coefficient (PPMCC), relationships exploration, large data sets, security assessment, transient stability, critical clearing time (CCT).

NOMENCLATURE

PG _i	Active power of generators at bus
QG _i	Reactive power of generators at bus
V _i	Voltage amplitude of bus
θ _i	Voltage phase angle of bus
P _{ij}	Active power from bus to bus
Q _{ij}	Reactive power from bus to bus
S _{ij}	Apparent power from bus to bus
Pi_LOAD_PQ/I/Y	Active power from bus to constant power, current, or impedance load
Qi_LOAD_PQ/I/Y	Reactive power from bus to constant power, current, or impedance load
Si_LOAD_PQ/I/Y	Apparent power from bus to constant power, current, or impedance load
Pi_X	Active power from bus to equipment
Qi_X	Reactive power from bus to equipment
Si_X	Apparent power from bus to equipment
I% _{i_j}	Load rate percent of the transmission line between bus and bus
I% _{i_j_1}	Load rate percent of the first transmission line between bus and bus
I% _{i_j_2}	Load rate percent of the second transmission line between bus and bus
I% _{i_X}	Load rate percent of the equipment at bus
PLOSS _{i_j}	Active power loss of the transmission line between bus and bus
QLOSS _{i_j}	Reactive power loss of the transmission line between bus and bus
PLOSS _{i_j_1}	Active power loss of the first transmission line between bus and bus
QLOSS _{i_j_1}	Reactive power loss of the first transmission line between bus and bus
PLOSS _{i_j_2}	Active power loss of the second transmission line between bus and bus
QLOSS _{i_j_2}	Reactive power loss of the second transmission line between bus and bus

1. Introduction

Security level assessment of transient stability is essential to the power system operation and control [1]. There has been a continually increasing interest and investigation into security level assessment of transient stability [2]–[4]. Transient stability or large disturbance rotor angle stability is concerned with the ability of the power system to maintain synchronism when subjected to a severe disturbance, such as a short circuit on a transmission line. At present security scanning and assessment for power system mainly rely on a lot of fault simulation. Considering the large scale of current power system, different types of equipment, the real-time changing load and changing generator output, the enumerated probabilistic fault simulation analysis method is not able to provide real-time assessment results or effective control measures information of improving the security level. In general, a single simulation method cannot meet the demand of intelligent decision for the power system control. Therefore, there is a pressing need to develop fast online security assessment method which could analyse the level of security and forewarn the system operators to take necessary preventive actions in case need arises [5], [6].

The security level assessment of transient stability is a problem with inherent complexity, non-linearity, uncertainty and the need for online monitoring. Seeking and establishing the mapping relationships between the power system operation state monitoring data and security level of transient stability based on knowledge engineering technology and data mining [7–9] is a very attractive idea. It is built on a large number of accumulated samples, which relies on fault simulation scan of transient stability. It is designed to discover the implicit relationships in the fault scan results and power flow information, which may be useful to assess security level. This security level assessment idea makes up for the deficiency of simulation scan. First of all, once the security level assessment rules or model have been established by offline data mining, the computation speed of online security assessment will be fast. Secondly, considering that power flow of power system can be easily observed, adjust and control, it will be convenient to improve the security level based on the relationships and it plays a role of aid decision making. However, it still faces many challenges to achieve direct security assessment based on operating information and data mining. We need to figure out how the power flow distribution and steady-state operating information of the system affect the security level of transient stability under a given fault. Another challenge is: the WAMS of a large power system may collect a huge amount of power flow and operating data, which not only contains features of high correlation for security level, but also the ones of weak correlation. How to effectively select the dimensions of the input feature, extract and classify the high correlation features, and eliminate redundant features is a key step in the security level assessment based on the artificial intelligence theory [10–12]. The purpose of feature selection is to select and classify high correlation features from a large number of original features. It requires reducing the dimension and minimum information loss of representing the research target. By selecting the features highly associating with the research target, the purpose of the d – dimensional feature extracted from the D – dimensional feature space ($d \ll D$) can be achieved [13], [14].

A lot methods have been applied to the transient stability assessment, such as artificial neural networks(ANN) [15], pattern recognition techniques [16], decision trees [17], and fuzzy neural networks [18]. Some optimisation algorithms such as simulated annealing algorithm and ant colony algorithm are also applied to transient stability assessment [19]–[21], and its purpose is to choose better input features. In [15], [22], ANN is adopted and correct estimation results are got. However, the input features used in the paper may not be the optimal ones and the size of selected features is not a small number for its test system. For a large system, it is necessary to select a small number of optimal input features from the massive features. The methods in these papers may fail because of the curse of dimensionality. In [20], [21], the number of variables in the optimal variable group given by optimisation algorithm is small, which reduce the dimension well. However, the final accuracy is not particularly high. Moreover, the new additional variable cannot be directly given by optimisation algorithm when the assessment accuracy needs to be improved. In [23], [24], the CCT in a case of assumption fault is calculated precisely with a short time, but the calculation time-consuming still will increase rapidly and cannot meet the needs of online assessment if the size of the actual power system is huge or with even more uncertain faults. In [17], [18], transient stability prediction accuracy for a fault is relatively high, but the security level assessment of transient stability for normal steady-state operation state is not given.

The online assessment scheme presented in this paper is based on relationships exploration in a large data set of offline power flow simulation and fault simulation. The optimal features are selected based on the implicit relationships explored in the data set. The relationships between these variables

and security level of transient stability are presented and explained. Finally, the optimal variables will be applied to online assessment scheme for power system security level of transient stability. The way to select features is different from the conventional optimisation algorithms of feature selection, and it can explain the variables group given by optimisation algorithm to a certain extent. The number of input features in the scheme can be chosen freely, which is based on the needed assessment accuracy. It can overcome the curse of dimensionality of large-scale power systems. The applicability will not be influenced by the change of the structure and scale since input features selected are based on data statistics and mining. The scheme has a certain requirement for the number of samples of the previous offline simulation. Steps of the scheme are shown on Figure 1.

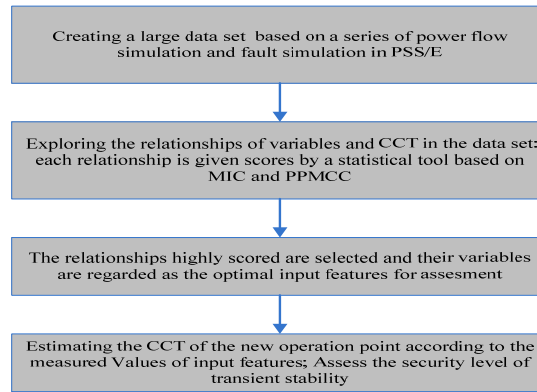


Figure 1. Assessment scheme

In the proposed approach, the results of power flow simulation and fault simulation in PSS/E are used to create a large data set, which include all kinds of operation variables and CCT. The relationship between CCT and each variable is explored and given scores by the maximal information coefficient (MIC) and Pearson's product moment correlation coefficient (PPMCC). The relationships highly scored determine their variables will be selected, and these variables are regarded as the optimal input features. The relationships highly scored are also presented and explained in the paper. Then the paper presents an estimation method using the optimal input features. The scheme is tested on a 21-bus system provided by PSS/E to assess security level for a lot of new operating points. The results of the assessment are verified to be correct. For real time application, the data of input features can be obtained from phase measurement units (PMUs). The scheme is economical since it requires a relatively small number of PMUs.

This paper is organized as follows: Section 2 provides a detailed statement of the problem and some supporting mathematical methods. Section 3 introduces the method to create a large data set based on simulation. Section 4 explores the relationships of variables and CCT. Section 5 presents the estimation method of CCT and security level assessment of transient stability. Section 6 concludes the paper.

2. Problem Statement and Supporting Mathematical Methods

2.1. Critical Clearing Time (CCT)

Given a certain fault, the transient stability of the Power system is usually described with the critical clearing time (CCT). The system with a longer CCT is considered to have a higher security level of transient stability. CCT can be used as the index for transient stability assessment. The delay in fault clearing from the CCT means loss of synchronous operation of the generators in the power system. Compared with other indices, CCT is easy for operators to understand how stable the power system is during operation.

2.2. Maximal Information Coefficient (MIC)

MIC is a measure of dependence for two-variable relationships and it captures relationships both functional and not in large data sets. The concept is presented recently by the paper [25]. MIC belongs to a larger class of maximal information-based nonparametric exploration statistics for identifying and

classifying relationships. MIC is applied to the data sets of biology and has detected novel relationships. In this paper, MIC is introduced into the field of power system and it is used to explore the relationships of CCT and lots of operation variables in power system operation.

MIC is based on the idea that if there is a relationship between two variables, then a grid can be drawn on the scatter plot of the two variables that partitions the data to encapsulate the relationship. MIC can give a score to measure the relationship between two variables based on the data pairs of variables. MIC can capture a wide range of interesting relationships, not only to specific function types (such as linear, parabolic, or sinusoidal), but also to even all functional relationships. For equally noisy relationships of different types, MIC can give similar scores to them.

Given a finite set D of ordered pairs, the x -values of D are partitioned into x bins and the y -values of D are partitioned into y bins, allowing empty bins. Such a pair of partitions can be called an x -by- y grid. Given a grid G , let $D|G$ be the distribution induced by the points in D on the cells of G . The distribution on the cells of G is obtained by letting the probability mass in each cell be the fraction of points in D falling in that cell. For a fixed D , different grids G result in different distributions $D|G$. For a data set D of two-variable, the MIC of their relationship is given by (1), (2).

For a finite set $D \subset R^2$ and positive integers x, y .

$$I^*(D, x, y) = \max I(D|G). \quad (1)$$

Where the maximum is over all grids G with x columns and y rows, and denotes the mutual information of. The MIC of two-variable data with sample size n and grid size less than is given by

$$MIC(D) = \max_{xy < B(x,y)} \left\{ \frac{I^*(D, x, y)}{\log \min\{x, y\}} \right\}. \quad (2)$$

Where for some.

In the research, is used because it's found to work well in practice [25]. MIC falls between 0 and 1. Some properties of MIC are as follows.

- 1) MIC assigns scores that tend to 1 to all never-constant noiseless functional relationships.
- 2) MIC assigns scores that tend to 1 for a larger class of noiseless relationships.
- 3) MIC assigns scores that tend to 0 to statistically independent variables.

2.3. Pearson's Product Moment Correlation Coefficient (PPMCC)

In statistics, PPMCC [26] is used to measure the linear correlation degree between two variables X and Y . In the field of natural sciences, the coefficient is widely adopted to detect the linear relationships in variables. In this paper, PPMCC is specially used to evaluate the degree of linearity for the relationship of a variable between CCT. For samples (X_i, Y_i) , a kind of expression for PPMCC is expressed as the mean of standard score, which is given by (3).

$$\rho = \frac{1}{n-1} \sum_{i=1}^n \left(\frac{X_i - \bar{X}}{S_X} \right) \left(\frac{Y_i - \bar{Y}}{S_Y} \right). \quad (3)$$

Where n is the size of samples, \bar{X} is the mean of samples, and S_X is the standard deviation of samples.

PPMCC falls between -1 and 1. Some properties of PPMCC are as follows.

- 1) If $\rho > 0$, it shows that the two variables are positive correlative.
- 2) If $\rho < 0$, it shows that the two variables are negative correlative.
- 3) The larger the absolute value of ρ is, the stronger linear relationship between the two variables exists.
- 4) If $\rho = 0$, it shows that the two variables are not linear correlative, but there may be another relationship between the two variables (such as a curvilinear association).

3. Creating a Large Data Set of CCT and Operation Variables in Power System Based on Simulation

In the practice of power system operation, the accidents of transient stability failure are unusual. It leads to the lack of instability data samples, which cannot satisfy the requirements of data mining. Therefore, simulation is usually used to obtain samples. A well-known software package named PEE/S is used to create the necessary data set. PSS/E is a software tool used for power system, and it can be used to analyse transient stability [27]. This paper uses Python programming language in PSS/E to achieve the follows: Initialise the data of loads randomly and the matching data of generators' output in a normal range. Solve the power flow of operating sample point, and then choose the convergent ones. Make a series of three-phase instantaneous short circuit fault simulation test at a set place and calculate its CCT for every selected operating sample point. The run will end until the set number of samples is satisfied. The program flow chart is illustrated on Figure 2.

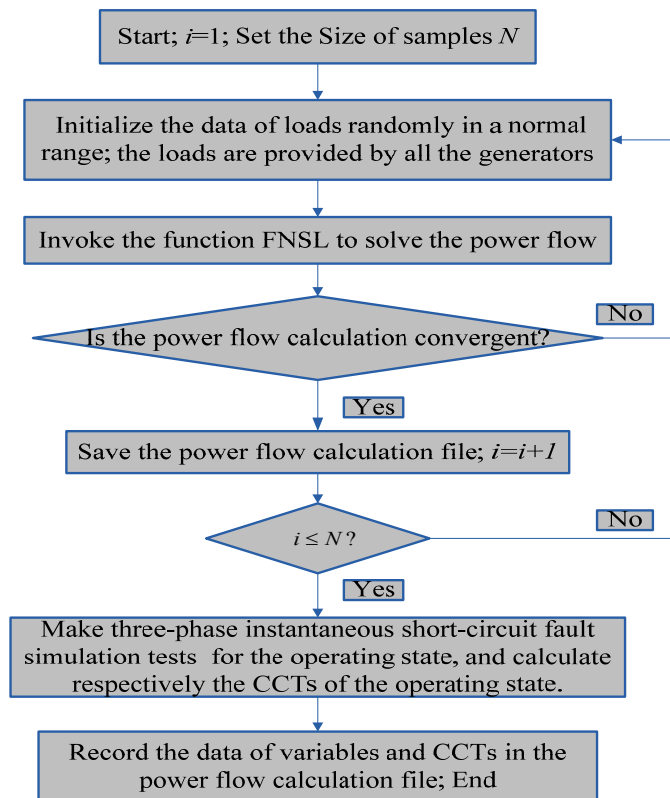


Figure 2. Program flow chart for creating a large data set of power flow and CCT based on simulation in PSS/E

Some explanatory notes for the program flow chart on Figure 2 are as follows.

- 1) N can be set according to the size of samples needed and $N = 150$ is used in this paper.
- 2) A lot of physical variables are extracted from the power flow results of the system: generator active power and reactive power of every generator; voltage amplitude and phase angle of every bus; active power, reactive power, apparent power, active power loss and reactive power loss of every branch; load rate percentage of every branch; active power and reactive power from a bus to an equipment.
- 3) According to the experience of the power system operation, some other variables are added because they are reasonably suspected to have a relationship with CCT. The additional variables are based on some fundamental variables in the power flow results. They are: phase angle difference between any two generators at steady-state, the maximum and minimum of absolute value of phase angle difference between any two generators at steady-state.

In the paper, a 21-bus test system [28] provided by PSS/E is used, which is shown on Figure 3.

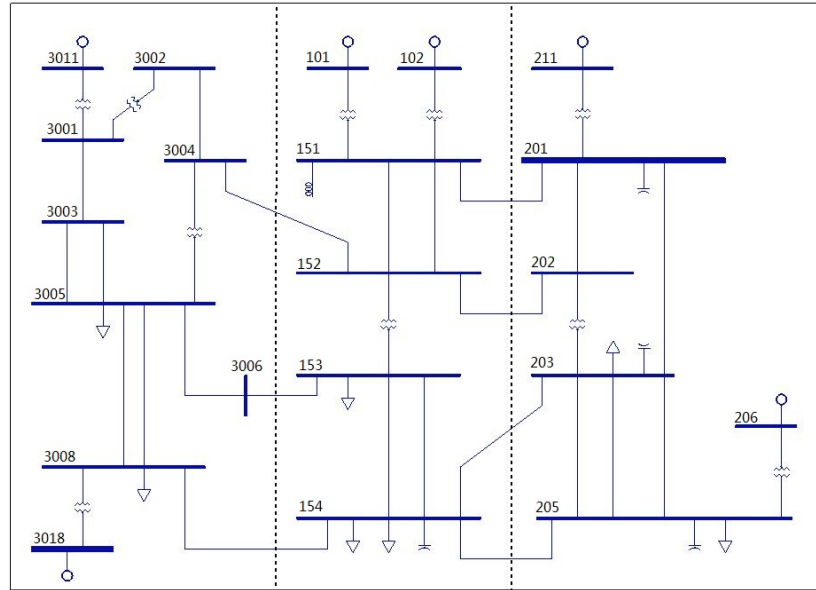


Figure 3. 21-bus test system provided by PSS/E

In the test system, 470 physical variables are finally extracted after eliminating all of the constant variables. Then a large data set of power flow variables and CCT is created, which is a matrix with 471 rows (470 physical variables and CCT) and 150 columns. The three-phase instantaneous short circuit fault simulation test is as follow: a fault occurs at the head of the first line between the bus 205 and the bus 203 when $t = 0s$, then disconnect the line after a set time.

4. Exploring the Relationships of Power Flow Variables and CCT

4.1. Top Relationships Explored by MIC and PPMCC

MIC and PPMCC are applied to detect the relationships in the data set. A statistical tool is provided by the paper [25], which can calculate MIC and PPMCC of each relationship. Table 1 shows the top 1% of relationships by MIC and Table 1 shows the top 1% of relationships by PPMCC. The relationships highly ranked by PPMCC have high degrees of linearity. A relationship highly ranked by MIC show a certain relationship between the two variables, and it doesn't necessarily have a high degree of linearity.

Table 1. Top 1% of relationships by MIC

Var1	Var2	MIC	MIC Rank	PPMCC (ρ)	PPMCC Rank
CCT	<i>S152 151 1</i>	0.778	1	-0.813	109
CCT	<i>S152 151 2</i>	0.778	2	-0.813	110
CCT	<i>PLOSS151 152 1</i>	0.773	3	-0.821	80
CCT	<i>PLOSS151 152 2</i>	0.773	4	-0.821	81
CCT	<i>PLOSS152 151 1</i>	0.773	5	-0.821	82

Table 2. Top 1% of relationships by PPMCC

Var1	Var2	PPMCC (ρ)	PPMCC Rank	MIC	MIC Rank
CCT	<i>Q3005 3003 1</i>	0.885	1	0.684	62
CCT	<i>Q3005 3003 2</i>	0.885	2	0.684	63
CCT	<i>Q3004 3002</i>	0.884	3	0.673	74
CCT	<i>Q3004 152</i>	-0.882	4	0.722	44
CCT	<i>0101</i>	-0.874	5	0.672	86

Specially, the relationship whose MIC rank is 1 in Table 1 and the ones whose PPMCC rank is 1 in Table 2 are shown successively on Figure 4 and Figure 5. These relationships are implicit in mass data, which are not easy to be found directly. After these relationships are detected out, generally reasonable

explanation can be given for the relationships from the perspective of power system. The variable $S_{152_151_1}$ is selected as an example, which represents the apparent power of the first line from bus 152 to bus 151 on Figure 6. In order to explain the relationship conveniently, a case can be imagined: with the increase of power system loads, the power on the transmission line will increase; when load rating of the system is low, the increase of load doesn't make CCT decrease significantly; when load rating of the system is high, a slight increase of load will make CCT decrease significantly.

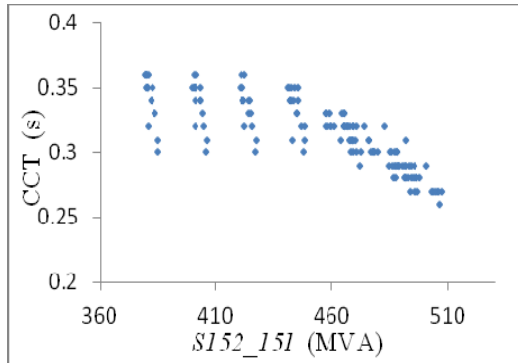


Figure 4. Scatter plot of the variable $S_{152_151_1}$ and CCT

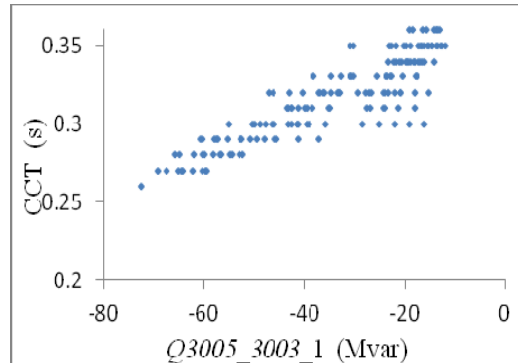


Figure 5. Scatter plot of the variable $Q_{3005_3003_1}$ and CCT

4.2. MIC versus PPMCC

Figure 6A shows that MIC versus PPMCC for all pair-wise relationships in the data set. In different areas of Figure 6A, different kinds of relationships can be found. Some examples are as follows.

- 1) Figure 6B: Both PPMCC and MIC yield low scores for unassociated variables. It indicates no specific relationship exist between the variable θ_{3001} and CCT.
- 2) Figure 6C: Ordinary linear relationships score high under both MIC and PPMCC tests. It indicates an obvious linear relationship between the variable θ_{101} and CCT.
- 3) Figure 6D: Relationships detected by MIC but not by PPMCC, because the relationships are nonlinear. It indicates a kind of nonlinear relationship between the variable the variable Q_{205_201} and CCT.

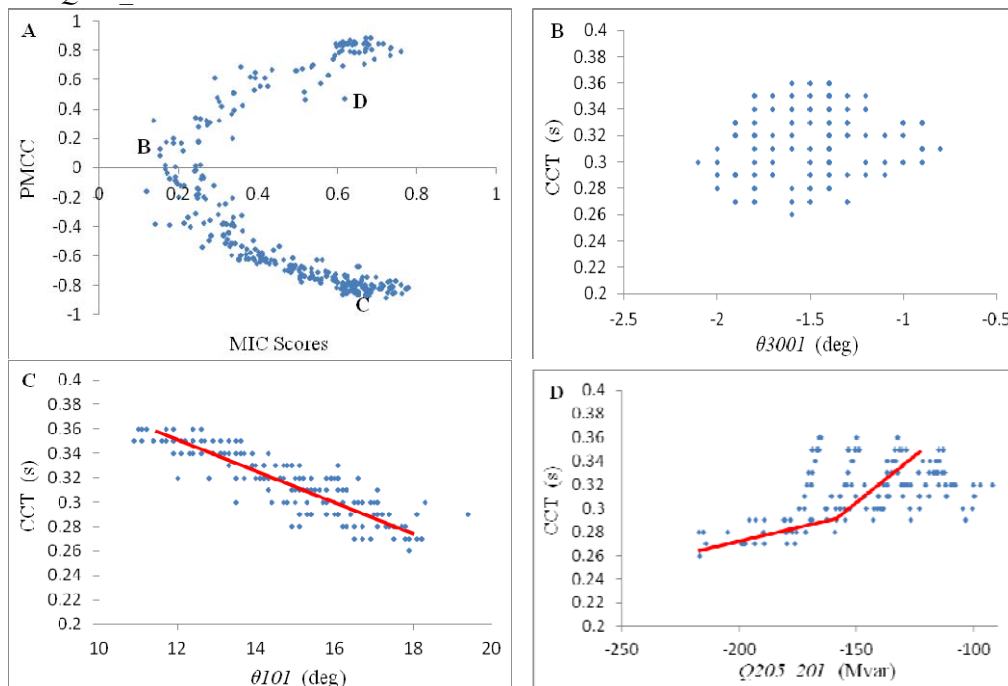


Figure 6. Application of MIC and PPMCC to the data set. (A) MIC versus PPMCC for all pair-wise relationships in the data set. (B)–(D) Examples of relationships from (A)

4.3. Top Nonlinear Relationships

In order to discover the nonlinear relationships of variables and CCT comprehensively and quickly, the statistic $MIC - \rho^2$ is adopted. For a relationship, a larger MIC and a smaller $|\rho|$ get a larger $MIC - \rho^2$. Table 3 shows the top 0.5% of relationships by $MIC - \rho^2$, and the relationships are shown on Figure 7.

Table 3. Top 0.5% of nonlinear relationships by $MIC - \rho^2$

Var1	Var2	$MIC - \rho^2$	$MIC - \rho^2$ Rank	MIC	PPMCC(ρ)
CCT	Q_{205_201}	0.395	1	0.618	0.471
CCT	Q_{205_206}	0.302	2	0.520	0.465

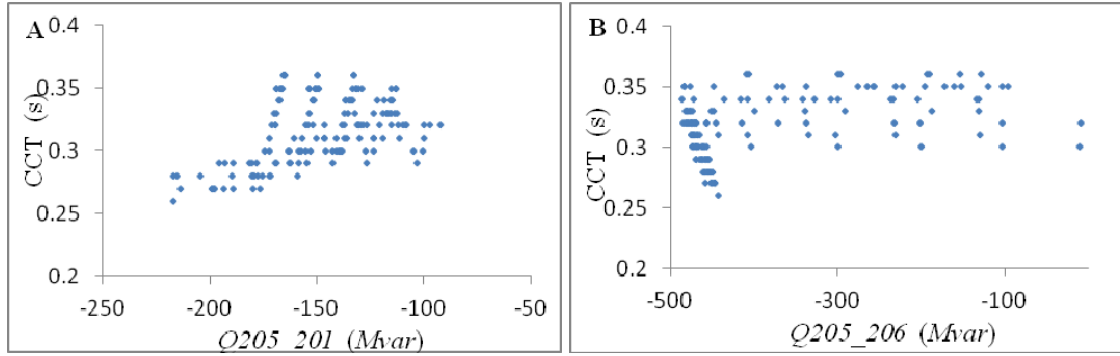


Figure 7. Scatter plot of the top 0.5% of nonlinear relationships selected by $MIC - \rho^2$

Some explanations for the relationships on Figure 7 from the perspective of power system are as follows.

1) Q_{205_201} represents the reactive power from bus 205 to bus 201. At a general operation state, the value of this variable is minus and will decrease gradually with the increase of power system loads. Compared to an operation state of low load rating, the decrease of CCT will become faster when the system is operated at a state of high load rating. Therefore the relationship between the variable Q_{205_201} and CCT is that shown on Figure 7A.

2) Q_{205_206} represents the reactive power from bus 205 to bus 206. When load rating of the system is low, the value of this variable will appear in the interval $(-500, 0)$ randomly. When load rating of the system is high, the variable will tend to its minimum value because there is a maximum reactive power limit for the generator at bus 206. Therefore the relationship between the variable Q_{205_206} and CCT is that shown on Figure 7B.

5. Estimation of CCT and Test Results

5.1. Selecting Input Features

After exploring the relationships of variables in power flow and CCT, these relationships can be used to estimate CCT and assess the security level of transient stability for a new operation state. The values of variables can be obtained from WAMS in practice. Obviously, the accuracy of estimation is affected by the variables selected and measured. The variables selected should be the ones who have obvious relationships with CCT. Moreover, the total number M of the variables selected should be appropriate. Setting M too low can lead to inaccurate estimation ranges, while setting M too high means the increase of economic cost in engineering application because of too many measuring points. An appropriate selection is given based on tests: the top 1% of relationships by MIC, the top 1% of relationships by PPMCC, and the top 0.5% of nonlinear relationships by $MIC - \rho^2$. Therefore the total number of relationships selected is 12 in the paper. It should be noted if a variable always remains the same with another one (such as $S152_151_1$ and $S152_151_2$ in Table 1), one of them will be

eliminated and a variable ranking behind the two variables will be selected to guarantee $M = 12$. The variables finally selected are in Tables 3–5, which are the optimal ones to be input features.

Table 4. Variables finally selected from the ranking list by MIC

Var1	Var2	MIC	MIC Rank
CCT	S152 151 1	0.778	1
CCT	PLOSS151 152 1	0.773	3
CCT	QLOSS151 152 1	0.773	7
CCT	QLOSS201 202	0.763	11
CCT	P152 151 1	0.760	13

Table 5. Variables finally selected from the ranking list by PPMCC

Var1	Var2	PPMCC (ρ)	PPMCC Rank
CCT	Q3005 3003 1	0.885	1
CCT	Q3004 3002	0.884	3
CCT	Q3004 152	0.882	4
CCT	$\theta 101$	0.874	5
CCT	Q3005 3006	0.871	8

5.2. Program Flow Chart for Estimation of CCT

For each input variable, the idea of estimation is as follow. As it is illustrated on Figure 8, the measurement value of the variable a205_201 is x_0 when the system is operated at a new point. In all the points on Figure 8, the smallest value of x -axis is X_{\min} and the largest value is X_{\max} . All the points with x -axis in the range (x_1, x_2) are searched out. The smallest value of y -axis in these points is y_1 and the largest value is y_2 . The CCT of the new operation state can be considered in the range (y_1, y_2) . Equations (4)–(8) are given for Figure 8. Specially, 3% is used in (5) and 0.5 is used in (6), which are found to work well in practice. A too wide search range leads to an imprecise estimation result. If the search range is too narrow, maybe no result is returned because the sample size is finite.

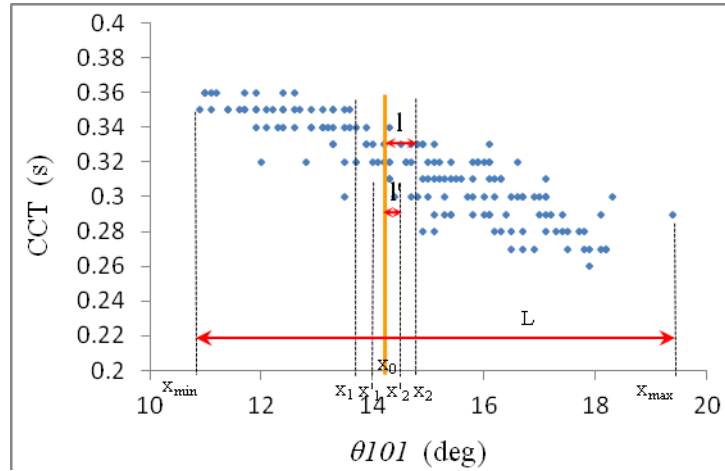


Figure 8. Estimation method for each variable

$$L = X_{\max} - X_{\min} \quad (4)$$

$$l = L * 3\% \quad (5)$$

$$l' = 0.5 * l \quad (6)$$

$$X_1 = X_0 - l \quad (7)$$

$$X_2 = X_0 + l \quad (8)$$

The selected variables are used to estimate CCT and the program flow chart is shown on Figure 9. The parameter t is introduced to update l when needed, which can increase the imprecision of estimation because the search range is narrower with a smaller l . If an estimation range (y_1, y_2) given at the first

search satisfies $Y_2 - Y_1 > 0.01$, the existence of parameter t can give it a more accurate search opportunity with the updated l . The method can try to make the final estimation range satisfies $Y_2 - Y_1 \leq 0.01$, which will be more precise.

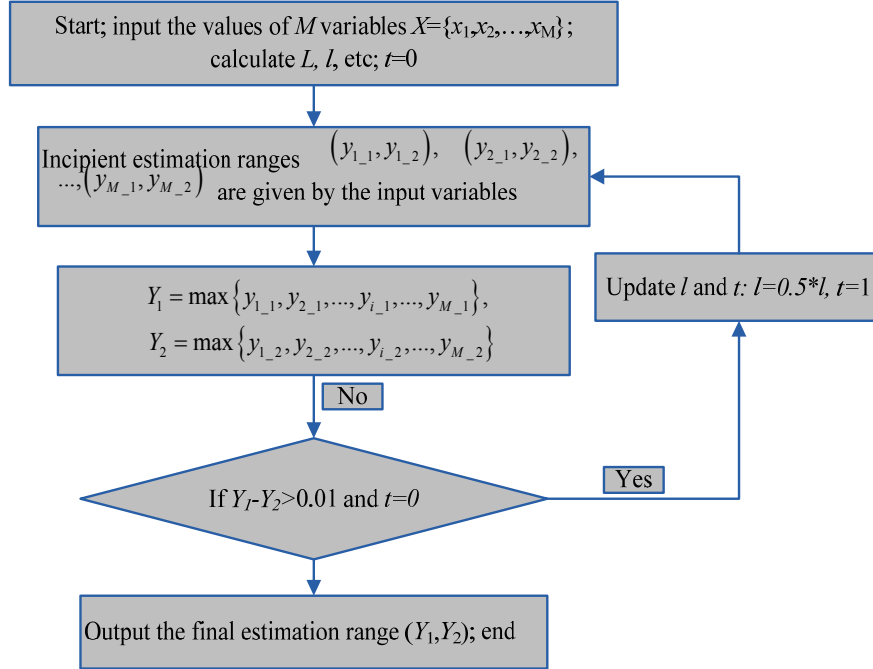


Figure 9. Program flow chart of estimating CCT

5.3. CCT estimation results and security level assessment of transient stability

In the tests, possible new operation states are set stochastically. 15 of them are randomly selected and shown in Table 6. Some explanatory notes for Table 6 are as follows.

- 1) R is the final estimation range of a new point, which is given by the program with the 12 selected variables as input features.
- 2) The span of R is shown to measure the precision of estimation range.
- 3) S is the value given by simulation, which is used to verify the correctness of estimation.
- 4) Occasionally, CCT is not visual enough to describe security level of transient stability for the power system operators. Therefore, samples can be classified as some levels according to their distribution. In this case, 5 levels are as follows: Level 1: 0.35–0.36; Level 2: 0.33–0.34; Level 3: 0.30–0.32; Level 4: 0.28–0.29; Level 5: 0.26–0.27. Level in Table 6 is security level assessment of transient stability for a new operation state.

Table 6. Estimation results of new operation states

No.	$R(s)$	Span of $R(s)$	$S(s)$	Level
1	0.27	0	0.27	5
2	0.27–0.28	0.01	0.27	5
3	0.28	0	0.28	4
4	0.28–0.29	0.01	0.29	4
5	0.29–0.30	0.01	0.30	3
6	0.30–0.31	0.01	0.31	3
7	0.32–0.33	0.01	0.32	3
8	0.32–0.33	0.01	0.33	2
9	0.34	0	0.34	2
10	0.35–0.36	0.01	0.35	1
11	0.35–0.36	0.01	0.36	1
12	0.33–0.34	0.01	0.34	2
13	0.27–0.28	0.01	0.28	4
14	0.29	0	0.29	4
15	0.31–0.32	0.01	0.31	3

In general, each simulation value S for new operation state is in the range R and this demonstrates the correctness of estimation ranges. S is slightly out of the range in a very few tests, which is due to the finiteness of previous samples. After the statistics of more tests, the possibility of S being out of the range R is lower than 1%.

6. Conclusions

This paper proposes a novel online transient stability assessment scheme based on the connotative relationship exploration in a large data set, which includes CCT and lots of different operation variables in power system. The scheme includes: a series of power flow simulation and fault simulation, creating a large data set of variables and CCT, giving scores to the relationships and ranking them, using the linear and nonlinear relationships to estimate CCTs for new operation states. The data set is created with a series of simulation in PSS/E. The relationships of variables and CCT are given scores by the statistical methods based on MIC and PPMCC. Some highly ranked linear and nonlinear relationships are detected out, shown, explained, and then used for estimation. The estimation results are verified to be accurate and can be used to assess the security level of transient stability.

Different from conventional feature selection methods, the input features are selected from a great number of variables based on data mining and relationships exploration in this paper. It will be more intelligent and efficient than conventional optimisation algorithms because each feature is given a score and ranked clearly. The applicability of the scheme will not be influenced by the change of the structure and scale since it based on data statistics and mining. The estimation results are with high precision, which relies on the total number of previous operation samples to a certain extent. The estimation of CCT and the online security level assessment of transient stability will be important basis for system operators to change operation state to improve the security level in practice.

Acknowledgements

This work was supported in part by the National Natural Science Foundation of China under Grant (61074101, 50477018, and 51007093) and in part by the Specialized Research Fund for the Doctoral Program of Higher Education (20090141120062).

References

1. Dong, Z.Y., Zhao, J.H. & D.J. Hil. (Nov. 2012). Numerical Simulation for Stochastic Transient Stability Assessment. *IEEE Trans. Power Syst.*, 27(4), 1741–1749.
2. Chatterjee, D. & A. Ghosh. (Aug. 2007). Transient Stability Assessment of Power Systems Containing Series and Shunt Compensators. *IEEE Trans. Power Syst.*, 22(3), 1210–1220.
3. Xu, Y., Dong, Z.Y., Meng, K. et al. Mar. (2011). Real-time transient stability assessment model using extreme learning machine. *IET Generation, Transmission & Distribution*, 5(3), 314–322.
4. Miah, A. M. (Apr. 2011). Study of a coherency-based simple dynamic equivalent for transient stability assessment. *IET Generation, Transmission & Distribution*, 5(4), 405–416.
5. Niazi, K. R., Arora, C. M., Surana, S. L. (2003). Power system security evaluation using ANN: feature selection using divergence. In Proc. 2003 Int. Joint Conf. Neural Networks, July 20–24, 2003, Vol. 3 (pp. 2094–2099). IJCNN 2003, Portland, Oregon, USA.
6. Amjady, N. & S. F. Majedi. (Aug. 2007). Transient stability prediction by a hybrid intelligent system. *IEEE Trans. Power Syst.*, 22(3), 1275–1283.
7. Tao, X., Renmu, H., Peng, W., Dongjie, X. (2004). Applications of data mining technique for power system transient stability prediction. In Proceedings of the 2004 IEEE International Conference on Electric Utility Deregulation and Restructuring and Power Technologies, during 5-8 April 2004, (pp. 1389–392). Hong Kong
8. Yu, Z. H., Zhou, X. X., Wu, Z. X. (2005). Fast Transient Stability Assessment Based on Data Mining for Large-Scale Power System. In Proc. Transmission and Distribution Conference and Exhibition, 2005 (pp. 1–6).
9. Wang, T. W. Guan, L. (2007). A data mining technique based on pattern discovery and k-nearest neighbor classifier for transient stability assessment. In Proc. Power Engineering Conference, IPEC 2007, 3–6 Dec. 2007 (pp. 118–123).
10. Silipo, R., Berthold, M. R. (Dec 2000). Input features' impact on fuzzy decision processes. *IEEE Transactions on Systems, Man, and Cybernetics, Part B: Cybernetics*, 30(6), 821–834.

11. Laine, T. I., Bauer, K. W., Jr., Lanning, J. W. et al. (Nov. 2002). Selection of input features across subjects for classifying crewmember workload using artificial neural networks. *IEEE Transactions on Systems, Man, and Cybernetics, Part A: Systems and Humans*, 32(6), 691–704.
12. Kwak, N., Choi, C.–Ha–H. (Jan. 2002). Input feature selection for classification problems. *IEEE Transactions on Neural Networks*, 13(1), 143–159.
13. Chen, J. X., Wang, S. (Sep./Oct. 2001). Data visualization: parallel coordinates and dimension reduction. *Computing in Science & Engineering*, 3(5), 110–113.
14. Shen, L., Tan, E. C. (April–June 2005). Dimension reduction–based penalized logistic regression for cancer classification using microarray data. *IEEE/ACM Transactions on Computational Biology and Bioinformatics*, 2(2), 166–175.
15. Verma, K., Niaz, K. R. (2011). Determination of vulnerable machines for online transient security assessment in smart grid using artificial neural network. In Proc. 2011 Annual IEEE India Conference (INDICON), 16–18 Dec. 2011 (pp. 1–5). Dept. of Electr. Eng., Indian Inst. of Technol., Kharagpur, India.
16. Garcia, G., Benussou, J. & M. Berbiche. (Jul. 1992). Pattern recognition applied to transient stability analysis of power systems with modeling including voltage and speed regulation. *IEE Proc. B Electric Power Applications*, 139(4), 321–325.
17. Rovnyak, S., Kretsinger, S., Thorp, J. & D. Brown. (Aug. 1994). Decision trees for real–time transient stability prediction. *IEEE Trans. Power Syst.*, 9(3), 1417–1426.
18. Amjady, V. (2005). Application of a new fuzzy neural network to transient stability prediction. In Proc. IEEE PES Summer Meeting, San Francisco, CA, Jun. 2005 (pp. 69–76). San Francisco, CA.
19. Cao, M., Wang, Y. J. (2011). Application of binary particle swarm optimization in feature selection for transient stability assessment. In Proc. 2011 International Conference on Electric Information and Control Engineering (ICEICE), 15–17 April 2011 (pp. 5719–5722 Wuhan, China, from <http://ieeexplore.ieee.org/xpl/mostRecentIssue.jsp?punumber=5766331>
20. Cao, M. (2006). *Feature Selection for Transient Stability Assessment Based on Genetic Simulated Annealing Algorithms*. Baoding: North China Electric Power University.
21. Zhang, X. Q., Guan, L., Wang, T. W. (Dec. 2010). Kernel Feature Identification Based on Improved Ant Colony Optimization Algorithm for Transient Stability Assessment. *Transactions of China Electrotechnical Society*, 25(12), 154–160.
22. Niazi, K. R., Arora, C. M., Surana, S. L. (2004). Power system security evaluation using ANN: feature selection using divergence. *Electric Power Systems Research*, 69, 161–167.
23. Al Marhoon, H.H., Leevongwat, I., Rastgoufard, P. (2012). A Practical Method for Power Systems Transient Stability and Security Analysis. In Proc. 2012 IEEE/PES Transmission & Distribution Conference and Exposition (T&D) 7–10 May 2012 (pp. 1–6). Orlando, FL, USA, from <http://www.ieceet-d.org/TECHPROfinal.pdf>
24. Yorino, N., Priyadi, A., Kakui, H., Takeshita, M. (Aug. 2010). A New Method for Obtaining Critical Clearing Time for Transient Stability. *IEEE Trans. Power Syst.*, 25(3), 1620–1626.
25. David, N. R., Yakir, A. R., Hilary, K. F., Sharon, R. G., Gilean, M., Peter, J. T., Eric, S. L., Michael, M. & C. S. Pardis. (Dec. 2011). Detecting novel associations in large data sets. *Science*, 334, 1518–1524.
26. Gayen, A. K. (1951). The frequency distribution of the product moment correlation coefficient in random samples of any size draw from non–normal universes. *Biometrika*. 38, 219–247.
27. Mohamad, A. M., Hashim, N., Hamzah, N., Nik, F., Abdul, L. & F. Mohd. (2011). Transient stability analysis on Sarawak’s grid using Power System Simulator for Engineering (PSS/E). In IEEE Symposium on Industrial Electronics & Applications (ISIEA 2011) (pp. 521–526). Langkawi, Malaysia on 25–28 September 2011, from <http://www.isiea.org/2011/>
28. Power Technologies, Inc. *PSS/E Application Program Interface*. Aug. 2004, from <http://www.energy.siemens.com/hq/en/services/power-transmission-distribution/power-technologies-international/software-solutions/pss-e.htm>

Received on the 20th of May 2013

NUMERICAL SIMULATION OF AIR LEAKAGE IN GOAF OF FULLY MECHANIZED FACE WITH HIGH DIP AND HARD ROOF

¹Zh. Xie, ²T. Luan, ²Na He

¹*Civil and Environmental Engineering School of University of Science and Technology Beijing
Beijing, 100083, China, xie0015@sina.com*

²*Civil and Environmental Engineering School of University of Science and Technology Beijing
Beijing, 100083, China*

Because the geological conditions of coal in goaf with high dip and hard roof are complex, and the law of air leakage is complicated and changeable, so the risk of coal spontaneous combustion in goaf is high. Mastering the law of air leakage in goaf is important to coal spontaneous combustion prevention. This paper detects the air leakage of 7162 working face in LongDong coal mine using SF₆ as tracer gas, and gets the basic distribution laws of air leakage in goaf of 7162 working face, furthermore collects relevant data for numerical simulation of airflow situation in goaf. The distribution laws of air pressure and wind speed in goaf have been obtained by simulating the seepage fields in goaf using FLUENT software. The research results provide scientific guidance for prevention measures of coal spontaneous combustion.

Keywords: goaf, coal spontaneous combustion, air leakage detection, numerical simulation

1. Introduction

The technology of fully mechanized top coal caving is widely used in coal mining, because of its mining intensity, high efficiency, and good economic benefits etc. But the risk of coal spontaneous combustion is higher, because the height of roof falling is big, and the remaining float coal is more and its distribution is uneven in goaf of fully mechanized top coal caving [1]. Especially, the risk of coal spontaneous combustion increases in goaf of fully mechanized face with high dip and hard roof. The main reasons include: the advance rate of working face is slow or stopping mining because the technology of fully mechanized top coal caving is difficult, to make oxidation time of float coal in goaf too long; the leakage air increases in goaf because the coal seam roof is hard, the coal pillar is easily crushed, and the filling of goaf falling is not dense.

The aim of air leakage measurement is to find the air leakage passage and grasp the law of air leakage. Generally, the tracer technique is used to detect air leakage passage and leakage air volume [2]. Qin Shuyu, Xu Jingcai, Du Liming and etc. had researched the oxygen concentration distribution, distribution laws of air leakage intensity, and the mathematical model of temperature fields in goaf [3]. Li Zongxiang, Hai Guozhi and etc. used finite element computer simulation, combining graphic display technology, studied the airflow movement regularity in goaf of coal face and calculation problems, visibly reflected the wind pressure distribution and airflow status in goaf by graphics modes [4]. Wang Jikai, Gao Jianliang and etc. set up seepage mathematical model of goaf through theoretical analysis and experimental measurement to seepage characteristics of porous medium in goaf. They used the FLUENT software to make numerical simulation for air leakage fields in goaf, and obtained air leakage velocity and pressure distribution law in goaf [5, 6]. These research results provide basic for numerical simulation of air leakage in goaf of fully mechanized face with high dip and hard roof, but are lack of verification of the actual test.

Based on the actual situation of 7162 goaf of fully mechanized face with high dip and hard roof in LongDong coal mine, this paper detected the air leakage laws in goaf using tracer gas with multiple release, got air pressure and wind speed distribution of air leakage in goaf by adopting computer simulation, and provide scientific guidance for prevention measures of coal spontaneous combustion.

2. General Situation of Working Face

The 7162 working face of LongDong coal mine has recoverable coal reserves of 576200 t, trend length is 800 m and tilt length is 150 m; the thickness of coal seam is from 5.2 to 6.9 m and the average thickness is 5.4 m; the dip angle of coal seam is from 22° to 31° and the average dip angle is 25°. Light mechanized long-wall mining is used in top-coal caving mining, which causes all caving full-seam mining, low recovery rate and more residual coal in goaf. Lithology of coal seam roof in 7162 working face is mainly fine-grained sandstone and sandstone, which belongs to the hard roof. Initial cross step distance of roof is 50 m, which has obvious cyclical, when cross step distance of roof is about 30 m, compaction time extended in goaf and there is a lot of pore space, so air leakage is serious.

The 7162 coal seam is spontaneous combustion coal seams, which has explosion risk and a low gas level. The geological structure of the face is more complex, roadway excavation revealed 13 faults, among them, F114, F108, F1, F2 and F156 are all cross protection pillar of 7162 working face and 7160 goaf, and the protection pillar will withstand the huge pressure with the face advancing and dismantling, the five faults will have a greater impact for protection pillar integrity. The coal at the top of fault is difficult to let out cleanly, a large number of coal stranded in goaf. Because of the influence of F108 fault, lower part of the working face has the jumping surface at the F108 fault, a 2 m gap, which left a 45 m coal pillar, the surround of coal pillar has been pressed and forms float coal, which has create conditions for coal spontaneous combustion [7]. Therefore, the goaf of 7162 working face has a high risk of spontaneous combustion.

3. Air Leakage Detection in Goaf

The aim to air leakage detection is to find the air leakage passage and master the law of air leakage, which can provide the scientific basis for the formulation of fire prevention measures. Air leakage detection usually adopts the tracer technique to detect air leakage passage and leakage air volume, and has a more unique superiority to the research of the gas flow, especially for underground goaf, coal pillar, sealing area and so on, which personnel cannot reach the location.

There are two types of air leakage in 7162 goaf, one is from 7162 working face to 7162 goaf, and other is from 7160 nearby goaf to 7162 goaf through the protection pillar.

To fully grasp gas flow changes in goaf of 7162 working face in the recovery process; air leakage detection is divided into two phases according to production schedule. The first phase to use instantaneous release method to detect air leakage of the working face, we have a total of four air leakage tests, respectively in the recovery process of 100 m, 150 m, 200 m, 250 m, when measured air speed of air leakage which is from stopping face to goaf internal because of the roof falling and false filling. The second stage to use continuous release method to detect air leakage nearby goaf, we have a total of four air leakage tests, respectively in the recovery process of 300 m, 450 m, 560 m, 680 m when measured air leakage of nearby 7160 goaf to the working face through the fault in late recovery. The detection of working face air leakage is illustrated as follows.

3.1. Arrangement and Method of Air Leakage Detection

The second air leakage test in the air leakage detection of the first phase is shown on Figure 1, which mainly tested air leakage situation of goaf depth within the scope of 0 to 80m in 7162 working face rear. Release point is in the 80 m of goaf. Setting four sampling point to collect gas through the 40 frame of stopping face, 20 frame of stopping face, the upper corner and fire dam of 7160 goaf return airway; to analysis concentration changes of trace gas and to grasp the air leakage situation of goaf depth within the scope of 0 to 80 m.

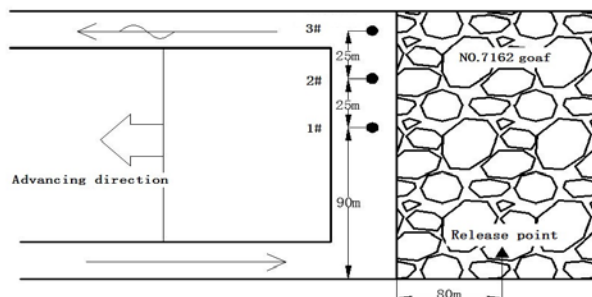


Figure 1. The schematic diagram of the second working face air leakage detection

Implementation method of air leakage detection is: to instantaneously release SF₆ gas to goaf through the reserve 80 m injection pipe in 7162 goaf, release flow is 15 L/min, release time is 30 min and release total is 450 L, to collect gas sample every 40 min respectively by three areas of No.40 frame and No.20 frame of stopping face and the upper corner after 500 min from releasing tracer gas, the collection number are 7 groups and 21 gas samples. The fourth sampling point can be further clear air leakage situation between 7162 working face and 7160 goaf. Only take three gas samples, sampling time respectively is 24 h, 48 h and 72 h.

3.2. Interpretation of Detection Results

We sent gas sample collected in the pit to the laboratory timely, and can get the tracer gas concentration of sampling points in the collection time through the analysis of gas chromatograph.

Detection results of the second working face air leakage is shown on Figure 2.

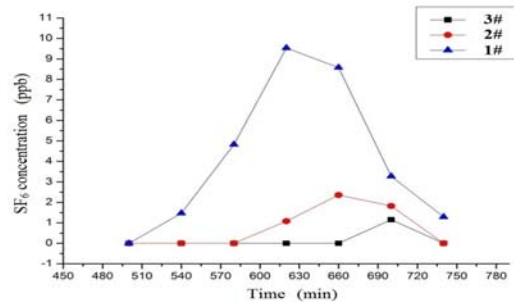


Figure 2. Tracer gas concentration changes of the second working face air leakage detection

We can reach the following conclusion from Figure 2:

- (1) SF₆ tracer gas is all detected in three sampling points, there are still air leakage passages even in the 80 m depth of goaf, but with the increase of the goaf depths, the compaction degree of goaf increases gradually, the air leakage intensity is also gradually weakened. The direction of air leakage is that air flow enters into goaf from below corner and gush from the working face near the return airway.
- (2) In 10 gas samples detected tracer gases, the gas samples collected at the same time are that the SF₆ concentration of upper corner is higher than the SF₆ concentration of the stopping face No. 20 frame, which higher than the SF₆ concentration of the stopping face No. 40 frame. It is confirmed that air leakage export in goaf is mainly the incompact roadway behind the upper corner, while the mid-lower of the stopping face is difficult to have air leakage passage due to compaction, the closer to axle wire of goaf, the little probability to air leakage.
- (3) The first occurrence time of tracer gas in each sampling point has interval, time difference is about 80 min. Each sampling point SF₆ concentration changing with time curve are approximate for normal distribution curve, through the curve fitting, to get the time of concentration peak to the upper corner, No. 20 frame, and No. 40 frame respectively for 637 min, 672 min and 700 min, and time difference is about 40 min. It shows that air leakage wind pressure from gas release point of the upper corner to each sampling point is greater when it is closer to return airway.
- (4) The time interval is 540 min from trace gases released to the first time detected the tracer gas, and the shortest distance between the release point to the sampling point is 168 m, the minimum air leakage speed is: $v = 168/540 = 0.0052$ m/s, air leakage wind speed is fall nearly 50% than the first air leakage detection speed.
- (5) The No. 4 sampling point still did not detect the tracer gas in the situation of prolonging the testing time, and at the same time, protection pillar has obvious mine pressure damage between 7162 working face and 7160 goaf in the test, and further remove the possibility which the air leakage direction is from 7162 working face to 7160 goaf, to master air leakage law from 7160 goaf to 7162 working face, air leakage test adjacent goaf is needed.

4. Model Establishment

4.1. Mathematical Model

4.1.1. Mathematical Model in Goaf

Goaf is generally regarded as porous media area composed of the crushing coal and rocks, and we can use the porous media seepage model to have the numerical simulation. To suppose that goaf gas is incompressible, its flow is steady state and isothermal process, porous medium in goaf is regarded as isotropic. Due to air leakage wind current relatively is small, we can approximately think airflow in goaf is laminar flow distribution, and airflow pattern complies with Darcy's law [8]. Usually there is an average of 27° dip angle in 7162 goaf, and there will be a 2 m head jump surface in the mining process, thus we have three-dimensional flow field simulation for goaf flow field.

Momentum (Navier-Stokes) equations are as follows:

$$\begin{aligned}
 & \frac{\partial(n\rho uu)}{\partial x} + \frac{\partial(n\rho uv)}{\partial y} + \frac{\partial(n\rho uw)}{\partial z} \\
 &= \frac{\partial}{\partial x} \left(n\mu \frac{\partial u}{\partial x} \right) + \frac{\partial}{\partial y} \left(n\mu \frac{\partial u}{\partial y} \right) + \frac{\partial}{\partial z} \left(n\mu \frac{\partial u}{\partial z} \right) - n \frac{\partial p}{\partial x} - \frac{\mu}{e} \cdot u \\
 & \frac{\partial(n\rho vu)}{\partial x} + \frac{\partial(n\rho vv)}{\partial y} + \frac{\partial(n\rho vw)}{\partial z} \\
 &= \frac{\partial}{\partial x} \left(n\mu \frac{\partial v}{\partial x} \right) + \frac{\partial}{\partial y} \left(n\mu \frac{\partial v}{\partial y} \right) + \frac{\partial}{\partial z} \left(n\mu \frac{\partial v}{\partial z} \right) - n \frac{\partial p}{\partial y} - \frac{\mu}{e} \cdot v \\
 & \frac{\partial(n\rho wu)}{\partial x} + \frac{\partial(n\rho wv)}{\partial y} + \frac{\partial(n\rho ww)}{\partial z} \\
 &= \frac{\partial}{\partial x} \left(n\mu \frac{\partial w}{\partial x} \right) + \frac{\partial}{\partial y} \left(n\mu \frac{\partial w}{\partial y} \right) + \frac{\partial}{\partial z} \left(n\mu \frac{\partial w}{\partial z} \right) - n \frac{\partial p}{\partial z} - \frac{\mu}{e} \cdot w
 \end{aligned} \tag{1}$$

In this pattern: u , v , and w are velocity vector component in the x , y , z direction, m/s ; ρ is goaf air density, m^3/kg ; μ is fluid dynamic viscosity, $kg/(m \cdot s)$; n is porous medium porosity.

The fluid motion in the porous medium is following Darcy's law:

$$\begin{aligned}
 u &= -K_x \frac{\partial \rho_x}{\partial x} \\
 v &= -K_y \frac{\partial \rho_y}{\partial y} \\
 w &= -K_z \frac{\partial \rho_z}{\partial z}
 \end{aligned} \tag{2}$$

In the pattern: K_x, K_y and K_z are respectively for permeability coefficient of x, y, z direction $m^2 / Pa \cdot s$.

4.1.2. Mathematical Model of the Working Face

The airflow of working face is turbulence, momentum equations are:

$$\begin{aligned}
 & \frac{\partial(\rho uu)}{\partial x} + \frac{\partial(\rho uv)}{\partial y} + \frac{\partial(\rho uw)}{\partial z} \\
 &= \frac{\partial}{\partial x} \left(\mu \frac{\partial u}{\partial x} \right) + \frac{\partial}{\partial y} \left(\mu \frac{\partial u}{\partial y} \right) + \frac{\partial}{\partial z} \left(\mu \frac{\partial u}{\partial z} \right) - \frac{\partial p}{\partial x} - \frac{\mu}{e} \cdot u \\
 & \frac{\partial(\rho vu)}{\partial x} + \frac{\partial(\rho vv)}{\partial y} + \frac{\partial(\rho vw)}{\partial z} \\
 &= \frac{\partial}{\partial x} \left(\mu \frac{\partial v}{\partial x} \right) + \frac{\partial}{\partial y} \left(\mu \frac{\partial v}{\partial y} \right) + \frac{\partial}{\partial z} \left(\mu \frac{\partial v}{\partial z} \right) - \frac{\partial p}{\partial y} - \frac{\mu}{e} \cdot v \\
 & \frac{\partial(\rho wu)}{\partial x} + \frac{\partial(\rho wv)}{\partial y} + \frac{\partial(\rho ww)}{\partial z} \\
 &= \frac{\partial}{\partial x} \left(\mu \frac{\partial w}{\partial x} \right) + \frac{\partial}{\partial y} \left(\mu \frac{\partial w}{\partial y} \right) + \frac{\partial}{\partial z} \left(\mu \frac{\partial w}{\partial z} \right) - \frac{\partial p}{\partial z} - \frac{\mu}{e} \cdot w
 \end{aligned} \tag{3}$$

Standard k - ε equations are:

$$\begin{aligned}
 & \frac{\partial(\rho ku)}{\partial x} + \frac{\partial(\rho kv)}{\partial y} + \frac{\partial(\rho kw)}{\partial z} \\
 &= \frac{\partial}{\partial x} \left(\mu + \frac{\mu_t}{\sigma_k} \right) \frac{\partial k}{\partial x} + \frac{\partial}{\partial y} \left(\mu + \frac{\mu_t}{\sigma_k} \right) \frac{\partial k}{\partial y} + \frac{\partial}{\partial z} \left(\mu + \frac{\mu_t}{\sigma_k} \right) \frac{\partial k}{\partial z} + G_k - \rho \varepsilon \\
 & \frac{\partial(\rho \varepsilon u)}{\partial x} + \frac{\partial(\rho \varepsilon v)}{\partial y} + \frac{\partial(\rho \varepsilon w)}{\partial z} \\
 &= \frac{\partial}{\partial x} \left(\mu + \frac{\mu_t}{\sigma_\varepsilon} \right) \frac{\partial \varepsilon}{\partial x} + \frac{\partial}{\partial y} \left(\mu + \frac{\mu_t}{\sigma_\varepsilon} \right) \frac{\partial \varepsilon}{\partial y} + \frac{\partial}{\partial z} \left(\mu + \frac{\mu_t}{\sigma_\varepsilon} \right) \frac{\partial \varepsilon}{\partial z} + \frac{\varepsilon}{k} (C_{1\varepsilon} G_k - C_{2\varepsilon} \rho \varepsilon)
 \end{aligned} \tag{4}$$

In this pattern: $C_{1\varepsilon} = 1.44$, $C_{2\varepsilon} = 0.09$, $\sigma_k = 1.0$, $\sigma_\varepsilon = 1.3$; k is turbulent kinetic energy, m^2/s^2 , ε is turbulent kinetic energy dissipation rate, m^2/s^3 ; μ is fluid turbulence kinetic viscosity, $kg/(m \cdot s)$; G_k is production item of the turbulent kinetic energy k caused by the average velocity gradient.

4.2. Physical Model

According to analysis results of the 7162 working face air leakage detection, make numerical simulation for 7162 goaf air leakage airflow field. The simulation aims at recovery stage which air leakage is larger, in this paper, we have eight times simulation, take the 6th numerical simulation as an example. The sixth numerical simulation simulates air leakage airflow field of recovery 450 m goaf, this is corresponding to goaf airflow field of the second adjacent goaf air leakage detection. The stopping face produced a gap of 2 m jump surface under the influence of the F108 fault, near the inlet airway, make a 45m × 15m coal pillar which cannot be recovery, because of the presence of coal pillar, near pillar roadway compaction situation will be affect.

The dip angle of 7162 goaf is bigger, without the influence of gas drainage, interlayer pressure regulating and other external conditions, accord with three dimensional nonlinear seepage laws, namely goaf physical model is three dimensional seepage models. The physical model of the 6th numerical simulation is shown on Figure 3. The length, width, height and angle of goaf is 200 m, 150 m, 6 m and 27°; in the inlet airway of goaf, apart 20 m distance from the working face, there is a 45m × 15m coal pillar; the length, width, height and angle of the working face is 150 m, 10 m, 3 m and 27°, inlet airway and outlet airway have the same length of 20 m, the same width of 5m, set up the 3D model two sources and

a convergence, and use GAMBIT software for meshing. The origin of coordinates set in left bottom of goaf, the direction to pointing inlet air side is the Y axis positive direction, the direction to pointing working face is the X axis positive direction, vertical XY flat surface external direction is Z axis positive direction, grid steps of three directions all take 0.5 m, namely mesh size is 0.5 m × 0.5 m × 0.5 m.

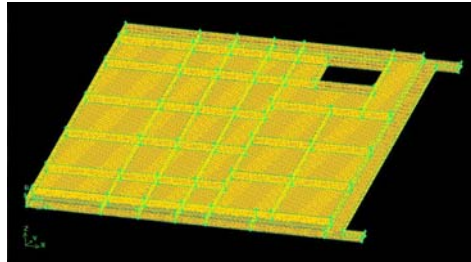


Figure 3. The physical model for the sixth time numerical simulation

4.3. Boundary Conditions

Inlet boundary: set two inlet airways for velocity – inlet, average wind speed is 1.1m/s, balance wind flow which is vertical inlet airway entrance enter into roadway;

Export boundary: set for free outflow;

Wall boundary: all walls are no slip boundary conditions, namely $u = v = w = 0$, the working face near wall can be used standard wall function method processing, regard wall as adiabatic treatment; roughness height of coal mining wall surface is set for 0 m; take the default value C_s for 0.5;

The boundary between working face and goaf: set for internal boundary;

Leakage wind source inlet boundary: set for velocity – inlet according to analysis results of 7162 working face air leakage detection.

According to the mathematical model, we need to set permeability and inertial resistance coefficient in goaf. The value of permeability e and inertial resistance coefficient C_2 can be got through two methods of the experimental measurement and the empirical formula, this article mainly uses Blake-Kozeny formula for the experience formula.

5. Results Analysis of Numerical Simulation

5.1. Air Pressure Distribution in Goaf

Usually roof management method in goaf is all caving, the air flow of working face and the air flow adjacent goaf under the action of pressure difference permeate goaf, forming leakage air field, and therefore the airflow situation in goaf depends on pressure distribution in goaf. The concrete results of the 6th numerical simulation are shown on Figure 4.

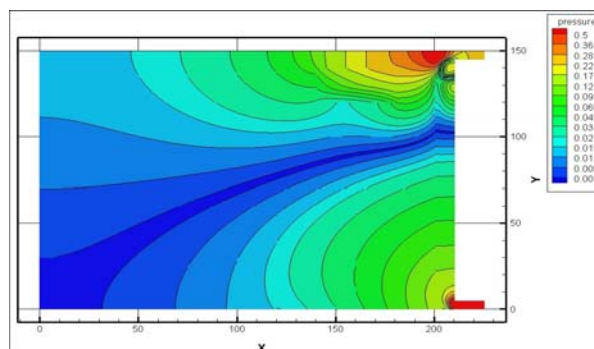


Figure 4. Air pressure distribution in goaf with 1.5 m height from the floor

In the analysis of cross section with 1.5 m height from the floor and parallel to the floor; the height of the roadway is 3 m, roadway resistance of air flow is least in this section. The wind pressure plane distribution in goaf with 1.5m height from the floor is as shown on Figure 4. In the picture, the left bottom in goaf subsurface is origin (0, 0), direction along goaf is X axis, direction along the working face is Y axis.

We can see from the Figure 4, the pressure of inlet airway in goaf is maximum, Along the goaf depth direction, wind present reduced gradually, the distance from the working face is about 120 m, wind pressure almost no longer change; Along the tendency direction, wind pressure distribution is diminishing from the entrance to the working face centre and is increasing from working face centre to export. At the same time, pressure gradient in both ends of goaf near the working face are maximum, isobar distribution in the Y axis direction is denser than in X axis direction; namely change trends of wind pressure along Y axis are larger than X axis. Due to the presence of coal pillar reserves, making the air pressure line discontinuity in the pillar position.

5.2. Air Speed Distribution in Goaf

Simulation results of air speed distribution in goaf are shown on Figure 5.

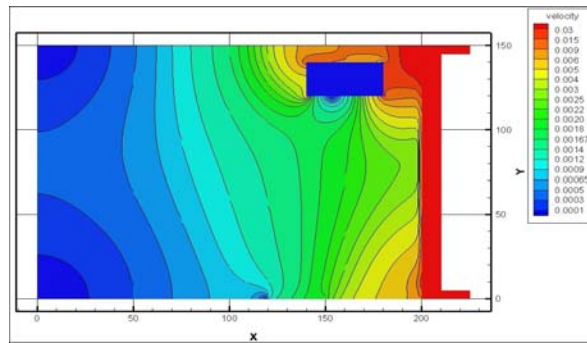


Figure 5. Air speed distribution in goaf with 1.5 m height from the floor

In the analysis of cross section with 1.5 m height from the floor and parallel to the floor; on Figure 5, left bottom in goaf subface is origin (0, 0), direction along goaf is X axis, direction along the working face is Y axis.

We can see from Figure 5, velocity change is maximum near air inlet and air outlet, in the middle of the working face, velocity change is minimum. In the depth of goaf, air leakage speed becomes smaller; in the distance from working face more than 100 m (X = 100 m) or so, air flow almost does not exist in goaf.

Due to the presence of reserve coal pillar, make “corridor effect” in reserve coal pillar and edge side, extended compaction time in goaf. In the “corridor” position, air speed is bigger than without reserve coal pillar, airflow can more easily into goaf inside, while in the other side of the reserve coal pillar, there is a calm area due to the blocking effect of the coal pillar.

Through curvilinear integral in the speed of 75 ~ 150m, we can respectively obtain leakage air volume with 0.035 m³/s, 0.073 m³/s and 0.184 m³/s, when X is 100 m, 150 m and 190 m. Namely leakage air volume from the working face to goaf when X is equal to the 190 m is 5 times than leakage air volume when X is equal to the 100 m.

5.3. Results Analysis of Numerical Simulation

- (1) The air leakage in goaf includes two kinds. One is that ventilation airflow of the working face leaks to own goaf; the other is that airflow adjacent goaf leaks to goaf through protection coal column, faults and so on.
- (2) Air leakage detection can get basic air leakage distribution law in goaf, and provide relevant data for the computer numerical simulation. Air leakage channels of working face in 7162 goaf are more obvious, minimum air leakage speed decreased with depth increasing; air leakage adjacent goaf related to completeness degree of the coal pillar and fault size.
- (3) Using the FLUENT software to simulate goaf seepage field and get distribution law of air pressure and air speed in goaf, and provide the basis for preventing coal spontaneous combustion. Due to the existence of reserve coal pillar, the coal pillar and face side together form a “corridor effect” to extend the compaction time in goaf, and the airflow is easier to enter goaf interior.

References

1. Yan Hu, Zhao Changjiang. (2010). The Analysis and Safety Technology of full-mechanized mining technology in steeply inclined coal seam. *Shandong Coal Science and Technology*, 16(1), 112–113.
2. Yang Yong, Shi Huitang. (2009). Application of tracing technology in testing air leakage in coal mine gob areas. *China Coal*, 35(2), 152–55.
3. Li Zongxiang, Hai Guozhi, Qin Shuyu. (2008). Numerical simulation and visual display of air flow pattern in goaf. *Journal of China Coal Society*, 55(1), 76–80.
4. Qin Shuyu, Zhao Shutian, Li Enru. (2006). Mathematical Models for Early Prediction of Mine Fires. *Systems Engineering Theory and Practice*, 22(1), 28–33.
5. Wang Jikai, Bao Xuebin, Ding Yangwei. (2009). Numerical Simulation on Gob Air Leakage Flow Field by Fluent. *Shandong Coal Science and Technology*, 12(1), 86–87.
6. Gao Jianliang, Wang Haisheng. (2010). Influence of Permeability Distribution on Airflow Field of Leakage in Gob. *China Safety Science Journal*, 20(3), 81–85.
7. Qin Botao, Wang Deming. (2007). Present Situation and Development of Mine Fire Control Technology. *China Safety Science Journal*, 17(12), 80–85.
8. Li Yongcun, Lin Aihui. (2008). Numerical Simulation and Experimental Research on Flow Field in Goaf Under the Airflow Fluctuating. *Engineering Sciences*, 10(2), 41–45.

Received on the 20th of May 2013

SIMULATION OF SYSTEMS INFORMATION SECURITY

S. Amanzholova, N. Zhakayev

International IT University
Department of the Computer Science and Software Engineering, Almaty, Kazakhstan
E-mail: shokataeva@gmail.com, nurik27_@mail.ru

As is well-known, the processes related to security – these are the same processes that take place in computer and telecommunication networks. IT Security involves the study processes starting from user authentication. Then came the authentication of users, and finally, began to use the authorization process. All these stages are only for customers or clients to have access to the necessary resources. After of the identification and authentication begins the processes related to access to resources, data integrity, password-protected sites, data encryption, adding digital signatures to documents, etc. For a detailed research of all processes involved in the creation of information security can be used very well established mathematical models queuing, i.e., queuing systems. The model of queuing systems, i.e., a perfect mathematical tool allows us to investigate any variants of information security systems. To create a reliable system of information security, we need to create a model of the system to accurately simulate the behaviour of the system being close to real conditions. Simulation of different objects lets us look at the problem from different points of view and identify system bottlenecks, as well as to offer the most appropriate option for the task.

Keywords: systems information security, computer and telecommunication networks, queuing systems

Introduction

Simulation of information security consists in the construction of its image of a corresponding (up simulation purposes) of the system, and gets through the necessary characteristics of the generated model of a real system [1, 2, 4]

For determining behavioural characteristics of the system one can use the well-known methods for modelling.

- Analytical – the model is a set of analytical and (or) logical dependencies, allowing to define the necessary characteristics by performing calculations on these dependencies.
- Statistics – the simulated system is represented in the form of an analogue reflecting for defined characteristics depending on the actual system. Determination of the values of these characteristics is accomplished by multiple imitation realization dependence of the characteristics of significantly important parameters of the real system and the external environment and the statistical treatment of the results set.

The most characteristic circumstances of imitating models are as follows:

- If there is a process of knowing the object simulation.
- If the analytical methods for studying are available but constituting them math routines are very complicated and time-consuming.
- If required to observe the behaviour of the components of the system for some time.
- If required control the flow of processes in the system by the deceleration or acceleration the phenomena in the course imitation.
- If the is of particular importance the sequence of events in the projected system and the model used to predict the so-called “narrow” places.
- By preparation of experts to acquire the necessary skills in the exploitation of new techniques.
- If the imitation modelling is the only way to research because of the inability of real experiments.

We indicate a number of basic merits and demerits of the method of simulation modelling [5].

The main advantages are as follows:

- Imitating model allows, in principle, to describe the simulated process with greater adequate than the others.
- Imitating model possesses a certain flexibility of varying structures, algorithms and parameters of the system.
- Use of electronic computers significantly reduces the duration of tests, compared with full-scale experimental data (if it is possible), and the estimated cost.

The main drawbacks are as follows:

- The solution obtained by imitation model, always is an individual, because it represents the fixed elements of the structure, algorithms, behaviour, and values of the system parameters;
- The high labour costs of creating a model and experiments, as well as the processing of their results.
- The use of the system assumes the participation of people in conducting machine experiment, the results may influence the effect of the so-called hautornsky (is the fact that people, knowing (feeling) that they are being watched, can change their usual behaviour).

Analytical modelling – is a mathematical method of research logistics systems, allowing to obtain accurate solutions.

For analytical modelling characteristic that processes of functioning the system are written as the functional relations (algebraic, differential, integral equations). The analytical model can be investigated by the following methods:

- 1) analytical, when seek to obtain in general form explicit dependencies for characteristics of systems;
- 2) number when one fails find a solution to the equations in general form and solve them for the specific initial data;
- 3) qualitative when for absence of a decision finding some of its properties.

Analytical models can be obtained only for comparatively simple systems. For complex systems often arise great mathematical problems. For the application of the analytical method are the substantial simplifications of the original model. However, a study on a simplified model helps to get only indicative results. Analytical models mathematically reflect connection between input and output variables and parameters. But their structure does not reflect the internal structure of objects.

Take as an example process of identification, authentication.

For the description of the given process one can use the usual and widely known single-channel two-phase model [6]. In the given model it can be assumed that an exponential character enables the query to the system. Between the first and second phases of the queue will be limited. Before the authentication phase will assume infinite queue. For the calculation of the model let's determine b_1 and b_2 ; where b_1 – the service time in the first phase; where b_2 - service time in the second phase.

In this model the first phase – a phase of identification, the second phase – the phase of authentication (Figure 1).

The given scheme can be represented as a two-phase model:

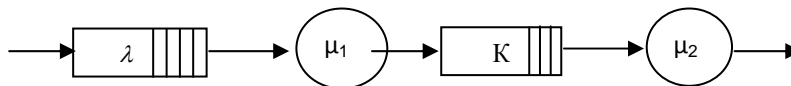


Figure 1. The single-channel two-phase model of identification and authentication

To exceptions loss of orders due to buffer overflow is entered the lock state into which the system in the absence buffer location the second phase. Quit this state occurs in if released of buffer space the second phase.

For exclusion from the analysis of the input stream applications the existence of an infinite input buffer queue is assumed (Figure 2).

In the present case two situations will be evaluated:

- 1) it is provided and applications are blocked in the devices of the corresponding phases;
- 2) in the phase places absent for service and blocked the application.

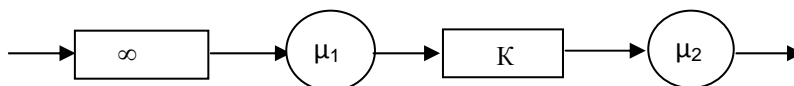


Figure 2. Model identification and authentication, where $\mu_1 = \frac{1}{b_1}$ and $\mu_2 = \frac{1}{b_2}$.

For a more detailed description of the model, we introduce the notation:

$P_{ij}(n)$ – the probability of state of the system where the state of the first phase is characterized by the index i , and the state of the second phase is characterized by the index j ,
 n – the number of applications in the buffer of the second phase, with values $n = 0 \div k$.

Computer Simulation

The first phase may take the values $i = \{1, \beta\}$, the second phase can take the values $j = \{0, 1\}$

If $i = 1$, this means that the phase is in a state service, if $i = \beta$, then this state is locked.

If $j = 0$, the second phase stands idle in anticipation orders from the first phase, if $j = 1$, the second phase is in a state service.

In the analytical simulation of queuing systems it is necessary to make the state graph transitions of the system (Figure 3):

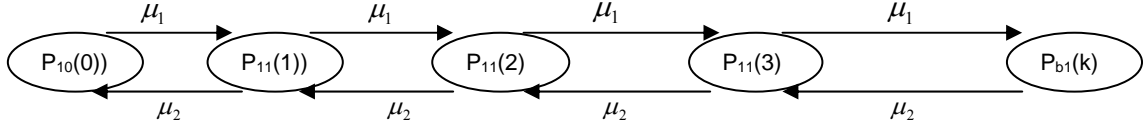


Figure 3. State graph transitions two-phase model

where

$P_{10}(0)$ – this is a zero state systems,

$P_{11}(n)$ – the state of the system at k -applications,

$P_{\beta 1}(k)$ – the last possible state of the system.

For this model, the equations of balance are true

$$\begin{aligned} \mu_1 P_{10}(0) &= \mu_2 P_{11}(1) \\ (\mu_1 + \mu_2) P_{11}(1) &= \mu_1 P_{10}(0) + \mu_2 P_{11}(2) \\ (\mu_1 + \mu_2) P_{11}(n) &= \mu_1 P_{11}(n-1) + \mu_2 P_{11}(n+1), \quad n = \overline{1, k} \\ &\dots\dots \\ &\dots\dots \\ \mu_2 P_{\beta 1}(K) &= \mu_1 P_{11}(K-1) \end{aligned} \quad (3)$$

with the normalization condition

$$P_{10}(0) + P_{\beta 1}(K) + \sum_{n=1}^{K-1} P_{11}(n) = 1. \quad (4)$$

From this normalization condition find the probability $P_{10}(0)$

$$P_{10}(0) = \left[\sum_{r=0}^k \rho^r \right]^{-1}, \quad (5)$$

while the remaining probabilities from recurrence formulas

$$P_{11}(n) = \rho^n \cdot P_{10}(0), \quad (6)$$

$$P_{\beta 1}(n) = \rho^k \cdot P_{10}(0). \quad (7)$$

To understand the behaviour of the model in real conditions let's use the following coefficients:

$$\eta_1 = 1 - P_{\beta 1}, \eta_2 = 1 - P_{10}, \quad (8)$$

where

$R_{\beta 1}$ – the probability of blocking I -th phase.

Throughput the system is equal $\varpi = \mu_1 \eta_1 = \mu_2 \eta_2$.

Average queue length in the buffer of the second phase is calculated by the formula:

$$m = \sum_{r=2}^{k-1} (r-1) * P_{11}(r) + P_{\beta 1}(K-1) * P_{\beta 1}(K). \quad (9)$$

The average waiting time in the queue:

$$q = \sum_{r=1}^{k-1} r * v_2 P_{11}(r) + k * v_2 P_{\beta 1}(k). \quad (10)$$

The average residence time in the system:

$$U = \frac{1}{\omega} + q + \nu_2, \quad (11)$$

where

$$\nu_2 = \frac{1}{\mu_2} \text{ -- the average time to the application in the first phase,}$$

$\frac{1}{\omega}$ -- average time of application in the first phase. It in turn is made up of the average service time

$$\nu_1 = \frac{1}{\mu_1} \text{ and blocking } \tau_{\beta 1} \text{ orders in the first phase, } \frac{1}{\omega} = \nu_1 + \tau_{\beta 1}.$$

Based on the calculated characteristics, we can estimate the behaviour of the system in real conditions.

References

1. Thesis "Stochastic Models and Methods of Information Security Processes in a Distributed Computing System Information System as on an Example of Distance Education". Almaty: KazNTU by K. I. Satpaeva. (In Russian)
2. Aliyev, T. (2009). *Basics of modelling discrete systems*. St. Petersburg: St. Petersburg State University of Information Technologies. (In Russian)
3. Vishnevsky, V. M. (2003). *Theoretical bases of designing computer networks*. M.: Tekhnosfera.
4. Amanzholova, S. T., Uskenbaeva, R. K. (2011). An integrated approach to the metric system of information security. In Proceedings of the 2nd International Scientific-practical Conference "Information and Innovative Technologies: Integration of Science, Education and Business", devoted to the 20th anniversary of Independence of the Republic of Kazakhstan, 1–2 December 2011. Almaty, Kazakhstan. (In Russian).
5. Ermakov, A., Amanzholova, S. T. (2006). The assessment of the parallel key generation by the "client-server" technology. In Proceedings of the Intern. Symp. "Information Technology and Systems in the Industry, Education and Science" (pp. 95–97). Karaganda. (In Russian).
6. Ermakov, A., Amanzholova, S. T. (2009). Model of identification and authentication information distributed computing system as on an example of distance education. *Math. NTO "Qakhaq"*, 1(23), 11–17. (In Russian)

Received on the 11th of March 2013

REAL-TIME FACIAL FEATURE POINT DETECTION AND TRACKING IN A VIDEO SEQUENCE

B. B. Abisheva¹, B. M. Baisakov², M. M. Maratov¹

*¹International IT University, Faculty of Information technologies
Almaty, Kazakhstan*

*²Kazakh-British Technical University, Faculty of Information technologies
Almaty, Kazakhstan*

Several algorithms for feature detection were compared and the most efficient ones were chosen to detect facial feature points such as eye corners, eyeballs, mouth corners and nostrils. To detect the desired feature points, first face detection was run using Viola-Jones's algorithm that is based on Haar-like features. Having found a face in an image, the face was searched for eyes, nose and mouth. Having found the necessary facial features, those regions of the image containing them were searched for the specific feature points described above.

For feature tracking several algorithms were compared as well. As a result of the comparison the algorithm of Lucas-Kanade was chosen to be performed on the detected points.

The resultant algorithm detects the feature points to be tracked in the first frame of a video-sequence and then uses these points in the Lucas-Kanade algorithm for tracking. In case more than two points are lost during tracking, feature point detection is run again. This way the algorithm tracks feature points accurately, without lagging in real-time.

Keywords: video sequences, real time tracking for the image points, Lucas-Kanade tracking algorithm

1. Introduction

Object detection and tracking in a video sequence is not a new topic in the area of computer vision, there already are a lot of algorithms proposed to solve this problem. However, a lot of research effort is still being put into this field because of an increased demand in various applications for this technology, such as video surveillance, video-conferencing, information security, access control, video search, etc. Each year more and more efficient and accurate algorithms are being proposed [2]. Mostly these algorithms are either for detecting some feature points in an image, or tracking movement in a video-stream. In this paper we are going to compare several existing algorithms for feature detection in an image, select the most suitable ones, add some modifications and present our own version of an algorithm for facial feature point's detection. This algorithm will be used to detect feature points of a human face in the first frame of a video-stream. After that detected points will be fed to the modified version of Lucas-Kanade algorithm, which was found to be the most useful for our purposes [1], for tracking.

2. Detecting Facial Feature Points

A feature point is a point that constitutes an "interesting" part of an image. It can be either a corner, or an edge, or a blob etc. For our purposes, facial feature points are the corners of eyes and mouth, eyeballs and nostrils.

First of all, our algorithm starts by detecting a face in an image using the famous Viola and Jones face detection algorithm [3]. This algorithm is based on Haar-like features, which encode the existing oriented contrast between regions in an image. For our purposes we use a cascade of boosted classifiers working with Haar-like features that was already trained to detect front faces. In the computer vision library OpenCV there is a function suitable for this problem.

CvSeq* `cvHaarDetectObjects(constCvArr* image, CvHaarClassifierCascade* cascade, CvMemStorage* storage, double scaleFactor, intminNeighbors, int flags, CvSizeminSize)`

Parameters:

image – Image to detect objects in

cascade – Haar classifier cascade in internal representation

storage – Memory storage to store the resultant sequence of the object candidate rectangles

scale_factor – The factor by which the search window is scaled between the subsequent scans, 1.1 means increasing window by 10%

min_neighbours – Minimum number (minus 1) of neighbour rectangles that makes up an object. All the groups of a smaller number of rectangles than min_neighbours-1 are rejected. If min_neighbours is 0, the function does not any grouping at all and returns all the detected candidate rectangles, which may be useful if the user wants to apply a customized grouping procedure

flags – Mode of operation. Currently the only flag that may be specified is CV_HAAR_DO_CANNY_PRUNING. If it is set, the function uses Canny edge detector to reject some image regions that contain too few or too much edges and thus cannot contain the searched object. The particular threshold values are tuned for face detection and in this case the pruning speeds up the processing

min_size – Minimum window size. By default, it is set to the size of samples the classifier has been trained on (for face detection) [10].

Having detected a face in an image, we define areas of the most probable locations of eyes, nose and mouth using existing anthropometric proportional dependencies of a human face [4], [5], [6]. Then these locations are scanned using appropriate Haar classifier cascades to detect the exact positions of facial features. From this point every facial feature is processed separately in order to find the necessary feature points for subsequent tracking (i.e. eye corners, eyeballs, nostrils and mouth corners).

For nostril detection we use the fact that nostrils differ with their darkness from the surrounding area [6]. The area where the nose was detected is searched for the two darkest patches and then the centres of these patches are identified as the nostrils.

For eye areas several algorithms, including Moreira algorithm [4], Canny edge detection and FAST corner detection algorithm [7], [8], were tested. Moreira’s algorithm introduced too much noise if images were not of a good quality and the eye corners could not be found accurately. However slight modification to the algorithm turned helpful in eyeball detection. Firstly non-skin pixels of the eye areas were highlighted by inverting the red component of every pixel. Then the area was binarized. The binary image B_w was found using the proposed equation:

$$B_w = \begin{cases} 1, & \text{if } I > (\bar{I} + Z\sigma) \\ 0, & \text{otherwise} \end{cases}, \tag{1}$$

where \bar{I} and σ are the average and the standard deviation of pixels’ intensity of I respectively, and Z is a score that controls the amount of pixels that will be selected to belong to the binary image B_w . The parameter Z was calibrated, as advised by the authors, in order to achieve the best results [4]. Then this binarized image was used to define the biggest blob in the middle and its centre was identified as the eyeball.

In order to find the eye corners, Canny edge detection was found unsuitable, as it did not give enough information and not all corners could be found. When trying FAST algorithm [7], [8], it showed accurate results in corner finding. Out of all corners retrieved by the FAST algorithm, the farthest left and farthest right ones were identified as eye corners.

For mouth corner detection we also used FAST algorithm for the same reasons as for the eye corner detection.

Figure 1 and Table 1 shows the results of running the algorithm on 48 2D images of 50 human faces.

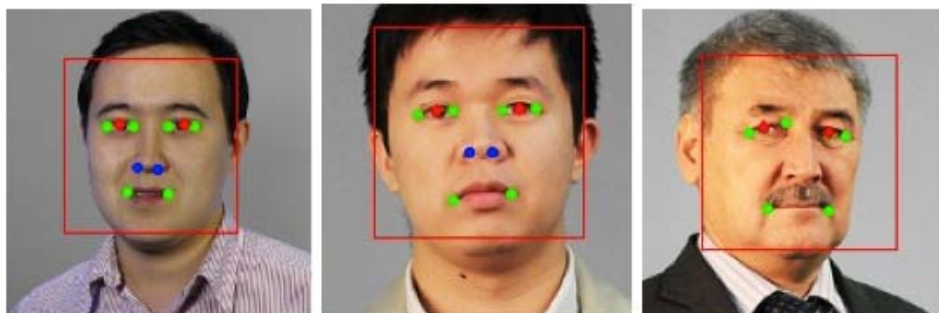


Figure 1. Results of testing the algorithm on 2D face images

Table 1. Results of running the algorithm on 2D face images

Feature being detected	Correctly detected	Incorrectly detected	Undetected
Face	49	0	1
Eye	96	0	4
Eyeball	91	3	6
Eye corners	70	19	11
Nose	39	0	11
Nostrils	67	4	29
Mouth	48	1	2
Mouth corners	89	6	7

3. Tracking Feature Points in a Video Sequence

Feature point tracking is performed using the optical flow algorithm. In the computer vision library OpenCV there are several functions that perform this task (void cvCalcOpticalFlow*).

Having compared three most popular algorithms for feature point tracking in a video sequence [1], it was decided that for the given task, a modified version of Lucas-Kanade algorithm [9] was the most suitable.

This algorithm is widely used in computer vision, also known as a local method of differential optical flow. The basic equation of optical flow comprises two unknowns and cannot be resolved unambiguously. Algorithm of Lucas-Kanade avoids ambiguity by using information of neighbouring pixels at each point. The method is based on the assumption that the local neighbourhood of each pixel value has the same optic flow, so you can write down the basic equation of optical flow for all pixels in the neighbourhood and solve the resulting system of equations by the method of least squares.

Lucas-Kanade algorithm is less sensitive to the noise in the images than point wise methods. However, it is purely local and cannot determine the direction of the pixels within the homogeneous regions. Let x – a feature of the first function F , to find a point $x + h$ function G , that the difference in area of these points as a minimum. The distance between the surroundings can be written as:

$$E = \sum [F(x + h) - G(x)]^2, \tag{2}$$

where you can get the value for h:

$$h = \left[\sum_x \left(\frac{dF}{dx} \right)^T [G(x) - F(x)] \right] \left[\sum_x \left(\frac{dF}{dx} \right)^T \left(\frac{dF}{dx} \right) \right]^{-1}. \tag{3}$$

In OpenCV, this algorithm is implemented by function:

void cvCalcOpticalFlowPyrLK(constCvArr* prev, constCvArr* curr, CvArr* prevPyr, CvArr* currPyr, const CvPoint2D32f* prevFeatures, CvPoint2D32f* currFeatures, int count, CvSizewinSize, int level, char* status, float* track_error, CvTermCriteria criteria, int flags)

Parameters:

prev – First frame, at time t

curr – Second frame, at time t + dt

prevPyr – Buffer for the pyramid for the first frame. If the pointer is not NULL, the buffer must have a sufficient size to store the pyramid from level 1 to level level; the total size of (image_width+8)*image_height/3 bytes is sufficient

currPyr – Similar to prevPyr, used for the second frame

prevFeatures – Array of points for which the flow needs to be found

currFeatures – Array of 2D points containing the calculated new positions of the input features in the second image

count – Number of feature points

winSize – Size of the search window of each pyramid level

level – Maximal pyramid level number. If 0, pyramids are not used (single level), if 1, two levels are used, etc

status – Array. Every element of the array is set to 1 if the flow for the corresponding feature has been found, 0 otherwise

track_error – Array of double numbers containing the difference between patches around the original and moved points. Optional parameter; can be NULL

criteria – Specifies when the iteration process of finding the flow for each point on each pyramid level should be stopped

flags –

Miscellaneous flags:

CV_LKFLOWPyr_A_READY pyramid for the first frame is precalculated before the call

CV_LKFLOWPyr_B_READY pyramid for the second frame is precalculated before the call

CV_LKFLOW_INITIAL_GUESSES array B contains initial coordinates of features before the function call [9].

The first image in the video sequence is scanned for the feature points and then Lucas-Kanade algorithm is fed the defined points for tracking. In the case of losing two or more feature points, the next frame of the video-sequence is used for detecting the feature points from scratch. This way, the window for Lukas-Kanade algorithm is reduced to produce more efficient results.

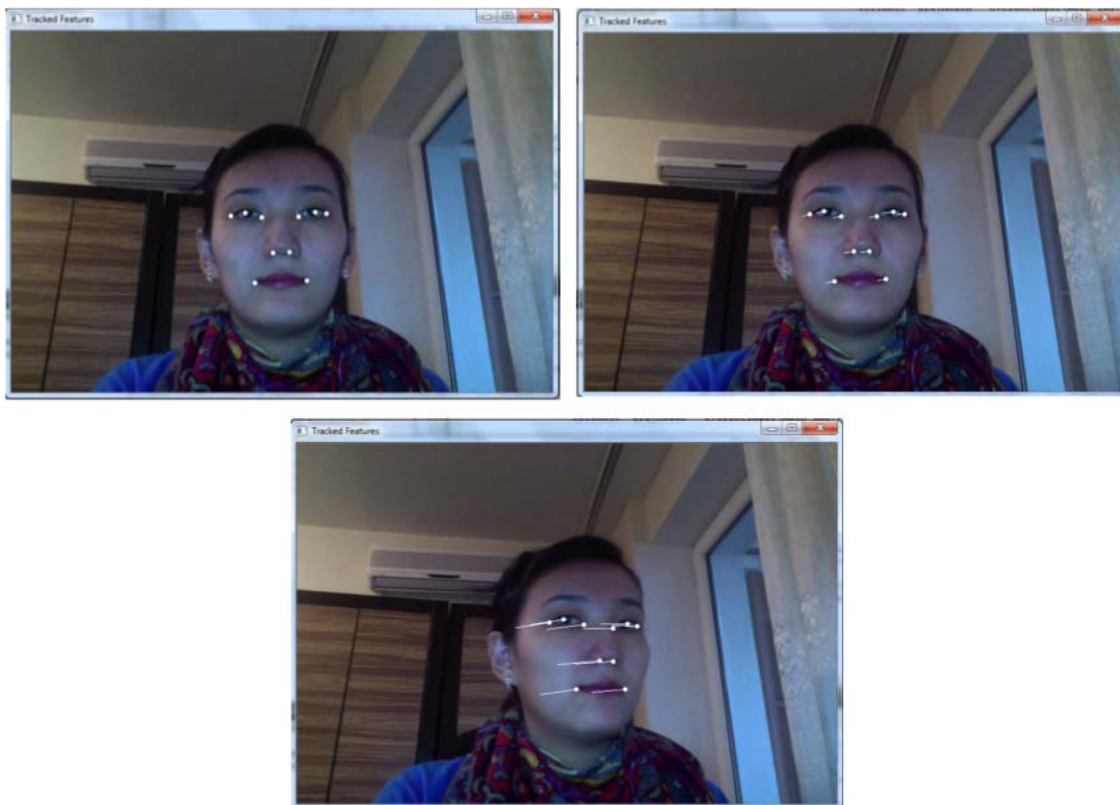


Figure 2. Testing the algorithm on a video sequence

4. Conclusions

As a result of testing several algorithms for feature detection, it was found that the best results are achieved using the combination of modified versions of several of them. It was found that FAST corner detection algorithm was the most accurate in finding the corners in an image. In order to increase efficiency the FAST algorithm was used only on previously reduced areas of interest. For nostril and eyeball detection modified versions of Chen [6] and Moreira [4] algorithms were used.

For feature tracking a modified version of Lucas-Kanade algorithm was used. It was given the specific points, which were detected in the first frame only, to track. This way the algorithm tracks the feature points without lagging.

In the end we received an algorithm that detects facial feature points and tracks them in a video sequence in real time.

References

1. Baisakov, B. M., Akshabayev, A. K., Maratov, M. M., Abisheva, B. B., Naizabayeva, L.(2012). The problem of tracking in real time for the image points in the video, *Bulletin of the Kazakh National University by K. I. Satpayev*, 4.
2. Yan Yan & Zhang Yu-Jin.(2009). State-of-the-Art on Video-Base Face Recognition,*Chinese Journal of Computers*, 32(5), 878–886.
3. Viola, P. & M. Jones. (2001). Robust real-time object detection.*International Journal of Computer Vision*, 57 (2), 137–154.
4. Moreira, J., Braun, A. & S. Musse. (2010). Eyes and Eyebrows Detection for Performance Driven Animation. In Proceedings of the 23rd Conference on Graphics, Patterns and Images (SIBGRAPI), Aug. 30 2010–Sept. 3 2010, GRAMADO, from BRAZIL <http://ieeexplore.ieee.org/xpl/mostRecentIssue.jsp?punumber=5719744>
5. Hua Gu Guangda & Su Cheng Du. (2003). Feature Points Extraction from Faces, *Image and Vision Computing NZ*, Palmerston North, November 2003 , pp.154–158 from <http://starttrinity.com/videorecognition/Resources/FacialFeaturePointsDetection/feature%20points%20extraction%20from%20faces.pdf>
6. Chen, J. & O. Lemon. (2009). Facial Feature Detection and Tracking in a New Multimodal Technology-Enhanced Learning Environment for Social Communication. In IEEE International Conference on Signal and Image Processing Applications, 2009 Signal and Image Processing Applications (ICSIPA), 2009 IEEE International Conference on 18–19 Nov. 2009 KUALA LUMPUR, MALAYSI from <http://ieeexplore.ieee.org/xpl/mostRecentIssue.jsp?punumber=5472904>
7. Rosten, E. & T. Drummond. (2005). Fusing points and lines for high performance tracking. In: IEEE International Conference on Computer Vision, 2005 Computer Vision, 2005. ICCV 2005. Tenth IEEE International Conference on 17–21 Oct. 2005, Beijing. China from <http://ieeexplore.ieee.org/xpl/mostRecentIssue.jsp?punumber=10347>
8. Rosten, E. & T. Drummond. (2006). Machine learning for high-speed corner detection. In European Conference on Computer Vision, 2006 9th European Conference on Computer Vision, Graz, Austria, May 7–13, 2006 from http://www.edwardrosten.com/work/rosten_2006_machine.pdf
9. http://opencv.willowgarage.com/documentation/c/video_motion_analysis_and_object_tracking.html
10. http://opencv.willowgarage.com/documentation/object_detection.html

DESIGN AND ANALYSIS OF NEGATIVE VALUE CIRCUIT COMPONENTS IN PSpICE SIMULATION SOFTWARE

A. Ferikoğlu¹, Ya. Sari², R. Köker³

¹*Sakarya University Technology Faculty
 Electrical and Electronics Engineering Department 54187 Sakarya – TURKEY
 E-mail: af@sakarya.edu.tr*

²*Sakarya University Hendek Vocational High School
 Electronics and Automation Department Hendek – Sakarya – TURKEY
 E-mail: sari@hotmail.com*

³*Sakarya University Technical Education Faculty
 Electronics and Computer Sciences Department 54187 Sakarya – TURKEY
 E-mail: rkoker@sakarya.edu.tr*

This paper describes the transaction to generate and measure negative valued resistors, capacitors and inductors in Pspice simulation medium for an educational purpose. Negative circuit components are designed and their defining characteristics are produced. An op-amp based generic circuit is used for obtaining negative components. To extract characteristics, a charge-meter and a flux-meter are designed and utilized, in addition to the conventional meters (markers) in the Pspice environment. The numerical examples verify the relevant background theory and validate the designed meters, namely flux meter and charge meter, in simulation medium. The study of the paper have educational value in making clear the meaning of negative impedance by experimentation in a simulation medium, thus relating theory to practice and also exhibit that ORCAD Pspice is highly visual and effective for both understanding the mathematical theory underlying the circuits and performing measurements of flux and charge which are needed to obtain the characteristics of negative inductors and negative capacitors.

Keywords: Simulation, Orcad PSpice, negative resistor, negative capacitor, negative inductor, flux-meter, charge-meter

1. Introduction

The development of computer technology has opened new perspectives in engineering education to prepare students for their needs. In this context computer simulation has been a commonly adopted technique for predicting the real world behaviour of a component, circuit or system. PSpice has existed for some time and is a much popular circuit analysis program used by many electrical engineers and by Universities in their engineering courses as a CAD tool to analyse and test circuitry, because of its simplicity and effectiveness [1–5]. Pspice Simulator also provides the advantage of using hierarchical structures, thus simplifying the design and rendering the drawings more manageable.

This paper presents a design and simulation study for negative impedance emulation in Pspice medium. Generally, negative impedances (admittances) can be used in generation of transfer functions or impedance functions, which are not physically realizable without active circuits. Specifically, negative impedance emulators play an important role in cancellation/compensation of parasitic impedances [6]. They also have applications in microwave circuits for impedance matching [6,7,8,9] and realization of chaotic oscillations [10,11,12]. The study presented is of educational value and has two facets: obtaining systematically all kind of negative valued circuit components, namely, resistors, capacitors and inductors, which are presented in Section 2; generating their characteristics using flux – meters and charge meters, additional to already existing voltage and current meters, designed in the same environment, which is provided in Section 3 together with simulation results. Finally, Section 4 covers the discussion.

2. Generation of Negative Components

The generic circuit used for obtaining negative components systematically is shown on Figure 1. The two-port active device is a universal operational device, such as an opamp or current conveyor and it does not draw any current at the input

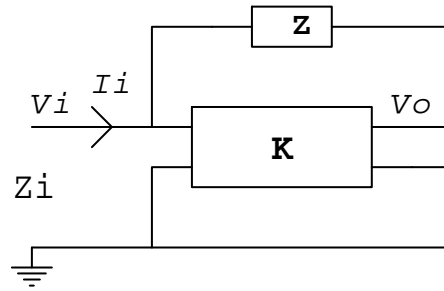


Figure 1. The generic circuit for obtaining grounded negative components

From the straightforward analysis of the circuit,

$$Z_i = \frac{V_i}{I_i} \tag{1}$$

and remembering the current input to the active element is zero,

$$I_i = \frac{V_i(1 - K)}{Z} \tag{2}$$

and finally substituting (2) in (1) yields,

$$Z_i = \frac{Z}{(1 - K)} \tag{3}$$

If K is chosen specifically as 2 then the input impedance of the overall becomes,

$$Z_i = -Z \tag{4}$$

from which negative value resistors, capacitors and inductors are derived.

3. Expression of Characteristics in Pspice Environment

In this Section negative components are obtained moving from the Figure 1 and numerical simulations are performed with an aim of extracting their defining characteristics. From the basic theory, the defining equations for the resistor, capacitor and inductor, respectively, are as follows

$$V = R I \tag{5}$$

$$Q = C V \tag{6}$$

$$\Psi = L I \tag{7}$$

In the measurement procedure for (5), the voltage and current markers, already existing within the structure of Pspice, are used. Whereas a charge-meter and flux-meter needed for (6) and (7), respectively, are constructed using sensing elements and integrators, whose details are illustrated on the relevant figures.

3.1. Negative resistor

The generative circuit and related measurement arrangement for producing the characteristic of the negative resistor is illustrated below on Figure 2. In Pspice dc analysis was performed changing V_{test} between -5V and 5V, thus obtaining the V-I characteristic as given on Figure 3.

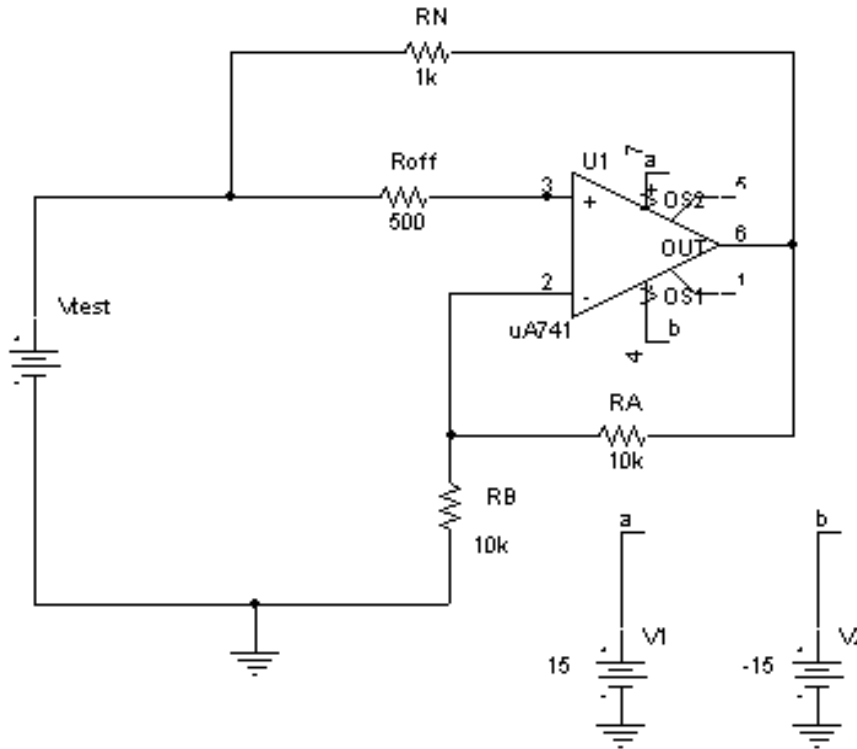


Figure 2. Negative resistor generation and measurement circuit

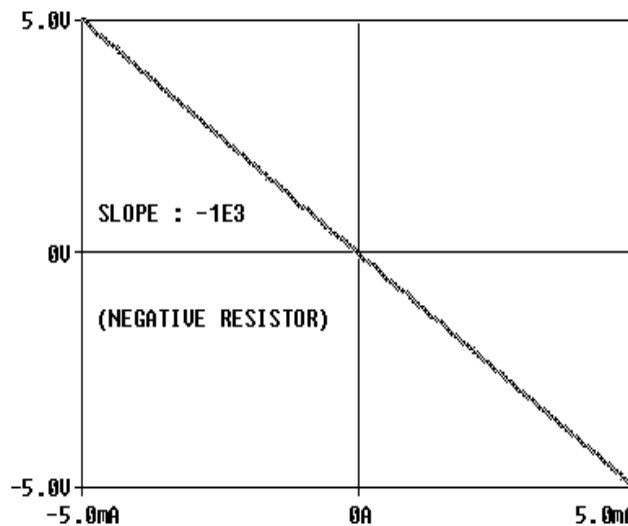


Figure 3. The defining characteristic for the negative resistor of Figure 2

The vertical and horizontal axis represents the voltage across and current through the component, respectively. The measurement was performed as required by (5) using a voltmeter and an ammeter.

3.2. Negative capacitor

The generative circuit and related measurement arrangement for producing the characteristic of the negative capacitor is illustrated below on Figure 4. In Pspice time analysis was performed for one period, thus obtaining the Q-V characteristic as given on Figure 6. The charge-meter designed for this aim is provided on Figure 4 both as a block and inside look.

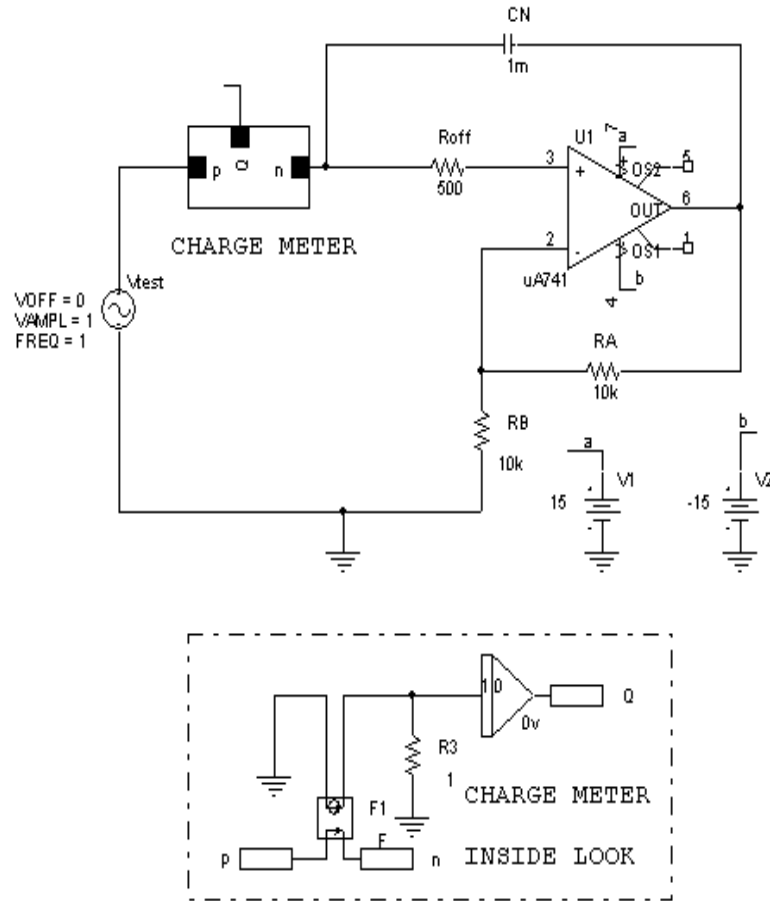


Figure 4. Negative capacitor generation and measurement circuit

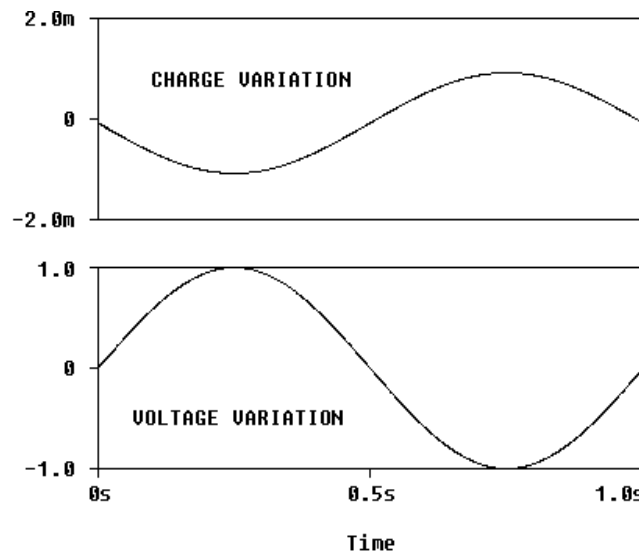


Figure 5. The voltage across and charge through the negative capacitor for one period of the alternating input voltage

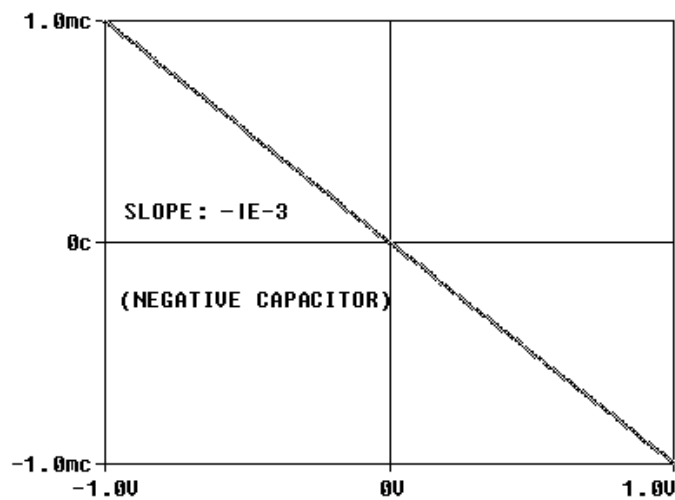


Figure 6. The defining characteristic for the negative capacitor of Figure 4. The vertical and horizontal axis represents the charge through and voltage across the component, respectively. The measurement was performed as required by (6) using a charge-meter and a voltmeter

3.3 Negative Inductor

The generative circuit and related measurement arrangement for producing the characteristic of the negative inductor is illustrated below on Figure 7. In Pspice time analysis was performed for one period, thus obtaining the Ψ -I characteristic as given on Figure. 9. The flux-meter designed for this aim is provided on Figure 7 both as a block and inside look.

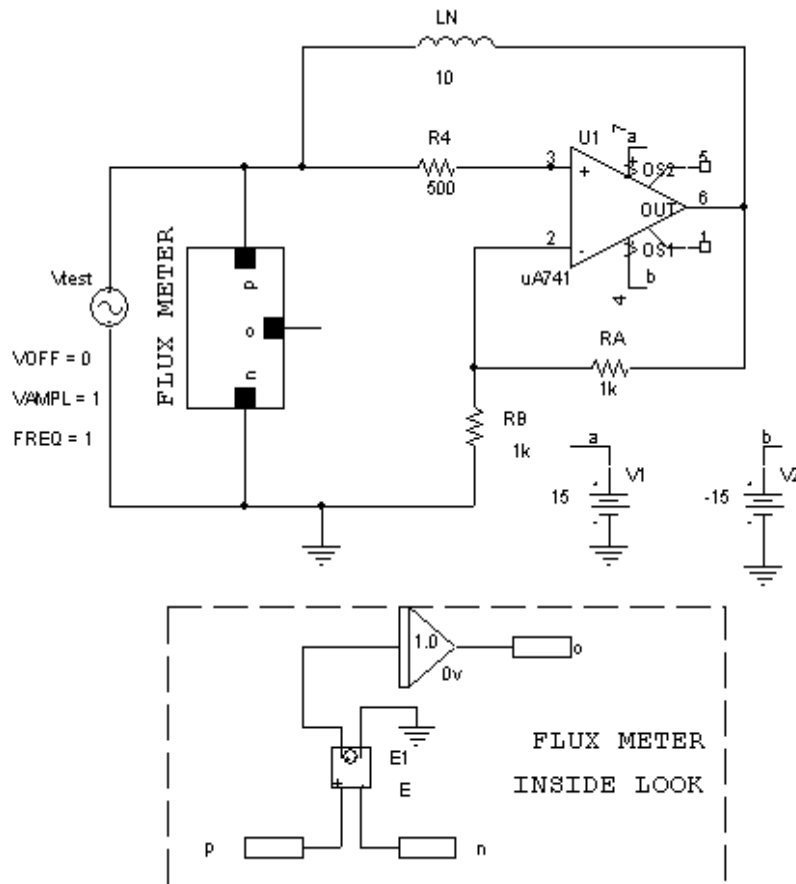


Figure 7. Negative inductor generation and measurement circuit

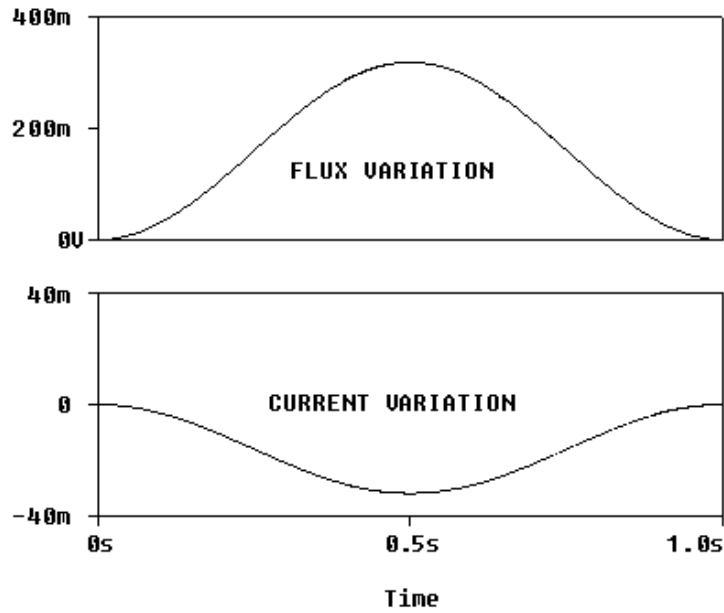


Figure 8. The flux across and current through the negative inductor for one period of alternating input voltage

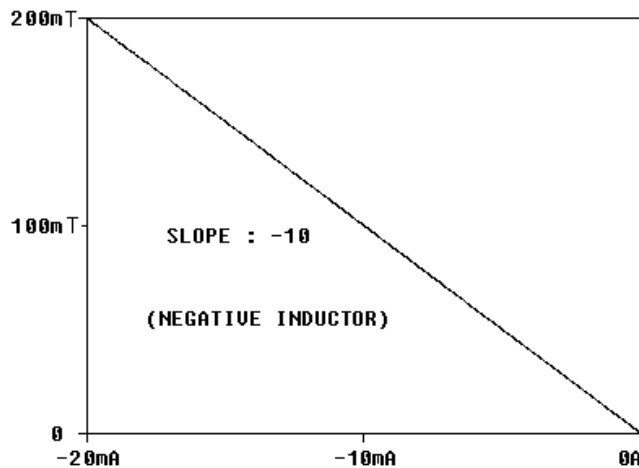


Figure 9. The defining characteristic for the negative inductor of Figure 7. The vertical and horizontal axis represents the flux across and current through the component, respectively. The measurement was performed as required by (7) using a flux-meter and an ammeter

4. Conclusions

In this study all types of two-terminal negative circuit components are generated from a single opamp circuit, complete with a simulation work in Pspice environment for obtaining their defining characteristics, which required the construction of a charge-meter (Fig. 4) and a flux-meter (Fig. 7) for educational purpose. The results are proved quite well in verifying and illustrating the underlined circuit theory, and as such have an educational value. It is apparent (Fig. 1) that the components obtained are all grounded. Besides, the voltage and current range of them are determined by the supply voltage and output current, respectively.

References

1. PSpice User's manual. OrCAD Corp. (Cadence Design Systems, Inc.)
2. OrCAD Capture User's Guide. OrCAD Corp. (Cadence Design Systems, Inc.)

3. Tobin, P. (2007). The Role of PSpice in the Engineering Teaching Environment. In Proceedings of the International Conference on Engineering Education – ICEE 2007, September 3 – 7, 2007, (77–81). Coimbra, Portugal, from http://www.academia.edu/818992/Role_of_PSpice_In_the_Teaching_Environment
4. Ferikoğlu, A., Sarı, Y., Köker, R. (2010) Simulating Solutions of Linear Differential Equations Using Various Active Circuits. In Proceedings of the XI International Workshop on Symbolic and Numerical Methods, Modeling and Applications to Circuit Design (SM2ACD), Sept. 2010, Oct. 4–6, 56-62. Gammarth, Tunisia
5. Sarı, Y., Ferikoğlu, A. (2011). The Role of PSpice in Analogue and Mixed-Signal Simulation of Electrical Circuits, 6th International Advanced Technologies Symposium (IATS'11), 16–18 May, 2011, 21-22. Elazığ, Turkey.
6. Kılınç, S., Salama, K. N., Çam, U. (2006). Realization of Fully Controllable Negative Inductance With Single Operational Trans-resistance Amplifier, *Circuit Systems Signal Processing*, *Birkhauser Boston*, 25(1), 147–57.
7. El Houry, S. (1995). The design of active floating positive and negative inductors in MMIC technology. *IEEE Microwave Guided Wave Lett.*, 5, 321–323.
8. Podell, A. F., Cristal, E. G. (1971). Negative-Impedance Converters (NIC) for VHF through Microwave Circuit Applications. *Microwave Symposium Digest*, 182–183.
9. Poklonski, N. A., Shpakovski, S.V., Gorbachuk, N. I. & Lastovskii, S. B., Negative capacitance (impedance of the inductive type) of silicon p+-n junctions irradiated with fast electrons. *Semiconductors*, 40(7), 803–807. DOI: 10.1134/S1063782606070128
10. Prokopenko, V. G. (2002). Chaotic oscillator with negative inductance. *J. Commun. Technol. Electron.*, 47, 1131–1133.
11. Pehlivan, İ., Uyaroğlu, Y. (2010). A New Chaotic attractor from General Lorenz System Family and its Electronic Experimental Implementation. *Turkish Journal of Electrical Eng. Comput. Sci.*, 18(2), 171–184.
12. Pehlivan, İ., Uyaroğlu, Y. (2007). Simplified Chaotic Diffusionless Lorenz Attractor and Its Application to Secure Communication Systems. *IET Communications*, 1(5), 1015–1022.

Received on the 12th of April 2013

IS THERE ANY TRUTH IN „PROJECTLIBRE THE OPEN SOURCE REPLACEMENT OF MICROSOFT PROJECT”?

Konstantin Stoychev Tsvetkov¹, Mariana Mateeva Petrova²

*¹Konstantin Preslavsky University of Shumen
4, Oboriste Str., Veliko Turnovo 5000, Bulgaria*

Phone: +359 887719785. E-mail: kscvetkov@gmail.com

*²University of Veliko Turnovo “St.Cyril and St.Methodius”,
32, Al.Burmov str., Veliko Turnovo 5000, Bulgaria*

Phone: +359 886842129. E-mail: petrova_mariana@abv.bg

An intensely intriguing announcement of major producers of open source software stir specialists in project management, namely message “ProjectLibre: the open source replacement of Microsoft Project”. In 2012 the founders of OpenProj announced that they forked the project and will be releasing a new version of OpenProj in August 2012. The name of the fork is ProjectLibre. Is it going to try to prove and is it possible to use this software in the learning process for the preparation of students and professionals will try to answer in this article. This issue is especially actual in Higher Education, as the main reason for people to university is a good realization that he would have offered and given trend more and more employers to run a Linux-based systems and to use free software in the near future, their experience with open source products would definitely give them a significant advantage in the labour market .

Keywords: Microsoft Project, OpenProj, ProjectLibre, Project management, open source

1. Introduction

The rise of open source software has been discussed in many places and it is obvious to anyone who likes a bit of development in information technology. Its introduction in education, however, is still the exception rather than the rule. This, of course, is a mistake. For one-sided consideration of IT disciplines only from the perspective of mainstream proprietary software is contrary to the very idea of education, which is rather a person to learn to operate a computer than to learn how to use specific products. Even specialty student has nothing to do with information technology in nearly every major person will have to use specified type of software. It is difficult to compare in detail any free alternative to correspond and commercial application. But not being ungrounded, you should give at least one specific example in more detail. It would be appropriate to countering Microsoft Project 2007 & 2010 against ProjectLibre, due to their widespread use in automation in the field of Project management.

2. Description

The product OpenProj was developed at Projity by Marc O'Brien, Howard Katz and Laurent Chretienneau in 2007 by Serena Software [3]. It moved out of beta with the release of Version 1.0, on January 10, 2008 [2]. As of early 2009 support for OpenProj and communication about development of OpenProj seems to have been suspended [4]. There has been no improvement in the past four years and it is not longer compatible with new versions of Microsoft Project and in particular there is a good compatibility of new versions 2007 and 2010.

Recently, the original founders of OpenProj started to develop a complementary server for OpenProj, comparable to Microsoft Project Server for Microsoft Project. During development they realized, that the fact that OpenProj had not been updated anymore by Serena Software during the last four years will become problematic to their goal, so they needed to develop first a significantly updated version of OpenProj. This version was released as a fork called ProjectLibre in August 2012 [4]. Source forge has issued a note that ProjectLibre <http://www.projectlibre.org> has superseded ProjectLibre and is the new replacement.

ProjectLibre project management software is an open source alternative to Microsoft Project. It has been downloaded in 146 [5] countries the first month of release and was just voted “Project of the Month”. ProjectLibre is compatible with Microsoft Project 2003, 2007 and 2010 files. ProjectLibre runs on the Java Platform, allowing it to run on a variety of different operating systems [1]. You can simply open them on Linux, Mac OS or Windows and if desired save results back.

A ProjectLibre is envisaged that in the future to moan could be used as an alternative to a cloud/server replacement of Microsoft Project Server.

On the site of OpenProj / ProjectLibre one can find various examples of projects. You can take advantage of opportunities to download, for each subproject that you remember, and the overall management of your business.

Working with the program is very intuitive and hardly difficult even to those people who are not engaged in project planning. From a technical point of view, we do not comment on the performance of the program.

Example proximity of MS project 2007 (Figure 1) with ProjectLibre (Figure 2) is the design of the task solved with both the products the conclusion is "it's the same". When comparing MS Project and ProjectLibre (Figure 1 and Figure 2) clearly visible large external similarities between the two products.

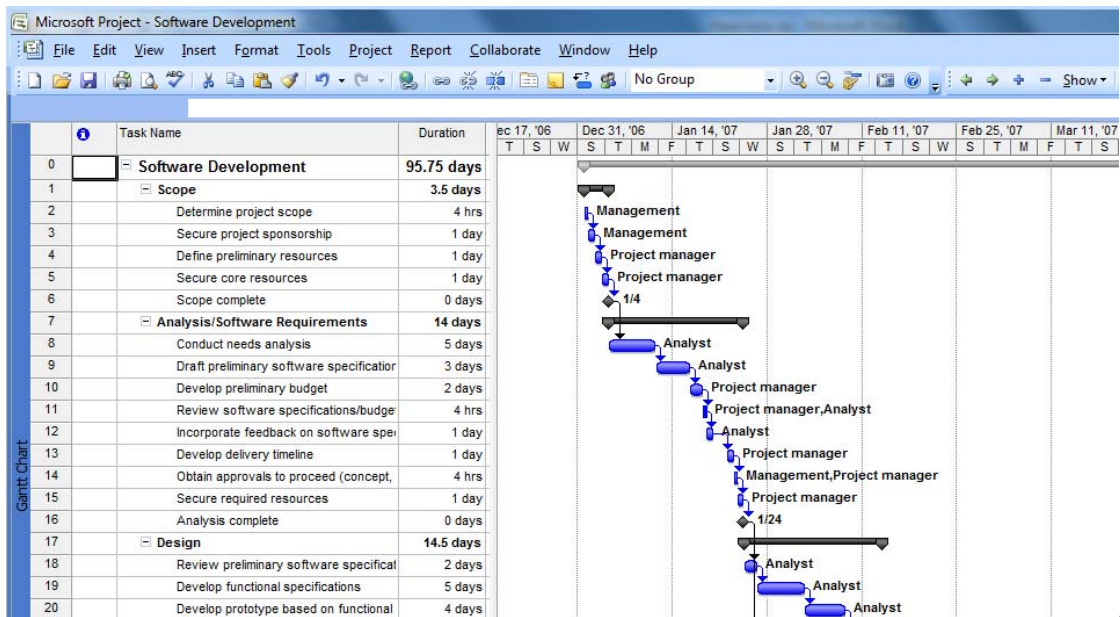


Figure 1. Gantt chart of MS Project 2007

Figure 1 shows the Gantt chart for project implementation, it is used to test for compatibility option.

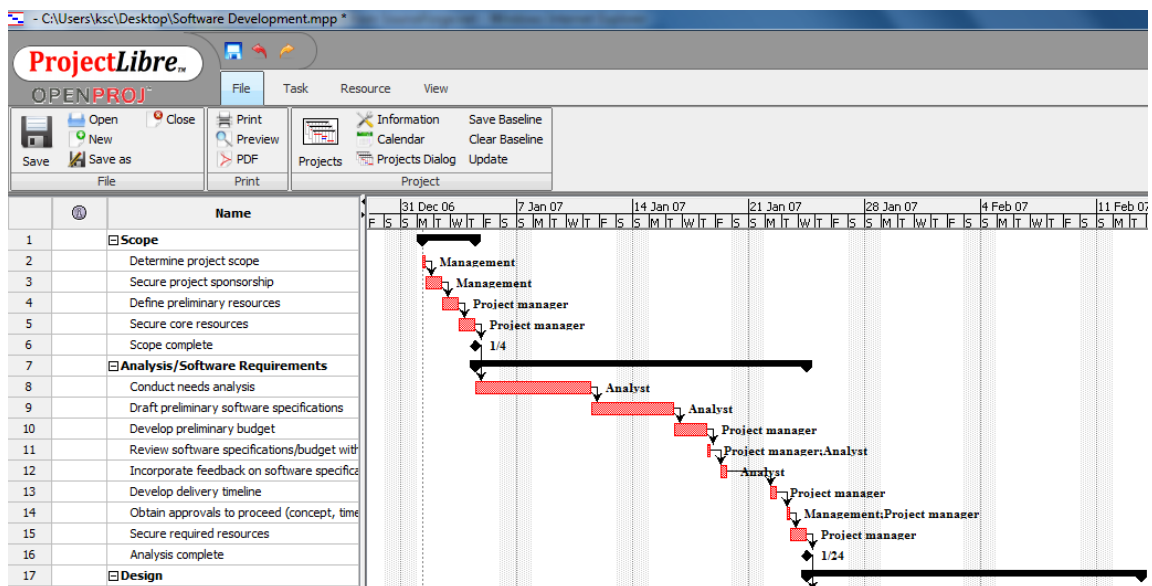


Figure 2. Gantt chart in ProjectLibre

3. Comparison of Packages

The most popular program in the field of project management is undoubtedly the package Microsoft Project. Microsoft Project is suitable for everyone who meets basic needs for project management and has a very large set of highly complex tools for collaboration and management. There is however one of its features, which certainly is not positive and this is the price – \$ 999. Naturally for such a price, one has to wonder if there is any other program with similar functionality that would be compatible with MS Project and with a lower price. The answer is there and the price is so low that less cannot be – they are free.

What are the main differences in the two platforms of Project management, implemented on the basis of open and proprietary software, which also belongs to the advantages/disadvantages comparing two packages?

- Application based on open source is free. Everybody would have loved to use the free software that is legally free, not pirated. In the case of ProjectLibre it is, and in the words of its creators, it always will be free.
- Updates open source application is also free. This is a direct consequence of the philosophy of the license under which it is running these applications. Microsoft updates are also generally free, but they can make them pay when they want without due explanation to someone about it.
- Application code open source is outside the control of a single company. This makes applications independent of the current developers of these products and if the company disappears behind application code will be lost and the product can continue to live.
- The application uses open source open standards. ProjectLibre file formats such as publicly documented, consistent and affordable. Many people do not understand what the advantage of file formats that are open is and their specifications are not known, but it is a great advantage in terms of transparency of what makes your computer data. It is also a great convenience for anyone who wants to create a product that is compatible with that format.

Now let's get to the actual comparison of the two Project packages.

General Stuff

Microsoft Project and ProjectLibre are two very powerful desktop applications for project management with the following features:

- **Gantt chart.** This is a bar chart that is used for project planning. It divides the design task into several subtasks and shows their relationship, start and end dates – Figure 1 and Figure 2.
- **Project Network.** It shows “pre”, “next” and “intermediate” tasks in graphical mode; and called PERT chart; it is shown on Figure 3 and Figure 4. Again it is seen close to the same product of MS.

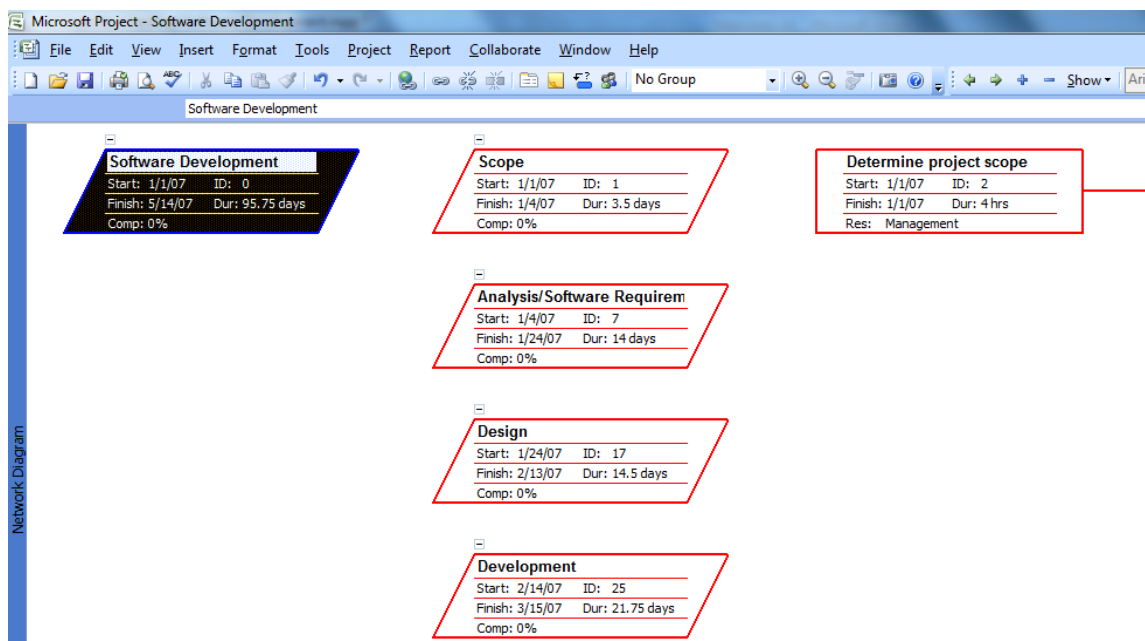


Figure 3. Networking diagram of MS Project 2007

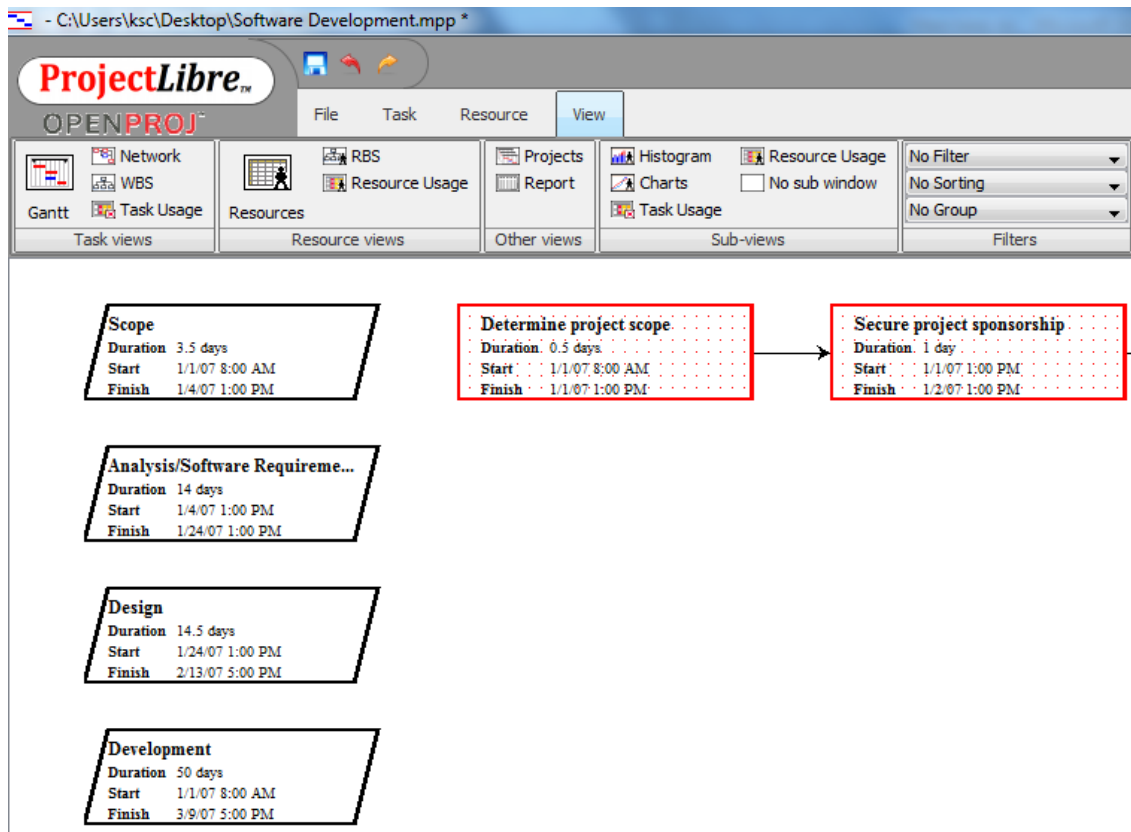


Figure 4. Networking diagram of ProjectLibre

- **Resources Chart.** These are the entries for the available resources listed to the right of the bars.
- **WBS (Work Breakdown Structure).** Component structure of the work. It shows the structure of subordination and systematic breakdown of tasks into subtasks.
- **RBS (Resource Breakdown Structure).** Resource breakdown or RBS is the categorization of resources according to different functions.
- **Output.** Microsoft Project and ProjectLibre offer several methods for tracking consolidated financial statements and for the use of tasks / resources.

Note: In this article we are not given any figures with diagrams near, but above are analogous according to the authors of the article to those of Figure 1–4.

Some advantages of Microsoft Project

- **Rich supporting documentation.** Microsoft Project has a really good support documentation that is available both online and offline, so that learning is easy.
- **Java is needed** (debatable advantage). Unlike ProjectLibre, no need to install Java on your machine to run Microsoft Project.

Some of the advantages of ProjectLibre

- **ProjectLibre is a free software** project management, so you will save \$ 700–1000.
- **Easy to system requirements.** In most computers and ProjectLibre and Microsoft Project 2007 & 2010 will go smoothly. In older computers ProjectLibre will have a significant advantage. Its minimum requirements are a Pentium 166 MHz and 128 Mb RAM, while Microsoft Project 2007 & 2010 are Pentium 450 MHz with 266 Mb Ram. Which is more important, ProjectLibre and will run Linux (and Solaris and BSD), and Linux runs much more efficiently than older computers running Windows 2000 or XP. This makes Linux ProjectLibre practical combination even for very old computers.
- **Independence of the operating system. Multiplatform.** This is undoubtedly one of the biggest advantages of ProjectLibre. It is available for each architecture, the three major

platforms (Windows, Linux, and Mac). It relies on its Microsoft formats, and many others. Own file formats are extremely effective and generally the same document is smaller than the format as MS format. By comparison, Microsoft Project 2007 & 2010 only supports its own formats and is available only for Windows.

- **Usability, Training, Support.** In general, anyone who has used MS Project 2003 & 2007 & 2010 will be feeling comfortable with ProjectLibre. Interfaces are almost identical, see Figure 1 and Figure 2; even in ProjectLibre syntax is identical. You can think of migration as ProjectLibre migration to Microsoft Project 2007 & 2010. While this is slightly different, but the concepts are the same.
- **Part of Star Office.** OpenProj by 2008 it was a part of Star Office at Sun Microsystems [6], we assume a large percentage of security as its successor and ProjectLibre becomes a part of the package.

Be asked if there are other programs like ProjectLibre, can confidently answer “Yes” and such are Ganttter [41], Teambox [7], Rally Community Edition [8], FreedCamp [9], and many others.

4. Conclusions

In conclusion, we emphasize three things.

Firstly, the differences between the philosophies of open and closed software mentioned in the beginning, is perhaps the most important argument in favour of this application. These are advantages, which cannot be neutralized or removed, no matter how its competitors change.

Secondly, the flexibility of open source software should be used to implement partial least in the beginning, if possible overall migration. Many open source programs have versions for Windows. Using ProjectLibre under Windows, it saves money; even Windows have to be paid or otherwise. Sometimes a person just needs the specific commercial applications. But he does not have to use them on Windows. One can use commercial software, without having to pay extra for Windows.

And finally, the third thing I want to point out is that financial arguments in favour of open source are far from the most important ones. Since so much of open source programs are free, it creates a false impression to some people that these are decisions for poorer ones, and as such are incomplete. These people carry the logic of the material world, where it has no place. And since we're talking about higher education, I can say that even Harvard began steps for the introduction of open source software in their curricula (for we are not ungrounded – news can be found at http://news.cnet.com/8301-13505_3-9916323-16.html) and they all would agree, it is certainly not suffering from a shortage of funds, so the example is quite telling, considering the topic of this report.

Acknowledgement

The article was designed by project PД-05-282/15.03.2012 of Konstantin Preslavsky University of Shumen.

References

1. Heck, Mike. *Preview: OpenProj brings free, robust project management to the desktop*. InfoWorld. International Data Group. Retrieved August 11, 2007, from http://weblog.infoworld.com/tcdaily/archives/2007/10/preview_openpro.html
2. *OpenProj 1.0 Released*. SourceForge.net. Retrieved January 17, 2008, from http://sourceforge.net/forum/forum.php?forum_id=775275
3. Serena Software Acquires Open Source Alternative to Microsoft Project. Serena Software. Retrieved January 19, 2009, from http://www.serena.com/company/news/pr_spr_09232008.html
4. http://en.wikipedia.org/wiki/OpenProj#cite_note-IW200710-0
5. <http://sourceforge.net/projects/projectlibre/>
6. <http://en.wikipedia.org/wiki/OpenProj>
7. <https://app.ganttter.com/>
8. <http://teambox.com/>
9. <http://www.rallydev.com/product-features/rally-community-edition>
10. <http://freedcamp.com/>

STUDY ON MODEL OF COMPONENT RELIABILITY BASED ON DYNAMIC STRENGTH INTERFERENCE THEORY

X. Ma, Cu. Jiang

*Department of Finance and Economics Shandong University of Science and Technology
 Jinan Shandong 250031
 E-mail: maxinbin@126.com*

The strength variation of a product can be regarded as a degeneration process as well as an antagonistic process with the stress imposed on the product during the whole life of the product. In this paper, we used the dynamic strength interference theory to construct a structural reliability model that the relationship between components and the stress acting on it. The system is a continued degeneration process with the variation of time t before their failure. The calculating methods of reliability were given for kinds of common strength and stress distribution.

Keywords: Structural reliability, dynamic strength interference model, strength, stress, degeneration

1. Introduction

The strength interference theory is an important issue on research on mechanical reliability. It is the research on the antagonism between the intrinsic strength of a product and the stress imposed on it [1]. The traditional design method is based on safety coefficient and semi-empirical coefficient, without the consideration of failure probability caused by random factors of the strength and stress of the product. Therefore, probabilistic design based on structural reliability has attracted people's attention and gained significant achievements [1, 2]. However, during the whole product life, the strength variation of the product is a degeneration process, and it is related to time t , the operation time of the product. Besides, because of the uncertainty of the inner structure of the product [3], it is impossible to foretell the variation of the state of the product's strength. On the other hand, the functionary load is dynamic load and dynamic stress and it varies and fluctuates with time variation. Dynamic strength interference theory is put forward based on this situation. And it has theoretical and practical significance. For one thing, it provides a new method to research on reliability of product [2]. For another thing, it lays the foundation for reliability forecast, remaining life forecast and making the optimum maintenance policy [5, 6]

2. Background

If the product consists of discrete component, $Y(t)$ denotes the state of the component. $Y(t)$ constantly changes with time variation because of the influence of various kinds of factors [7, 8]. The components will fail when $Y(t)$ changes to a limitation. The typical situation is $Y(t)$ changing to 0 or ∞ . For example, let $Y(t)$ be numerical value of electric resistance, the components will be short circuit and fail when $Y(t) = 0$; the component will be open circuit and fail when $Y(t) = \infty$. To summarize, the types of change of $Y(t)$ are as follows:

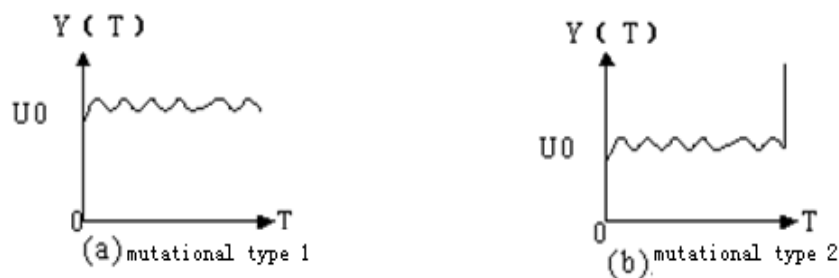


Figure 1. Mutational Degeneration

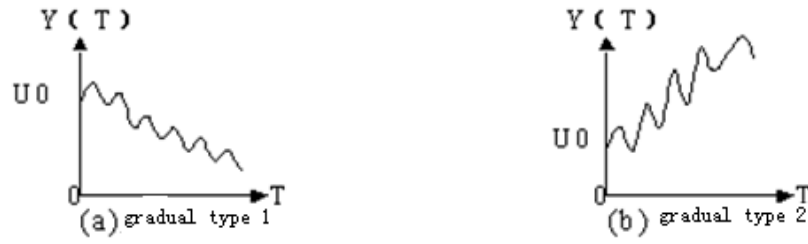


Figure 2. Gradual Degeneration



Figure 3. Hybrid Degeneration

Figure 1 means $Y(t)$ random variation around U_0 before some time point, then mutate to 0 or ∞ . The component is called mutational degeneration, and mutational type 1 when $Y(t)$ mutates to 0 (Figure 1(a)), and it is called mutational type 2 when $Y(t)$ mutates to ∞ (Figure 1(b)); Homoplastically, Figure 2(a) is called gradual type 1; Figure 2(b) is called gradual type 2; Figure 3(a) is called hybrid type 1; Figure 3(b) be called hybrid type 2.

Let $F(y, t)$ be one dimensional distribution function of $Y(t)$, there is:

$$F(y, t) = \Pr\{Y(t) \leq y\}$$

If one dimensional density function of $Y(t)$ exists, there is:

$$f(y, t) = \frac{\partial F(y, t)}{\partial y}$$

Let η be mutations moment, its distribution function is $F_\eta(t)$, there is:

$$F_\eta(t) = \Pr\{\eta < t\}$$

Its density function is as follows:

$$f_\eta(t) = \frac{\partial F_\eta(t)}{\partial t}$$

$$\text{Then: } F(y, t) = \Pr\{Y(t) \leq y\} = \Pr\{Y(t) \leq y / \eta \geq t\}P\{\eta \geq t\} + \Pr\{Y(t) \leq y / \eta < t\}P\{\eta < t\} \quad (1)$$

It is marked as: $\Phi(y, t) = \Pr\{Y(t) \leq y / \eta \geq t\}$

$$\varphi(y, t) = \frac{\partial \Phi(y, t)}{\partial t}$$

$\Phi(y, t)$ and $\varphi(y, t)$ denote conditional distribution function and conditional distribution density respectively under the condition of $Y(t)$ without mutation.

Formula 1 can be written in this way: to hybrid type 1.

$$\Pr\{Y(t) \leq y / \eta \geq t\} = \Pr\{0 \leq y\} = I(y)$$

$I(t)$ is unit step function, here, Formula (1) is:

$$F(y, t) = (1 - F_\eta(t))\Phi(y, t) + F_\eta(t)I(y) \quad (2)$$

So

$$f(y, t) = (1 - F_\eta(t))\varphi(y, t) + F_\eta(t)\delta(y) \quad (3)$$

Hybrid type 2 can be done in the same manner:

$$f(y, t) = (1 - F_\eta(t))\ell(y, t) + F_\eta(t)\delta(y - \infty) \quad (4)$$

Apparently, the distribution densities of mutational type 1 and mutational type 2 are the special cases in (3) and (4) respectively.

To gradual degeneration,

let $Y(t) = U_0$ be the failure of state of the component, there is:

$$F(y, t) = (1 - F_\eta(t))\Phi(y, t) + F_\eta(t)I(y - u_0) \quad (5)$$

$$\text{So: } f(y, t) = (1 - F_\eta(t))\Phi(y, t) + F_\eta(t)\delta(y - u_0) \quad (6)$$

Gradual type 2 can be done in the same manner and there is:

$$f(y, t) = (1 - F_\eta(t))\Phi(y, t) + F_\eta(t)\delta(y - u_0 - \infty) \quad (7)$$

3. The Strength-Dynamic Interference Model

The structure reliability can be defined as the probability that strength is greater than stress [9], that is,

$$R = P\{Y - X > 0\} \quad (8)$$

Y is strength; X is stress.

If X 's probability distribution density and Y 's are respectively $f_X(x), f_Y(y)$; X and Y are mutually independence, there is

$$R = \iint_D f_X(x)f_Y(y)dxdy$$

$Y > x$ is domain of integration, so:

$$R = \int_{-\infty}^{\infty} f_X(x) \int_x^{\infty} f_Y(y)dydx. \quad (9)$$

The unreliability is

$$\bar{R} = \int_{-\infty}^{\infty} f_X(x) \int_{-\infty}^x f_Y(y)dydx. \quad (10)$$

If X 's probability distribution function and Y 's are respectively.

$F_X(x), F_Y(y)$, and $f_X(x), f_Y(y)$ are density function, we can conclude:

$$R = 1 - \int_{-\infty}^{\infty} f_X(x)F_Y(x)dx \quad (11)$$

$$\text{and because } R = P\{Y > X\} = \int_{-\infty}^{\infty} f_Y(x)F_X(x)dx. \quad (12)$$

We can also draw a conclusion:

$$\bar{R} = \int_{-\infty}^{\infty} f_X(y)F_Y(y)dy \quad (13)$$

$$\text{or } \bar{R} = \int_{-\infty}^{\infty} f_Y(y)[1 - F_X(x)]dy. \quad (14)$$

If $Z = Y - X$ is defined as Interference random variables, there is:

$$\bar{R} = \int_0^{\infty} \int_0^{\infty} f_Y(x+z)f_X(x)dx dz \quad (15)$$

and

$$\bar{R} = \int_{-\infty}^0 \int_z^{\infty} f_Y(x+z)f_X(x)dx dz . \quad (16)$$

The model of strength-dynamic interference is defined as

$$R(t) = P\{Y(t) - x(t) > 0\} \quad (17)$$

In (17), intensity $Y(t)$ and stress $X(t)$ are both stochastic process, and for convenience, if we set random variables of stress on components as $X = X(t)$, there is:

$$R(t) = P\{Y(t) - x > 0\}. \quad (18)$$

As for hybrid degradation, we can come up with a new formula when inserting (2) into (11), that is,

$$\begin{aligned} R(t) &= P\{Y(t) - x > 0\} = 1 - \int_{-\infty}^{\infty} f_X(y)[(1 - F_{\eta}(t))\Phi(y, t) + F_{\eta}(t)I(y)]dy \\ &= 1 - F_{\eta}(t) \int_0^{\infty} f_X(y)dy - (1 - F_{\eta}(t)) \int_{-\infty}^{\infty} f_X \Phi(y, t)dy \end{aligned} \quad (19)$$

The Unreliability is

$$\bar{R}(t) = F_{\eta}(t) \int_0^{\infty} f_X(y)dy + (1 - F_{\eta}(t)) \int_{-\infty}^{\infty} f_X(y)\Phi(y, t)dy . \quad (20)$$

Or a new formula forms when (3) is inserted into (12); that is,

$$\begin{aligned} R(t) &= P\{Y(t) - x > 0\} = \int_{-\infty}^{\infty} f(y, t)F_X(y)dy = \int_{-\infty}^{\infty} [(1 - F_{\eta}(t))\varphi(y, t) + F_{\eta}(t)\delta(y)]F_X(y)dy \\ &= (1 - F_{\eta}(t)) \int_{-\infty}^{\infty} \varphi(y, t)F_X(y)dy + F_{\eta}(t) \int_{-\infty}^{\infty} \delta(y)F_X(y)dy \\ &= (1 - F_{\eta}(t)) \int_{-\infty}^{\infty} \varphi(y, t)F_X(y)dy + F_{\eta}(t)F_X(0) \end{aligned} \quad (21)$$

The Unreliability is

$$\bar{R}(t) = (1 - F_{\eta}(t))(1 - \int_0^{\infty} \varphi(y, t)F_X(y)dy) + F_{\eta}(t)(1 - F_X(0)) . \quad (22)$$

4. The Application of the Dynamic Strength Interference Theory

The following is the expression of probability of structural reliability concerning common distribution of strength and stress.

4.1. Strength and stress are both normal distribution

If Intensity $Y(t) \sim N[U(t), \delta^2(t)]$,

stress $X(t) \sim N[U_1, \delta_1^2]$, and $Y(t)$, $X(t)$ are mutually independence, there is $Y(t) - X(t) \sim N[u(t) - u_1, \sigma^2(t) + \sigma_1^2]$, according to probability theory.

So as for hybrid type 1, we can get a formula as follows:

$$\begin{aligned} R(t) &= 1 - F_{\eta}(t) \\ &\int_{-u/\sigma_1}^{\infty} \varphi_{0,1}(x)dx - (1 - F_{\eta}(t))(1 - \Phi(\frac{u(t) - u_1}{\sqrt{\sigma^2(t) + \sigma_1^2}})) = F_{\eta}(t)\Phi(-\frac{u_1}{\sigma_1}) \\ &+ (1 - F_{\eta}(t))\Phi(\frac{u(t) - u_1}{\sqrt{\sigma^2(t) + \sigma_1^2}}) \end{aligned} \quad (23)$$

In (23), $\varphi_{0,1}(x)$ means distribution density of standard normal distribution and $\Phi(x)$ means distribution function.

$$\text{If } \beta(t) = \frac{u(t) - u_1}{\sqrt{\sigma^2(t) + \sigma_1^2}}.$$

We can prove: when $\frac{d\beta(t)}{dt} \leq 0$, there is $\frac{dR(t)}{dt} < 0$.

That is because

$$\frac{dR(t)}{dt} = -f_\eta(t) \int_{-u_1/\sigma_1}^{\beta(t)} \varphi_{0,1}(x) dx + (1 - F_\eta(t)) \frac{d\beta(t)}{dt}.$$

Then we can conclude: when $\frac{dR(t)}{dt} = 0$, two items on the right side of “=” are all less than 0 in above formula.

4.2. Strength and stress are both lognormal distribution

There is $\ln Y(t) \sim \ln x(t) \sim N[u(t) - u_1, \sigma^2(t)\sigma_1^2]$ if $Y(t) \sim \ln[u_1(t), \sigma^2(t)]$ and $x(t) \sim \ln[u_1, \sigma_1^2]$ are mutually independent.

If $\overline{k(t)} = EY(t)/EX$ is Average safety coefficient; $Cx = \sqrt{Dx}/Ex$ is coefficient of variation of strength and $Cy(t) = \sqrt{DY(t)}/EY(t)$ is the coefficient of variation of stress in such formula

$$\beta(t) = \frac{\ln \left[\overline{k(t)} \left(\frac{1 + c_x^2}{1 + c_y^2(t)} \right)^{\frac{1}{2}} \right]}{\sqrt{\ln \left[(1 + c_y^2(t))(1 + c_x^2) \right]}}, \text{ there is}$$

$$R(t) = (1 - F_\eta(t))\Phi(\beta(t)) \tag{24}$$

According to the quality of lognormal distribution; from (24) we can conclude that the monotonicity of $R(t)$ depends on $\beta(t)$ completely.

4.3. Stress Intensity all obey the distribution of Γ

$$Y(t) \sim \Gamma(y/m(t), \lambda(t)) \stackrel{\Delta}{=} \frac{u(t)^{m(t)}}{\Gamma(m(t))} y^{m(t)-1} e^{-\lambda(t)y}, y > 0$$

$$x(t) \sim \Gamma(x/n(t), u(t)) \stackrel{\Delta}{=} \Gamma(x/n, u) \stackrel{\Delta}{=} \frac{u^n}{\Gamma(n)} x^{n-1} e^{-ux}, x > 0$$

Arrange the Average Safety Factor $\overline{k(t)} = EY(t)/EX(t) = \frac{m(t)u}{n\lambda(t)}$, here, $EY(t) = m(t)/\lambda(t)$, $EX = n/u$.

According to properties of the distribution of Γ :

$$R(t) = (1 - F_\eta(t)) P \left\{ \frac{um(t)}{\lambda(t)n} w \geq 1 \right\} = (1 - F_\eta(t)) I \frac{u}{u + \lambda(t)}(n, m(t)) \tag{25}$$

$W \sim F_{2m(t),n,F_{2m(t),2n}$ is Degree of Freedom, the distribution of F in $2m(t),2n$,

$$I_x(s, f) = \frac{1}{B(s, f)} \int_0^1 x^{s-1} (1-x)^{f-1} du.$$

In this equation, $\beta(s, f) = \int_0^1 x^{s-1} (1-x)^{f-1} dx$ is the Function of Incomplete B, when $m(t) = n = 1$,

$$R(t) = (1 - F_\eta(t)) \frac{u}{u + \lambda(t)} \tag{26}$$

4.4. Stress Intensity obey the distribution of Weibull

When $Y(t) \sim w(m(t), n(t), r(t))$, the distribution of three PL models Weibull, $x \sim N[U, \sigma^2]$.

According to $Fr(y) = 1 - e^{-\left(\frac{y-r(t)}{\eta(t)}\right)^{m(t)}}$

There is

$$\begin{aligned} R(t) &= 1 - F_\eta(t) \int_{-u/\sigma}^{\infty} \varphi_{0,1}(x) dx - (1 - F_\eta(t)) \int_r^{\infty} \Phi(y, t) f_x(y) dy \\ &= 1 - F_\eta(t) \Phi(u/\sigma) - (1 - F_\eta(t)) \frac{1}{\sqrt{2\lambda\sigma}} \int_{r(t)}^{\infty} e^{-(y-u)2/2\sigma^2} \left\{ 1 - e^{-\left(\frac{y-r(t)}{n(t)}\right)^{m(t)}} \right\} dy \\ &= 1 - F_\eta(t) \Phi(u/\sigma) - (1 - F_\eta(t)) \left[\Phi(-A) - \frac{c}{\sqrt{2\pi}} \int_0^{\infty} \exp\left\{-\frac{1}{2}(cu + A)^2 - u^{m(t)}\right\} du \right] \end{aligned} \tag{27}$$

Here, in the equation (27), $c = n(t)/\sigma$, $A = \frac{r(t) - u}{\sigma}$, the calculation of the third Integral Type can be found in Table [10].

5. Special Cases of Nonnumeric Columns

5.1. Element strength and stress all obey the distribution of normality

The Element Strength $Y(t) \sim N[u(t), \sigma^2(t)]$, $u(t) = T15.1 - 10t$, $\sigma^2(t) = 80 - 0.03t$, the received Stress $x \sim N[u_1, \sigma_1^2]$, $u_1 = 70$, $\sigma_1^2 = 200$. Failure Probability of element $\eta \sim F_\eta(t) = 1 - e^{-\lambda t}$, try to make out the dynamic reliability. According to (23), the result is on Figure (4).

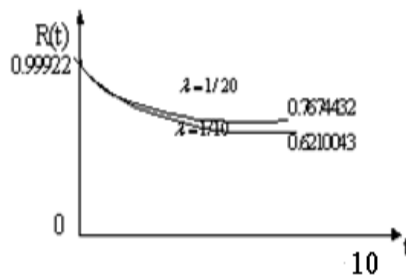


Figure 4. Result of calculation

5.2. Elements and stresses all obey the distribution of Γ

The Element Strength and Stress all obey the distribution Γ , $Y(t) \sim \Gamma(y/m(t), \lambda(t))$, $x \sim \Gamma(x/n, u)$. But, both $m(t) = 1, n = 1$, $\lambda(t) = \frac{1}{600 - 0.01t}$, $u = \frac{1}{40}$ and Failure Probability of element $\eta \sim F_\eta(t) = 1 - e^{-\lambda t}$, try to make out the dynamic reliability. According to (26), the result is on Figure (5).

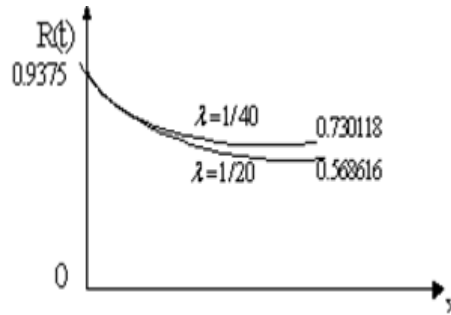


Figure 5. The result of the dynamic reliability

6. Conclusions

The strength interference theory offers a great tool to work out reliability of system and components. The components and system is a process of degenerate procedure varying with time before it fills. We will lose some important information when design strengths of components and structure make use of conventional safety factor. The degenerate will fill when it reaches the given level but it has safety in another stress system.

Combine loading system and strengths and dynamic of component make use of strength interference theory to build dynamic model relate to time. We can get the conclusion through calculating the model as follows.

The degenerate process of component can imitate if assume both caption values and external voltage obey to normal distribution, the component reliability depend on $\beta(t) = \frac{u(t) - u_1}{\sqrt{\sigma^2(t) + \sigma_1^2}}$ in this

state, if $\frac{d\beta(t)}{dt} \leq 0$, that $\frac{dR(t)}{dt} < 0$. That is, the components reliability decreases gradually with mean value of component's caption values decrease gradually.

We can conclude that component reliability decrease quickly at the beginning phase and entry in stable phase for later on and fail at last through assuming component obey to Lognormal distribution and Weibull distribution have simulations.

According strength interference theory to work out the probability of the reliability, we can decide to repair and change for components and structure when reliability reaches t_0 and combine with a casualty expected value.

Acknowledgment

This work was supported by Natural Science Foundation of China, under the Grants 71071089; supported by Science and Technology Development Planning of Shandong, under the Grants 2012RKB01457

References

1. Zhou, Y. Q., Weng, Zh. X. (1990). *Reliability evaluation*. Beijing: Science Press.
2. Ingram, G. E. (1964). A Basic Approach for Structural Reliability. In Proceedings of the Eleventh National Symposium on Reliability and Quality Control, August, 1964. Arinc Rrinc Research Corp.

Mathematical Modeling

3. Haugen, E. B. (1985). *Mechanical Probability Design*, translated by Wang Yilin, Yu Kanglin, Xu Qixiang, et al. (pp. 103–151). Beijing, China: Machine Press.
4. Goble, W. M., Brombacher, A. C., Bukowski, J. V. et al. (1998). Using Stress-strain Simulations to Characterize Common Cause. In A. Mosleh, R.A. Bari (Eds.), *Probabilistic Safety Assessment and Management (PSAM4)*. New York: Springer.
5. Chen, W. G. (1998). *The Practical Basis of Power Distribution System Reliability*. Beijing China: Electric Power Press.
6. Adem Kilicman, Hassan Eltayeb. (2012). Note on Partial Differential Equations with Non-Constant Coefficients and Convolution Method. *Applied Mathematics and Information Sciences*, 6(1), 59–6.
7. Lv Zhenzhou, Feng Yuansheng, (1996). The general reliability model about structure strength. *Mechanical Science and Technology*, 32(1), 53–61.
8. Tian, Sh. P., Wei, H. Y. (2004). Mechanical parts reliability design method based on the Matlab [J]. *Machinery Design & Manufacture*, 8(4).
9. Guo, Y. J. (2002). *Reliability Engineering Principles*. Beijing: TsingHua University Press, Springer Press.
10. Kapur, K. C. & Lamberson, L. R. (1984). *The Reliability in Engineering Design*, translated by Zhang Zhitie. Beijing: China Machine Press.

Authors' index

Abisheva, B.	48
Amanzholova, S.	44
Baisakov, B. M.	48
Chai, Y.	15
Fan, Y.	24
Ferikoğlu, A.	53
He, N.	36
Jiang, C.	15
Jiang, C.	65
Köker, R.	53
Li, Y.	15
Liu, S.	24
Luan, T.	36
Ma, S.	15
Ma, X.	65
Maratov, M.	48
Meng, X.	15
Petrova, M.	60
Qian, F.	24
Rebezova, M.	7
Sarı, Y.	53
Shen, L.	15
Tsvetkov, K.	60
Wei, H.	24
Xie, Z.	36
Xu, L.	15
Yang, W.	24
Zhakayev, N.	44



Yuri N. Shunin (born in Riga, March 6, 1951)

- Vice-rector on Academic Issues (Information Systems Management Institute), professor, Dr.Sc.Habil., Member of International Academy of Refrigeration
- Director of Professional Study Programme Information Systems (Information Systems Management Institute)
- Director of Master Study Programme Computer systems (Information Systems Management Institute)
- **University studies:** Moscow physical and technical institute (1968–1974).
- Ph.D. (physics & mathematics) on solid state physics (1982, Physics Institute of Latvian Academy of Sciences), Dr.Sc.Habil (physics & mathematics) on solid state physics (1992, Ioffe Physical Institute of Russian Academy of Sciences)
- **Publications:** 460 publications, 1 patent
- **Scientific activities:** solid state physics, physics of disordered condensed media, amorphous semiconductors and glassy metals, semiconductor technologies, heavy ion induced excitations in solids, mathematical and computer modelling, system analysis, nanotechnologies, nanodevices, nanoeducation, nanorisks



Igor V. Kabashkin (born in Riga, August 6, 1954)

- Vice-rector for Research and Development Affairs of Transport and Telecommunication Institute, Professor, Director of Telematics and Logistics Institute
- Ph.D in Aviation (1981, Moscow Institute of Civil Aviation Engineering) Dr.Sc.Habil. in Aviation (1992, Riga Aviation University), Member of the International Telecommunication Academy, Member of IEEE, Corresponding Member of Latvian Academy of Sciences (1998)
- **Publications:** 485 scientific papers and 67 patents
- **Research activities:** information technology applications, operations research, electronics and telecommunication, analysis and modelling of complex systems, transport telematics and logistics



Xingbin Ma

- Associate Professor of Shandong University of Science and Technology
- Director of the management science and engineering department
- **Research project:** management science and engineering



Xiaoyan Liu

- Associate Professor of Shandong University of Science and Technology
- **Research project:** Applied mathematics



Feng Qian

- Doctor of electrical engineering, mainly engaged in power system analysis and control, operation and management
- **University studies:** China Electric Power Research Institute (2005–2009). Ph.D. on power system and automation
- **Publications:** 10 papers



Songkai Liu

- Ph.D. student of Wuhan University
- **Research interests:** operation and control of power system



WenJia Yang

- Master of electrical engineering; The secondary assistant Technical specialists of Guangdong Power Grid Corporation, mainly engaged in power system operation analysis, control and management
- **University studies:** Tsinghua University, in the Department of Electrical Engineering, Sep. 2004–July. 2006. North China Electric Power University, in the School of Electrical & Electronic Engineering, Sep. 2000–July. 2004
- **Publications:** 2 Patents, 5 papers



Hong Wei

- Master of electrical engineering, mainly engaged in power system operation analysis, control and management.
- **University studies:** Huazhong University of Science and Technology, in the School of Electrical and Electronic Engineering (2003–2009)
- **Publications:** 2 papers



Youping Fan

- Wuhan University; Professor
- **Research interests:** artificial intelligence and knowledge engineering, modelling and control of complex system, security analysis and risk control technology of power system, parameter identification of power system



Zhenhua Xie (born August 26, 1968)

- University of Science and Technology Beijing, Professor, Ph.D.
- **Professional interests:** Safety science and technology
- **Research interests:** Mine safety and safety management



Tingting Luan

- Doctoral candidate at University of Science and Technology Beijing, major in Safety science and technology



Na He

- Master degree candidate at University of Science and Technology Beijing, major in Safety science and technology



Yingying Chai

- Master of Environmental Engineering, Dalian University of Technology
- **Professional interests:** Environmental impact assessment



Konstantin Tsvetkov

- Professor at Konstantin Preslavsky University of Shumen, 4, Oboriste Str., Veliko Turnovo 5000, Bulgaria



Mariana Petrova

- Professor at University of Veliko Turnovo “St.Cyryl and St.Methodius”, 32, Al.Burnov str., Veliko Turnovo 5000, Bulgaria

Marina Rebezova (born in Moscow, Russia)

- **Present position:** Programme Leader Metal Forming and Tribology, Programme: Materials Technology Division Educational Qualification: B .E., (Mechanical Engineering), MSc.E., (Mechanical Engineering); Head of the Department at Transport Clearing House
- **University study:** State institution of higher professional education – Moscow Aviation Institute (State University of Airspace Technology): Systems engineer
- **Publications:** 6 publications, 3 intra-branch ATSS standards, materials for study guide
- **Fields of research:** billing and settlement systems and technologies

CUMULATIVE INDEX

COMPUTER MODELLING and NEW TECHNOLOGIES, volume 17, no. 2, 2013

(Abstracts)

M. Rebezova. Repayment Problem at a Settlement of Debts, *Computer Modelling and New Technologies*, vol. 17, no. 2, 2013, pp. 7–14.

In different areas of practical activity the mutual payment liabilities occur between the subjects. Mutual repayment can be done to reduce the real money transfers between subjects. The problem consists in finding the corresponding chain of subjects. The problem is formulated in language of the graph theory and on the one hand it is the classical linear programming problem, on the other hand it is the classical problem of the graph theory. The algorithm and software have been developed for the solution of the problem.

Keywords: graph theory, tree, contour, linear programming, settlement of debts

Y. Chai, X. Meng, Sh. Ma, L. Xu, Ya. Li, Lu Shen, Ch. Jiang. A Research on Transport Planning Strategic Environmental Assessment (Sea): Incorporating System Dynamics into the Environmental Carrying Capacity, *Computer Modelling and New Technologies*, vol. 17, no. 2, 2013, pp. 15–23.

Transport construction plays an important role in promoting prosperity in the development process of a city. However, the environmental impacts it bring shouldn't be ignored. It is necessary to adopt strategic environmental assessment (SEA) before the transport planning is carried out. Environmental carrying capacity (ECC) is often used as a measuring tool in SEA to see whether a region is suitable to exploit. However, this static snapshot of ECC accounting fails to present the dynamic, multi-levelled relationship among the driving forces. In order to refine the SEA theory and conduct the transport planning in Dalian, China, this paper attempts to incorporate system dynamic (SD) into ECC to develop a SD-ECC forecasting framework, and provide a platform to support policy making for urban transport planning.

Keywords: Transport planning; Strategic environmental assessment; System dynamic; Environmental carrying capacity; Scenario analysis

F. Qian, S. Liu, W. Yang, H. Wei, Yo. Fan. A Novel Online Assessment Scheme for Power System Security Level of Transient Stability Based on Relationships Exploration in a Large Data Set, *Computer Modelling and New Technologies*, vol. 17, no. 2, 2013, pp. 24–35.

In this paper, a scheme based on data mining and relationships exploration is presented for security level assessment of transient stability. The proposed scheme can select the optimal variables as input features by detecting the relationship between critical clearing time (CCT) and each variable in a large power flow data set. The data set is created based on a series of power flow simulation and fault simulation in the software PSS/E. The relationships exploration statistical tool used is based on the maximal information coefficient (MIC) and the Pearson product-moment correlation coefficient (PPMCC). The variables selected are corresponding to the relationships highly ranked by MIC and PPMCC, including linear relationships and especially nonlinear ones. These relationships are also shown in the paper and some of them are explained from the perspective of power system operation. If the measured values of these variables are obtained in real-time from wide area measurement system (WAMS), the CCT can be estimated in real time since its relationships with these variables are explored. Then the security level of transient stability can be assessed for a new operation state. The scheme is tested on a 21-bus system provided by PSS/E and various test results indicate the scheme is accurate and effective, as well as the way to select input features is more intelligent than the current techniques.

Keywords: Maximal information coefficient (MIC), Pearson product-moment correlation coefficient (PPMCC), relationships exploration, large data sets, security assessment, transient stability, critical clearing time (CCT)

Zh. Xie, T. Luan, Na He. Numerical Simulation of air Leakage in Goaf of Fully Mechanized Face with High Dip and Hard Roof, *Computer Modelling and New Technologies*, vol. 17, no. 2, 2013, pp. 36–43.

Because the geological conditions of coal in goaf with high dip and hard roof are complex, and the law of air leakage is complicated and changeable, so the risk of coal spontaneous combustion in goaf is high. Mastering the law of air leakage in goaf is important to coal spontaneous combustion prevention. This paper detects the air leakage of 7162 working face in LongDong coal mine using SF₆ as tracer gas, and gets the basic distribution laws of air leakage in goaf of 7162 working face, furthermore collects relevant data for numerical simulation of airflow situation in goaf. The distribution laws of air pressure and wind speed in goaf have been obtained by simulating the seepage fields in goaf using FLUENT software. The research results provide scientific guidance for prevention measures of coal spontaneous combustion.

Keywords: goaf, coal spontaneous combustion, air leakage detection, numerical simulation

S. Amanzholova, N. Zhakayev. Simulation of Systems Information Security, *Computer Modelling and New Technologies*, vol. 17, no. 2, 2013, pp. 44–57.

As is well-known, the processes related to security – these are the same processes that take place in computer and telecommunication networks. IT Security involves the study processes starting from user authentication. Then came the authentication of users, and finally, began to use the authorization process. All these stages are only for customers or clients to have access to the necessary resources. After of the identification and authentication begins the processes related to access to resources, data integrity, password-protected sites, data encryption, adding digital signatures to documents, etc. For a detailed research of all processes involved in the creation of information security can be used very well established mathematical models queuing, i.e., queuing systems [1]. The model of queuing systems, i.e., a perfect mathematical tool allows us to investigate any variants of information security systems. To create a reliable system of information security, we need to create a model of the system to accurately simulate the behaviour of the system being close to real conditions [2]. Simulation of different objects lets us look at the problem from different points of view and identify system bottlenecks, as well as to offer the most appropriate option for the task.

Keywords: systems information security, computer and telecommunication networks, queuing systems

B. B. Abisheva, B. M. Baisakov, M. M. Maratov. Real-Time Facial Feature Point Detection and Tracking in a Video Sequence, *Computer Modelling and New Technologies*, vol. 17, no. 2, 2013, pp. 48–52.

Several algorithms for feature detection were compared and the most efficient ones were chosen to detect facial feature points such as eye corners, eyeballs, mouth corners and nostrils. To detect the desired feature points, first face detection was run using Viola-Jones's algorithm that is based on Haar-like features. Having found a face in an image, the face was searched for eyes, nose and mouth. Having found the necessary facial features, those regions of the image containing them were searched for the specific feature points described above.

For feature tracking several algorithms were compared as well [1]. As a result of the comparison the algorithm of Lucas-Kanade was chosen to be performed on the detected points.

The resultant algorithm detects the feature points to be tracked in the first frame of a video-sequence and then uses these points in the Lucas-Kanade algorithm for tracking. In case more than two points are lost during tracking, feature point detection is run again. This way the algorithm tracks feature points accurately, without lagging in real-time.

Keywords: video sequences, real time tracking for the image points, Lucas-Kanade tracking algorithm

A. Ferikoğlu, Ya. Sarı, R. Köker. Design and Analysis of Negative Value Circuit Components in Pspice Simulation Software, *Computer Modelling and New Technologies*, vol. 17, no. 2, 2013, pp. 53–59.

This paper describes the transaction to generate and measure negative valued resistors, capacitors and inductors in Pspice simulation medium for an educational purpose. Negative circuit components are designed and their defining characteristics are produced. An op-amp based generic

circuit is used for obtaining negative components. To extract characteristics, a charge-meter and a flux-meter are designed and utilized, in addition to the conventional meters (markers) in the Pspice environment. The numerical examples verify the relevant background theory and validate the designed meters, namely flux meter and charge meter, in simulation medium. The study of the paper have educational value in making clear the meaning of negative impedance by experimentation in a simulation medium, thus relating theory to practice and also exhibit that ORCAD Pspice is highly visual and effective for both understanding the mathematical theory underlying the circuits and performing measurements of flux and charge which are needed to obtain the characteristics of negative inductors and negative capacitors.

Keywords: simulation, Orcad PSpice, negative resistor, negative capacitor, negative inductor, flux-meter, charge-meter

K. S. Tsvetkov, M. M. Petrova. Is There Any Truth in „Projectlibre the Open Source Replacement of Microsoft Project”? *Computer Modelling and New Technologies*, vol. 17, no. 2, 2013, pp. 60–64.

An intensely intriguing announcement of major producers of open source software stir specialists in project management, namely message "ProjectLibre: the open source replacement of Microsoft Project". In 2012 the founders of OpenProj announced that they forked the project and will be releasing a new version of OpenProj in August 2012. The name of the fork is ProjectLibre. Is it going to try to prove and is it possible to use this software in the learning process for the preparation of students and professionals will try to answer in this article. This issue is especially actual in Higher Education, as the main reason for people to university is a good realization that he would have offered and given trend more and more employers to run a Linux-based systems and to use free software in the near future, their experience with open source products would definitely give them a significant advantage in the labour market.

Keywords: Microsoft project, OpenProj, ProjectLibre, project management, open source

X. Ma, Cu. Jiang. Study on Model of Component Reliability Based on Dynamic Strength Interference Theory, *Computer Modelling and New Technologies*, vol. 17, no. 2, 2013, pp. 65–72.

The strength variation of a product can be regarded as a degeneration process as well as an antagonistic process with the stress imposed on the product during the whole life of the product. In this paper, we used the dynamic strength interference theory to construct a structural reliability model that the relationship between components and the stress acting on it. The system is a continued degeneration process with the variation of time t before their failure. The calculating methods of reliability were given for kinds of common strength and stress distribution.

Keywords: structural reliability, dynamic strength interference model, strength, stress, degeneration

M. Rebezova. Atmaksas problēma parādu nokārtošanā, *Computer Modelling and New Technologies*, 17. sēj., Nr. 2, 2013, 7.–14. lpp.

Dažādu jomu praktiskās darbībās savstarpējās maksājumu saistības rodas starp subjektiem. Savstarpējo atmaksu var veikt, lai samazinātu reālos naudas pārskaitījumus starp subjektiem. Problēma pastāv atbilstošas ķēdes subjektu atrašanās. Problēma ir formulēta grafu teorijas valodā, un, no vienas puses, tā ir klasiskās lineārās programmēšanas problēma, no otras puses, tā ir klasiska grafu teorijas problēma. Algoritms un programmatūra ir izstrādāta, lai atrisinātu šo problēmu.

Atslēgvārdi: grafu teorija, koks, kontūra, lineārā programmēšana, parādu nokārtošana

J. Čai, H. Meng, Š. Ma, L. Hu, Ja. Li, Lu Šen, Č. Džiang. Transporta plānošanas stratēģiskā ietekmes uz vidi novērtējuma pētniecība: iekļaujot sistēmdinamiku vides ekoloģiskajā kapacitātē, *Computer Modelling and New Technologies*, 17. sēj., Nr. 2, 2013, 15.–23. lpp.

Transporta attīstībai ir nozīmīga loma, veicinot labklājību pilsētas attīstības procesā. Tomēr nedrīkst ignorēt ietekmi uz vidi, ko tā izraisa. Ir jāpieņem stratēģisks ietekmes uz vidi novērtējums pirms tiek veikta transporta plānošana. Vides ekoloģiskā kapacitāte, bieži tiek izmantota kā mērīšanas līdzeklis stratēģiskajā ietekmes uz vidi novērtējumā, lai redzētu, vai reģions ir piemērots izmantošanai. Tomēr šīs vides ekoloģiskās kapacitātes aprēķina statiskais momentuzņēmums nesniedz dinamisku, multi-izlīdzinātu attiecību starp virzītājspēkiem. Lai precizētu stratēģisko ietekmes uz vidi novērtējuma teoriju un veiktu transporta plānošanu Dalian reģionā, Ķīnā, šajā rakstā tiek mēģināts iekļaut sistēmdinamiku vides ekoloģiskajā kapacitātē (SD-VEK), lai izstrādātu (SD-VEK) prognozēšanas sistēmu, un nodrošinātu platformu politikas veidošanai pilsētas transporta plānošanā.

Atslēgvārdi: transporta plānošana; stratēģiskais ietekmes uz vidi novērtējums, sistēmdinamika, vides ekoloģiskā kapacitāte; scenāriju analīze

F. Kvian, S. Liu, V. Jang, H. Vei, Jo. Fan. Jauna tiešsaistes novērtēšanas sistēma pārejošas stabilitātes enerģijas sistēmas drošības līmenim, balstītam uz attiecību izpēti lielā datu kopā, *Computer Modelling and New Technologies*, 17. sēj., Nr. 2, 2013, 24.–35. lpp.

Šajā rakstā tiek izskatīta sistēma, kas balstās uz datu ieguvī un attiecību izpēti, un ir nepieciešama pārejošas stabilitātes drošības līmeņa novērtēšanai. Piedāvātā shēma var izvēlēties optimālos mainīgos kā ievades funkcijas, atklājot saikni starp kritisko notīrīšanas laiku un katru mainīgo lielā spēcīgā datu kopas plūsmā. Datu kopa ir izveidota, pamatojoties uz jaudas plūsmas simulācijas sēriju un bojājumu simulāciju programmatūrā PSS/E. Attiecību izpētes statistiskais izmantotais līdzeklis ir balstīts uz maksimālās informācijas koeficientu (*MIC*) un Pīrsona produkta-momenta korelācijas koeficientu (*PPMCC*). Izvēlētie mainīgie ir atbilstoši attiecībām, kas augsti sarindoti pēc *MIC* un *PPMCC*, tostarp lineārās attiecības un, it īpaši, nelineārās attiecības. Šīs attiecības arī ir parādītas rakstā, un dažas no tām ir izskaidrotas no enerģijas sistēmas darbības perspektīvas viedokļa. Ja šo mainīgo izmērītās vērtības tiek iegūtas reālā laikā no plašas teritorijas mērījumu sistēmas (*WAMS*), kritisko notīrīšanas laiku var novērtēt reālā laikā, kopš tās attiecības ar šiem mainīgajiem tiek izpētītas. Tad pārejošas stabilitātes drošības līmeni var novērtēt jaunam darbības stāvoklim. Shēma ir pārbaudīta uz 21-autobusa sistēmas, ko paredz PSS/E, un dažādu testu rezultāti liecina, ka shēma ir precīza un efektīva, kā arī veidu, lai izvēlētos ievades funkcijas, ir vairāk vieds nekā pašreizējās metodes.

Atslēgvārdi: maksimālās informācijas koeficients, Pīrsona produkta-momenta korelācijas koeficients, attiecību izpēte, lielas datu kopas, drošības novērtēšana, pārejoša stabilitāte, kritiskais notīrīšanas laiks

Ž. Ksie, T. Luan, Na He. Gaisa noplūdes skaitliska simulācija krāvējumā ar pilnībā mehanizētu plakni ar augstu kritumu un cietu grēdu, *Computer Modelling and New Technologies*, 17. sēj., Nr. 2, 2013, 36.–43. lpp.

Tā kā ogļu krāvējuma ar augstu kritumu un cietu grēdu ģeoloģiskie apstākļi ir sarežģīti, un gaisa noplūdes likums ir sarežģīts un mainīgs, tāpēc ogļu spontāna aizdegšanās risks krāvējumā ir liels. Ir svarīgi uzlabot likumu par gaisa noplūdi krāvējumā, lai novērstu ogļu pašziedēšanos.

Pētījuma rezultāti sniedz zinātniskus ieteikumus par profilakses pasākumiem ogļu pašziedēšanās gadījumā.

Atslēgvārdi: krāvējums, ogļu pašziedēšanās, gaisa noplūdes konstatēšana, skaitliska simulācija

S. Amanžolova, N. Žakajevs. Informācijas drošības sistēmu simulācijas, *Computer Modelling and New Technologies*, 17. sēj., Nr. 2, 2013, 44.–47. lpp.

Kā ir labi zināms, ka procesi, kas saistīti ar drošību - tie ir tie paši procesi, kas notiek datoru un telekomunikāciju tīklos. IT drošība saista studiju procesu sākt ar lietotāja autentifikāciju. Tad nāca lietotāju autentifikācija, un, visbeidzot, sāka izmantot autorizācijas procesu. Visi šie posmi ir domāti tikai klientiem, lai būtu pieeja nepieciešamiem resursiem. Pēc identifikācijas un autentifikācijas sākas procesi, kas saistīti ar piekļuvi resursiem, datu integritāti, ar paroli aizsargātiem saitēm, datu šifrēšanu, pievienojot digitālo parakstu uz dokumentiem, utt. Par visu iesaistīto procesu detalizētu pētījumu, kas iekļauti informācijas drošības procesu izveidē, var izmantot ļoti labi izveidotas matemātisko modeļu rindas, t.i., rindošanas sistēmu [1]. Rindas sistēmu modelis, t.i., ideāls matemātiskais rīks ļauj mums izpētīt visus informācijas drošības sistēmas variantus. Lai izveidotu informācijas drošības uzticamu sistēmu, mums ir jāizveido sistēmas modelis, precīzi jāmodelē sistēmas uzvedība esot tuvu reālajiem apstākļiem [2]. Dažādu objektu simulācija ļauj apskatīt problēmu no dažādiem skatu punktiem un noteikt sistēmas vājās vietas, kā arī piedāvāt vispiemērotāko uzdevuma variantu.

Atslēgvārdi: sistēmas informācijas drošība; datoru un telekomunikāciju tīkli; rindošanas sistēmas

B. Abiševa, B. Baisakovs, M. Maratovs. Reālā laika sejas vaibstu iezīmes punkta noteikšana un izsekošana A video secībā, *Computer Modelling and New Technologies*, 17. sēj., Nr. 2, 2013, 48.–52. lpp.

Vairāki algoritmi iezīmes noteikšanai tika salīdzināti un visefektīvākie tika izvēlēti, lai noteiktu sejas vaibstu punktus piemēram, acu kaktiņus, acs ābolus, mutes kaktiņus, nāsis. Lai noteiktu vajadzīgo līdzekli punktiem, vispirms sejas noteikšana tika palaista, izmantojot *Viola-Jones* algoritmu, kas balstās uz *Haar-like* funkcijām. Konstatējot sejas attēlu, sejai piemēklēja acis, degunu un muti.

Bez tam iezīmes izsekošanai tika salīdzināti arī vairāki algoritmi [1].

Iegūtais algoritms atrod iezīmes punktus, kas jāizseko pirmajā video secības ietvarā, un pēc tam šos punktus izmanto *Lucas-Kanade* algoritmā. Gadījumā, ja vairāk nekā divi punkti tiek zaudēti izsekošanas laikā, iezīmes punkta noteikšana ir palaista vēlreiz. Tādā veidā algoritms izseko iezīmes punktus precīzi, bez atpalikšanas reālajā laikā.

Atslēgvārdi: video sekvenču, reālā laika uzskaites attiecībā uz attēlu punktiem, Lucas-Kanade uzskaites algoritms

A. Ferikoglu, Ja. Sari, R. Kokers. Negatīvi vērtētu ķēžu komponentu plānošana un analīze Pspice simulācijas programmatūrā, *Computer Modelling and New Technologies*, 17. sēj., Nr. 2, 2013, 53.–59. lpp.

Šajā rakstā tiek apskatīta transakcija, lai radītu un novērtētu negatīvi vērtētus rezistorus, kondensatorus un induktorus Pspice simulācijas vidē izglītošanas nolūkā. Negatīvās ķēdes komponenti ir izstrādāti un to definēšanas raksturlielumi ir izveidoti. Uz op-amp balstīta vispārēja shēma tiek izmantota negatīvu sastāvdaļu iegūšanai. Lai ekstrahētu īpašības, uzlādes-mērītājs un plūsmas-mērītājs tiek izstrādāts un izlietots, papildus parastajiem mērītājiem (markieriem) šajā PSpice vidē. Skaitliskie piemēri pārbauda attiecīgās fona teorijas un apstiprina izstrādātos mērītājus, proti, plūsmas mērītāju un uzlādes mērītāju simulācijas vidē. Pētījumam dotajā rakstā ir izglītojoša vērtība, padarot skaidru, ko nozīmē negatīvā pretestība eksperimentāli simulācijas vidē, tādējādi attiecinoši teoriju praksei, kā arī uzrādot, ka ORCAD PSpice ir izteikti vizuāla un efektīva gan matemātiskās teorijas izpratnei ķēžu pamatā, gan plūsmu un uzlādes mērījumu veikšanā, kuras ir vajadzīgas, lai iegūtu negatīvu indukcijas spoļu un negatīvu kondensatoru īpašības.

Atslēgvārdi: simulācija, Orcad PSpice, negatīva pretestība, negatīvs kondensators, negatīvs induktors, plūsmas mērītājs, uzlādes mērītājs

K. Cvetkovs, M. Petrova. Vai pastāv kāda patiesība „ProjectLibre atvērta koda aizvietošanā ar *Microsoft Project*”? *Computer Modelling and New Technologies*, 17. sēj., Nr. 2, 2013, 60.–64. lpp.

Atvērta pirmkoda programmatūras lielāko ražotāju intensīvi intriģējošs paziņojums iesaista speciālistus projektu vadībā, proti, ziņojums „ProjectLibre: atvērta koda nomaiņa ar Microsoft Project”. 2012. gadā OpenProj dibinātāji paziņoja, ka tie sazarāja projektu un laidīs klajā jaunu versiju OpenProj 2012.gada augustā. Atzara nosaukums ir ProjectLibre. Vai tas notiek, lai mēģinātu pierādīt, un vai ir iespējams izmantot šo programmatūru mācību procesa sagatavošanā studentiem un profesionāļiem, centīsimies atbildēt šajā rakstā. Šis jautājums ir īpaši aktuāls augstākajā izglītībā, kā galvenais iemesls ir laba realizācija universitātes darbiniekiem, ka viņiem tiks piedāvāts un dota tendence arvien vairāk darba devējiem palaist Linux balstītas sistēmas un izmantot bezmaksas programmatūru tuvākajā nākotnē, viņu pieredze ar atklātā pirmkoda produktiem noteikti dotu viņiem būtiskas priekšrocības darba tirgū.

Atslēgvārdi: Microsoft Project, OpenProj, ProjectLibre, projektu vadība, atvērts avots

X. Ma, Cu. Džiang. Komponenta drošuma modeļa pētījums, pamatojoties uz dinamiskas izturības interferences teoriju, *Computer Modelling and New Technologies*, 17. sēj., Nr. 2, 2013, 65.–72. lpp.

Produkta stipruma variāciju var uzskatīt par deģenerācijas procesu, kā arī par antagonistisku procesu ar stresu, uzliktu uz produkta visas dzīves laikā. Šajā rakstā mēs izmantojam dinamisko izturības interferences teoriju, lai izveidotu strukturālu drošuma modeli tā, ka attiecības starp sastāvdaļām un stresu iedarbojas uz to. Sistēma ir deģenerācijas procesa turpinājums ar izmaiņām laikā t pirms tās atteices. Drošuma aprēķina metodes tika dotas kopējo spēku veidiem un stresa izplatīšanai.

Atslēgvārdi: konstrukciju drošums, dinamiska spēka interferences modelis, izturība, stress, deģenerācija

**COMPUTER MODELLING
&
NEW TECHNOLOGIES**

ISSN 1407-5806 & ISSN 1407-5814 (on-line)

EDITORIAL BOARD:

Prof. Igor Kabashkin (Chairman of the Board), *Transport & Telecommunication Institute, Latvia*;
Prof. Yuri Shunin (Editor-in-Chief), *Information Systems Management Institute, Latvia*;
Prof. Adolfas Baublys, *Vilnius Gediminas Technical University, Lithuania*;
Dr. Brent Bowen, Dr. Brent D. Bowen, *Purdue University, USA*;
Prof. Olgierd Dumbrajs, *University of Latvia, Solid State Physics Institute, Latvia*;
Prof. Sergey Maksimenko, *Institute for Nuclear Problem, Belarus State University, Belarus*;
Prof. Litovchenko, V. *Lashkaryov Institute of Semiconductor Physics of National Academy of Science of Ukraine*;
Prof. Pavel D'yachkov, *Kurnakov Institute for General and Inorganic Chemistry, Russian Academy of Sciences, Russia*;
Prof. Stefano Bellucci, *Frascati National Laboratories – National Institute of Nuclear Physics, Italy*;
Prof. Eugene Kopytov, *Transport & Telecommunication Institute, Latvia*;
Prof. Arnold Kiv, *Ben-Gurion University of the Negev, Israel*;
Prof. Juris Zakis, *Higher School of Social Technologies; Latvia*;
Prof. Edmundas Zavadskas, *Vilnius Gediminas Technical University, Lithuania*;
Prof. Michael Schenk, *Fraunhofer Institute for Factory Operation and Automation IFF, Germany*.

Host Organization:

Transport and Telecommunication Institute

Supporting Organizations:

Latvian Transport Development and Education Association
Latvian Academy of Sciences
Latvian Operations Research Society

**THE JOURNAL IS DESIGNED FOR PUBLISHING PAPERS CONCERNING
THE FOLLOWING FIELDS OF RESEARCH:**

- mathematical and computer modelling
- mathematical methods in natural and engineering sciences
- physical and technical sciences
- computer sciences and technologies
- material science, solid state physics and chemistry
- nanomaterials, nanodevices and nanotechnologies
- aviation and aerospace technologies
- electronics and telecommunication
- transport and logistics
- economics and management
- innovative education
- social sciences

In journal articles can be presented in English. All articles are reviewed.

EDITORIAL CORRESPONDENCE

Transporta un sakaru institūts (Transport and Telecommunication Institute)
Lomonosova iela 1, LV-1019, Riga, Latvia. Phone: (+371) 67100593. Fax: (+371) 67100535
E-mail: journal@tsi.lv, www.tsi.lv

Computer Modelling & New Technologies * Preparation of publication

COMPUTER MODELLING AND NEW TECHNOLOGIES, 2013, vol. 17, no. 2

ISSN 1407-5806, ISSN 1407-5814 (on-line: www.tsi.lv)

Scientific and research journal of Transport and Telecommunication Institute (Riga, Latvia)

The journal is being published since 1996.

The papers published in Journal “Computer Modelling and New Technologies” are included in

INSPEC (since 2010), **VINITI** (since 2011), **CAS Database**

www.theiet.org/resources/inspec/

<http://www2.viniti.ru/>

<http://www.cas.org/>

Computer Modelling & New Technologies * Preparation of publication

PREPARATION OF CAMERA-READY TYPESCRIPT: COMPUTER MODELLING AND NEW TECHNOLOGIES

1. In order to format your manuscript correctly, see the Page Layout Guideline for A4 (21 cm x 29,7 cm) paper size. Page Layout should be as follows: Top – 3 cm, Bottom – 3 cm, Left – 3 cm, Right – 3 cm.
2. Maximum length for the article is **10 pages**.
3. **Using of other Styles with the exception of Normal is not to be allowed!**
4. **Articles** should be Times New Roman typeface, single-spaced.
5. The article should include:
 - title;
 - author's name(s) and information (institution, city, country, the present address, phones, and e-mail addresses);
 - abstract (100–150 words);
 - keywords (max. 6);
 - introduction – clear explanation of the essence of the problem, previous work, purpose of the research and contribution;
 - description of the research;
 - conclusion section (this is mandatory) – should clearly indicate the advantages, limitations and possible applications;
 - references.
- Attention!** First name, last name, the title of the article, abstract and keywords must be submitted in the English and Latvian languages (in Latvian it is only for Latvian authors) as well as in the language of the original (when an article is written in different language).
6. The text should be in clear, concise English (or other declared language). Please be consistent in punctuation, abbreviations, spelling (**British English**), headings and the style of referencing.
7. **The title of the article** – 14 point, UPPERCASE, style Bold and centred.
8. **Author's names** – centred, type size 12 point, Upper and lower case, style Bold Italic.
9. **Author's information** – 10 point, Upper and lower case, style Italic, centred.
10. **Abstract and keywords** – 8 point size, style Normal, alignment Justify.
11. **The first level Headings** – 11 point, Upper and lower case, style Bold, alignment Left. Use one line space before the first level Heading and one line space after the first level Heading.
12. **The second level Headings** – 10 point, Upper and lower case, style Bold, alignment Left. One line space should be used before the second level Heading and 1/2 line space after the second level Heading.
13. **The third level Headings** – 10 point, Upper and lower case, style Italic, alignment Left. One line space should be used before the second level Heading and 1/2 line space after the third level Heading.
14. **Text** of the article – 10 point, single-spaced, alignment Justify.
15. The set of **formulas** on application of fonts, signs and a way of design should be uniform throughout the text. The set of formulas is carried out with use of editors of formulas MS Equation 3.0 or MathType. The formula with a number – the formula itself should be located on the left edge of the text, but a number – on the right one. Font sizes for equations are the following: 11pt – full, 7pt – subscripts/superscripts, 5pt – sub-subscripts/superscripts, 16pt – symbols, 11pt – subsymbols.
16. All **Figures** – must be centred. Figure number and caption always appear below the Figure, type size 8 point.

Figure 1. This is figure caption

Diagrams, Figures and Photographs – must be of high quality, in format *.TIFF, *.JPG, *.BMP with resolution not less than 300 dpi. Also formats *.CDR, *.PSD are possible. Combination of Figures in format, for instance, *.TIFF with elements of the in-built Figure Editor in MS Word is prohibited.

17. **Table Number and Title** – always appear above the Table. Alignment Left. Type size 8 point. Use one line space before the Table Title, one line space after the Table Title and 1/2 line space after the Table.

Computer Modelling & New Technologies * Preparation of publication

Table 1. This is an example of a Table

Heading	Heading	Heading
Text	Text	Text
Text	Text	Text

18. **References** in the text should be indicated by a number in square brackets, e.g. [1].

References should be numbered in the order cited in the manuscript. The correct format for references is the following:

Book: Author(s). (Year of publication). *Book title (in Italics)*. Place of publication: Publisher.

Example: 1. Kayston, M. and Fried, W. R. (1969). *Avionic Navigation Systems*. New York: John Wiley and Sons Inc.

Conference Proceedings: Author(s). (Year of publication). Title of an article. In Conference name, Date (Page range). Place of publication: Publisher.

Example: 2. Canales, Romero J. (2003). A First Step to Consolidate the European Association of Aerospace Students in Latvia (Presented by the Munich Local Group). In 'Research and Technology – Step into the Future': Programme and Abstracts. Research and Academic Conference, Riga, Latvia, April 7–11, 2003 (pp. 20–29). Riga: Transport and Telecommunication Institute.

Journal article: Author(s). (Year of publication). Article title. *Journal Title*, Volume (issue), range of pages. DOI.

Example: 3. Nikora, V. (2006). Hydrodynamics of aquatic ecosystems. *Acta Geophysica*, 55(1), 3–10. DOI:10.2478/s11600-006-0043-6.

Report: Author(s). (Year of publication). *Title*. Place of publication: Publisher. (Report number).

Example: 4. Osgood, D. W., & Wilson, J. K. (1990). *Covariation of adolescent health problems*. Lincoln: University of Nebraska. (NTIS No. PB 91-154 377/AS).

Government publication: Institution name. (Year of publication). *Title*. Place of publication: Publisher.

Example: 5. Ministerial Council on Drug Strategy. (1997). *The national drug strategy: Mapping the future*. Canberra: Australian Government Publishing Service.

19. **Authors Index**

Editors form the author's index of a whole Volume. Thus, all contributors are expected to present personal colour photos with the short information on the education, scientific titles and activities.

20. **Acknowledgements**

Acknowledgements (if present) mention some specialists, grants and foundations connected with the presented paper. The first page of the contribution should start on page 1 (right-hand, upper, without computer page numbering). Please, paginate the contributions in the order they are to be published. Use simple pencil only.

21. **Articles poorly produced or incorrectly formatted may not be included in the proceedings.**